Università degli Studi di Milano

PhD Thesis

Epigenetics of Energy Metabolism:
Focus on Class I Histone Deacetylases

Doctorate School of Biochemical, Nutritional,
and Metabolic Sciences

Doctorate of Biochemistry

Dipartimento di Scienze Farmacologiche e Biomolecolari

Cycle XXVII

BIO 10

Alessandra Ferrari

Matr. R09683

Tutor: Prof. Maurizio Crestani

Coordinator: Prof. Francesco Bonomi

Table of Contents

Introduction 1

Aim of the study 24

Materials and Methods 28

Results 43

Introduction

Obesity: epidemiology and classification

Obesity is a metabolic disease, whose diffusion has been exponentially increased in the last thirty years[1]. In the light of this alarming data, the world health organization defined obesity as a global epidemic. Particularly relevant is the explosion of infantile obesity: recent data demonstrated that the number of obese children in France is dramatically increased in the last decade[2], and the prevalence of over-weight children in USA has doubled in the last forty years[3]. The fast increase in obesity incidence is linked to an excessive food intake and to a sedentary life style, typical of western population. But, at individual level, can be exacerbate by genetic susceptibility. The weight gain is in fact the result of interaction among genetic, environmental and psychosocial signals that, integrated by physiological factors, regulate energy store and consumption[4]. Obesity is strictly related to deep changes in physiological functions, leading to an altered and ectopic distribution of adipose tissue. This can severely compromise cardiac and respiratory function, due to fat accumulation around heart and rib cage. Moreover the increase of intra-abdominal visceral fat deposition correlates to insulin-resistance, type 2 diabetes, dyslipidemia and hypertension[5]. These comorbidities contribute to raise the mortality rate associated to the pathology that positively correlates to body weight gain[6]. Obesity is the result of an altered energy balance that results in excessive accumulation of adipose tissue. Clinical diagnosis of obesity is based on the Body Mass Index (BMI), calculated as the ratio between the body weight (kilograms) and the square of the height (meters). Based on the indication of the World Health Organization a BMI over 25 correlates with overweight, while a value of BMI over 30 is considered indicative of obesity[4].

Insulin resistance: the evil partner of obesity

Recent studies highlighted a strong correlation between obesity, insulin resistance, and type 2 diabetes[7]. In the early phase, this pathology is characterized by a reduced insulin sensitivity of skeletal muscle, adipose tissue and liver[8]. In the later state of disease the ability to secrete insulin by pancreatic beta cells is also impaired[9]. In physiological condition, insulin secreted from pancreatic beta cells in response to increased glucose plasma level, exerts multiple systemic effects by binding its receptor (insulin receptor, IR) in several organs. In skeletal muscle and adipose tissue the binding of insulin to IR activates the phosphorylation on tyrosine residues of insulin receptor substrate (IRS) that in turn phosphorylates and activates the phosphatidylinositide 3-kinase (PI3K). Through a cascade of intracellular signals, insulin induces the membrane traslocation of the insulin-dependent glucose transporter Glut4 that allows the internalization of glucose in muscle and adipose cells[10]. In liver insulin stimulates the expression of genes involved in glucose metabolism and lipogenesis (glucokinase, pyruvate kinase, acetilCoA carboxylase, fatty acid synthase); concomitantly it inhibits transcription of gene encoding for

phosphoenolpyruvate carboxykinase (*Pepck*), key enzyme of gluconeogenesis[11]. In insulin resistance state the ability of skeletal muscle and adipose tissue to uptake circulating glucose is impaired because of reduced membrane translocation of Glut4[11]. Moreover in obese subjects the high levels of circulating free fatty acids and other metabolites such as ceramides and diacilglycerols, activate different protein kinases, such as protein kinase C (PKC), Jun kinase (JNK) and the inhibitor of nuclear factor kB (IKB) that increase serine residues of IRS, preventing the tyrosine phosphorylation[12]. This prevent the activation of insulin signaling, contributing to the onset of insulin resistance[13]. In this context, free fatty acids represent a dangerous enemy of liver: by inhibiting IRS activation, they block insulin-mediated activation of *Pepck*, leading to a higher synthesis of hepatic glucose that can be released in plasma and worsens the hyperglycemia[14]. The reduced insulin hepatic clearance leads to increased levels of insulin in peripheral districts, inducing a further down-sensitization of insulin receptors.

Hyperinsulinemia and insulin-resistance are also related to dyslipoproteinemia and contribute to alterations of plasma lipid profile typically associated to obesity: reduced high density lipoproteins (HDL), high levels of cholesterol and low density lipoprotein[4].

The adipose organ

In mammals the adipose organ is traditionally composed by white adipose tissue (WAT) and brown adipose tissue (BAT). Two types of WAT have been described: subcutaneous and visceral. Subcutaneous WAT is located anteriorly in axillary region and posteriorly from dorsal-lumbar to inguinal region. Visceral WAT is instead located in the rib cage and in abdominal cavity and consists of retroperitoneal, peritoneal, mesenteric, epicardial and gonadic (referred to as epidydimal in males) WAT[15]. BAT has been localized by positrons emission tomography (PET) in the inter-scapular region, and it has been demonstrated that this fat depot is functional even in adult human subjects[16]. The main function of adipose tissue is to store lipids as triglycerides and to release them in response to energy demands. However several publications demonstrated that adipose tissue plays an important role in multiple physiological processes, such as immunity[17] and thermogenesis[18]. Adipose tissue also has important mechanical properties, serving to protect delicate organs (the eye, for example, is surrounded by fat) and to cushion body parts exposed to high levels of mechanical stress[19].

Adipose tissue: white, brown and beige

White and brown adipocytes are different in term of morphology and function. The classical view of the function of WAT is the storage of lipids in form of trygliceride, so in the past it has been considered just a long-term fuel reserve, which can be mobilized during food deprivation with the release of fatty acids for oxidation in other organs. Thus, the size of the adipose tissue stores increases in periods of positive energy balance and

declines when energy expenditure is in excess of intake[20]. Nowadays it has been established that adipose tissue is not only a storage center for lipids but a master regulator of energy balance and nutritional homeostasis[21], that plays a key role in metabolic regulation. Moreover adipose tissue is now known to express and secrete a variety of bioactive peptides, known as adipokines, which act at both the local (autocrine/paracrine) and systemic (endocrine) level[22]. Adipose tissue, in fact, produces cytokines and cytokine-related protein (Leptin[23], TNF[24], IL-6[25], adiponectin[25], resistin[26]), proteins involved in the fibrinolytic system (PAI-1[27]), lipids and proteins for lipid metabolism or transport (lipoprotein lipase, apolipiprotein E, non esterified fatty acids), and enzymes involved in steroid metabolism[28]. In addition to these efferent signals, adipose tissue expresses numerous receptors that allow it to respond to afferent hormonal and nervous signals. Thus, besides the biological repertoire necessary for storing and releasing energy, adipose tissue contains the metabolic machinery to permit communication with distant organs including the central nervous system[22].

White adipose tissue is mostly composed of unilocular high dimensional (70-80 μm) cells with peripheral nucleus and a large cytoplasmic lipid vacuole that occupies 90% of cellular volume, where triglycerides are stored. This vacuole is separated from the rest of the cytoplasm by an electron-dense barrier, which contains important structural proteins such as perilipin[29]. During weight gain, different fat depots enlarge via hyperplasia (increase in the number of adipocytes), by hypertrophy (increase of adipocyte size) or both[30]. Different WAT depots showed relevant differences in terms of function and morphology. Visceral adipocytes have long been known to be smaller than their subcutaneous counterparts both in lean and in obese animals[31]. This is relevant especially in pathological condition such as obesity that is related to a global inflammatory status. It has been proposed that obesity-related inflammation is the result of macrophage infiltration in WAT[32]. Several studies suggest that adipose tissue inflammation is attributable in large part to the pro-inflammatory actions of bone marrow-derived white adipose tissue (WAT) macrophages. These studies demonstrate that macrophage numbers and/or gene expression of macrophage inflammatory markers in WAT are positively correlated with adipocyte size and body mass index (BMI) in mice[33] and negatively correlated with weight loss in obese humans[34]. Macrophages are the predominant source of tumor necrosis factor-α (TNF-α) and a significant source of interleukin-6 (IL-6) and nitric oxide in WAT of obese (*ob/ob*, *db/db*) mice and humans[35]. These molecules affect cellular metabolism: TNF, for example, reduces insulin sensitivity and increases lipolysis in adipocytes, inhibiting in this way adipogenesis[36]. It in fact represses the master regulator of adipocyte differentiation, Peroxisome Proliferator-Activated Receptor γ (PPARγ) at transcriptional, translational and post-translational level[37]. Moreover increase in macrophage inflammatory gene expression in WAT immediately precedes or is coincident with the onset of hyperinsulinemia in murine diet-induced obesity[38], and obese mice with genetically ablated macrophage inflammatory (i.e., nuclear factor κB) signaling are protected from insulin resistance[39]. Together, these observations implicate macrophage activation in the development of obesity-associated WAT inflammation and insulin resistance. Saverio

Cinti and collaborators demonstrated that adipose tissue infiltrated macrophages (ATMs) surround dead adipocytes, whose number increases in obese state, and form a typical "crown-like structure" (CLS) that scavenges residual adipocyte lipids[40]. Cinti and colleagues also demonstrated that visceral depots are the prevalent sites of adipocyte death and macrophage infiltration. Their data suggest that the higher incidence of metabolic disorders associated with visceral fat accumulation could be due to a greater susceptibility to death of the adipocytes. The conclusion they reach is that visceral adipocytes reach the critical size triggering death before subcutaneous adipocytes[41]. Thus the established concept that larger adipocytes (such as subcutaneous adipocytes) correlate with greater insulin resistance[42] should be reconsidered in its pathogenic mechanism: it appears more appropriate to refer to positive correlation between inflammation (related to insulin resistance) and the critical size that adipocytes can reach before they collapse. A recent paper supports a preferential visceral versus subcutaneous macrophage infiltration also in obese human patients[43]. Some authors have hypothesized that the differences in size, function, and potential contribution to disease shown by the different fat depots may be due to regional intrinsic differences, including differences in preadipocyte characteristics[44,45]. Accordingly to this hypothesis, the greater propensity of visceral compared with subcutaneous adipocytes to die could be explained by intrinsic cellular differences among different fat depots. Regarding adipose tissue and macrophages it is important to underline the role of a population of resident macrophages, typical of functional adipose tissue: M2 macrophages (or "alternatively activated")[46]. These macrophages differ from the classic M1 macrophages, typically associated to a pro-inflammatory phenotype[47]. They play a role in tissue remodeling and wound healing and respond to IL-4 and IL-13 by secreting anti-inflammatory cytokines like IL-10 and IL-1 receptor antagonist[48]. In lean animals, M2 macrophages dominate the adipose tissue resident population. As obesity progresses, however, more M1 macrophages infiltrate the fat pad, causing insulin resistance[49]. Adipose M2 macrophage number does not diminish in obesity and, in fact, may increase; but there is a major shift in the M1/M2 ratio favoring a pro-inflammatory state[48] (Figure 1).
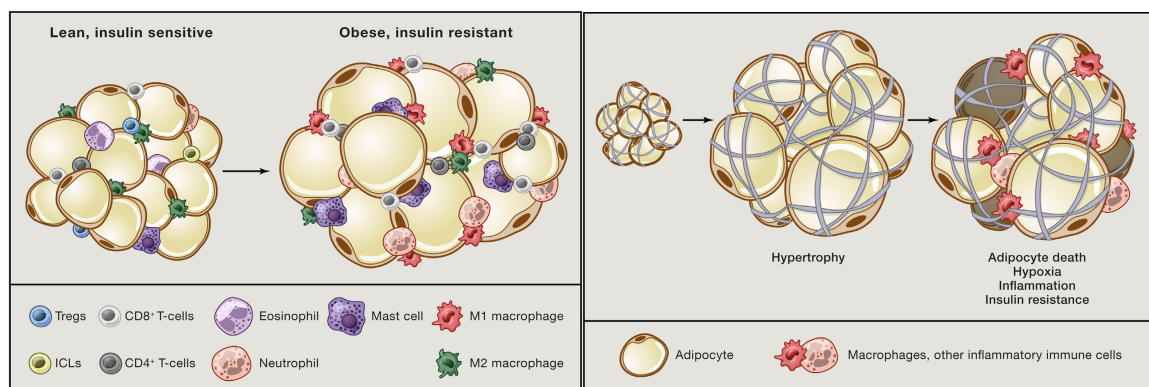

Figure 1: Adipose tissue hypertrophy consequent to obese state increases M1 macrophages recruitment. They surround dead adipocyte, form typical "crown-like structures" (CLS) that scavenge residual adipocyte lipid. *Adapted from Rosen and Spiegelman, 2014*[21]

In the recent years the fundamental role of another type of fat, brown adipose tissue, has been deeply investigated. The unequivocal discovery of brown fat in adult human subjects[50] opened a new way for studying whether metabolic potential of this fat depot can be exploited to treat metabolic disorders. Brown adipocytes are highly specialized cells that dissipate stored chemical energy in the form of heat. They do this through the actions of uncoupling protein-1 (UCP-1), a brown adipose tissue (BAT)-specific protein located within the mitochondria, which are densely packed in these cells. UCP-1 catalyzes a proton leak across the inner mitochondrial membrane, thus "uncoupling" fuel oxidation from ATP synthesis[51]. The function of BAT is to transfer energy from food into heat; in fact it regulates body temperature via non-shivering thermogenesis. Heat production and thermogenic capacity are under the control of norepinephrine released from sympathetic nerves. Heat production from brown adipose tissue is activated whenever the organism is in need of extra heat, e.g., postnatally, during entry into a febrile state, and during arousal from hibernation, and the rate of thermogenesis is centrally controlled via a pathway initiated in the hypothalamus[18]. Sympathetic nervous system (SNS) plays a key role in the activation of thermogenic program: several hypothalamic and extrahypothalamic areas act as integrators of the cold response[52]. The cold thermal afferent circuit from cutaneous thermal receptors, through thermosensory neurons in the dorsal horn of the spinal cord, ascends to activate neurons in the lateral parabrachial nucleus. These neurons drive GABAergic interneurons in the preoptic area (POA) to inhibit warm-sensitive, inhibitory output neurons of the POA. The resulting disinhibition of BAT thermogenesis-promoting neurons in the dorsomedial hypothalamus activates BAT sympathetic premotor neurons in the rostral ventromedial medulla, including the rostral raphe pallidus, which provide excitatory, and possibly disinhibitory, inputs to spinal sympathetic circuits to drive BAT thermogenesis[53]. The result of the activation of this intricate neural circuitry is the secretion of cathecolamines at the level of BAT: norepinephrine activates adrenergic receptors on adipocytes, which triggers a signal transduction cascade that leads to adaptive switch in the expression of thermogenic genes[54]. Sympathetic neurons release catecholamines, which bind to β3-adrenergic receptor, leading to activation of adenylyl cyclase (AC), increased cyclic AMP (cAMP) concentrations and enhanced PKA activity[18]. Recently it has been reported that also increased concentrations of natriuretic peptides trigger BAT thermogenesis through activation of cyclic GMP-dependent protein kinase (PKG)[55]: natriuretic peptides bind natriuretic peptide receptor A (Npra), which activates guanylyl cyclase (GC) to increase the concentrations of cyclic GMP leading to activation of PKG[55]. Activated PKA and PKG drive transcriptional responses in brown adipocytes through the activity of phosphorylated Creb and p38 Mapk[56]. p38 Mapk phosphorylates and activates the activating transcription factor 2 (Atf2) and the master regulator of mitochondrial biogenesis Pparγ coactivator 1α, Pgc-1α[57], which induce the transcription of downstream thermogenic genes, including *Ucp1*[58]. Pgc-1α binds DNA through interactions with Pparγ[59], Pparα, retinoid X receptors (Rxrs) and thyroid receptor (TFx)[60]. Additionally, catecholamines increase the amounts of miR-196a, resulting in increased C/ebpβ expression, which helps drive the thermogenic gene

program[61]. Importantly, activation of PKA and PKG also acutely induces lipolysis. Free fatty acids released from lipid droplets are oxidized by mitochondria to produce heat. Proton leak through Ucp1 is activated by long-chain fatty acids released from the mitochondrial membrane by phospholipase 2 (Pla2)[62].

In addition to nerve terminals, alternatively activated macrophages (M2) in BAT produce catecholamines in response to cold that further tighten up the thermogenic activation[63].
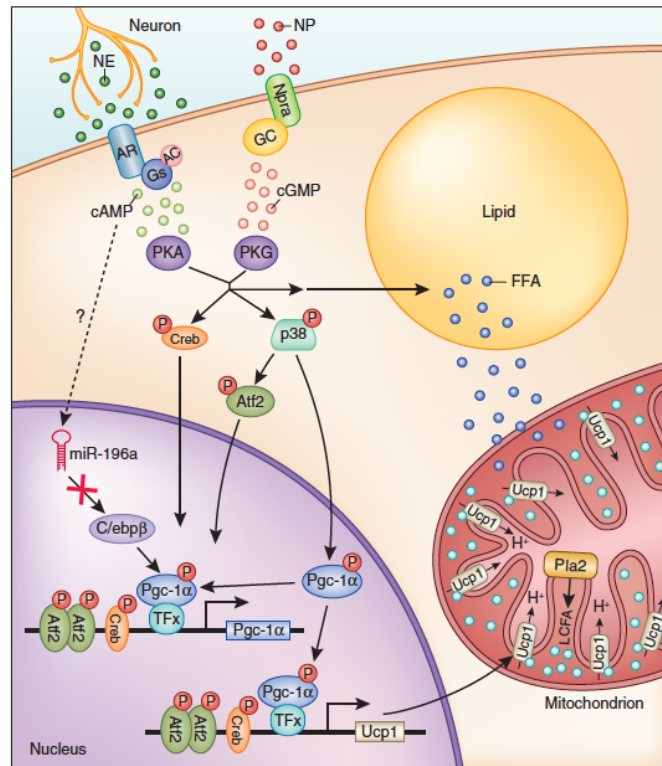
Figure 2: Induction of thermogenesis: cathecolamines and natriuretic peptide binding to brown adipocyte surface activate a molecular cascade leading to Ucp1 activation. *From Harms and Seale, 2013[54]*

Moreover the SNS distributes signals to white or brown adipose depots according to energy demand, thus both the effect of food deprivation and the effect of cold exposure determine SNS input to adipose tissue[64].

Human newborns have significant brown fat depots, presumably to provide heat in the cold environment encountered at birth. Adult humans, however, were felt to be largely devoid of brown fat unless specifically challenged by chronic cold[65] or by states of catecholaminergic excess[66]. The existence of significant depots of brown fat in adult humans was proven based upon radiological observations of symmetrical [18F]-2-fluoro-D-2-deoxy-Dglucose (FDG) positron emission tomography (PET)-positive loci in the supraclavicular and spinal regions of patients getting such scans for cancer diagnosis or staging. Biopsies confirmed the presence in these regions of UCP-1+ adipocytes, consistent with brown fat[50,67,68]. In rodents, prolonged cold exposure or adrenergic signaling can provoke the appearance of clusters of UCP-1+ cells with a brown fat-like

morphology within white fat depots. Their abundance varies dramatically between depots, with the highest numbers found in inguinal and retroperitoneal fat. These inducible cells have been called "beige" or "brite" adipocytes and share an overlapping but distinct gene expression pattern compared to classic brown adipocytes[21]. Both express a core program of thermogenic and mitochondrial genes, including Ucp1. However, murine beige cells also express the surface markers such as Cd137 and Tmem26 that are not expressed in brown adipocytes[69]. Other genes, like Zic1, appear to mark classic brown adipocytes, but not beige cells[70]. Classical brown fat cells have a higher basal UCP1 expression and elevated uncoupled respiration (relative to white or beige cells) before hormonal stimulation. Beige cells have low basal UCP1 expression and uncoupled respiration, comparable to white cells. However, stimulation with a β-adrenergic agonist elevates UCP1 to levels seen in brown fat cells. This suggests that beige cells are uniquely programmed to be bifunctional suited for energy storage in the absence of thermogenic stimuli but fully capable of turning on heat production when they receive appropriate signals[69]. Moreover selective loss of classic brown fat (for example by ablation of the type IA BMP receptor) causes compensatory induction of beige fat, restoring both body temperature and resistance to diet-induced obesity[71]. The thermogenic profile of beige adipocytes is reversible: beige adipocytes acquired in WAT during cold exposure lose Ucp1 expression and are retained after mice are moved back to warmer conditions. When these mice are re-exposed to cold, the same cells again induce Ucp1 expression[72]. Beige adipocytes are most abundant in the inguinal WAT, the major subcutaneous depot in rodents[73]. However, Ucp1-expressing adipocytes are evident in most WAT depots in response to cold exposure[74,75]. Petrovic and colleagues found that a subset of adipocytes isolated from epidydimal WAT (a visceral fat depot) differentiated *in vitro* from the stromal vascular fraction (an enriched source of preadipocytes) of WAT express Ucp1 in response to chronic treatment with Pparγ activators, highlighting the role played by Pparγ in the establishment of browning of visceral adipocytes[76]. There is evidence from animal models that enhancement of the function of brown adipocytes, beige adipocytes or both in humans could be very effective for treating type 2 diabetes and obesity[77]. In recent years several pathways and factors that can induce browning of white fat have been identified and potentially they represent new targets in the therapy of metabolic disorders. Spiegelman and collaborators, starting from the observation that increasing the amounts of Pgc-1α in muscle protects sedentary mice from obesity[78], found that WAT of Pgc-1α transgenic mice contained more beige adipocytes than that of wild-type mice[79]. In a search for effectors of the enhanced energy expenditure in these mice, they identified *Fndc5* (encoding fibronectin type III domain containing 5) as a Pgc-1α target gene and showed that its product was secreted from myocytes in the form of a previously undiscovered hormone, which they called irisin: irisin stimulates the browning of WAT through specific actions on the beige preadipocyte population[79]. Hepatic bile acids and FGF21 have also been shown to enhance browning, as have cardiac hormones like atrial and ventricular natriuretic peptides (ANP and BNP) and cardiotrophin-1[80]. These agents act through their respective receptors to induce browning by various overlapping mechanisms. Bile acids, for example, activate the TGR5

receptor, which in turn induces the deiodinase enzyme that promotes intracellular T3 formation[81]. Thyroid hormone and catecholamines both induce the local formation of BMP8b, which sensitizes the brown adipocyte to further adrenergic signaling. BMP8b also acts in the brain to direct SNS signaling specifically to BAT[82] (Figure 3).
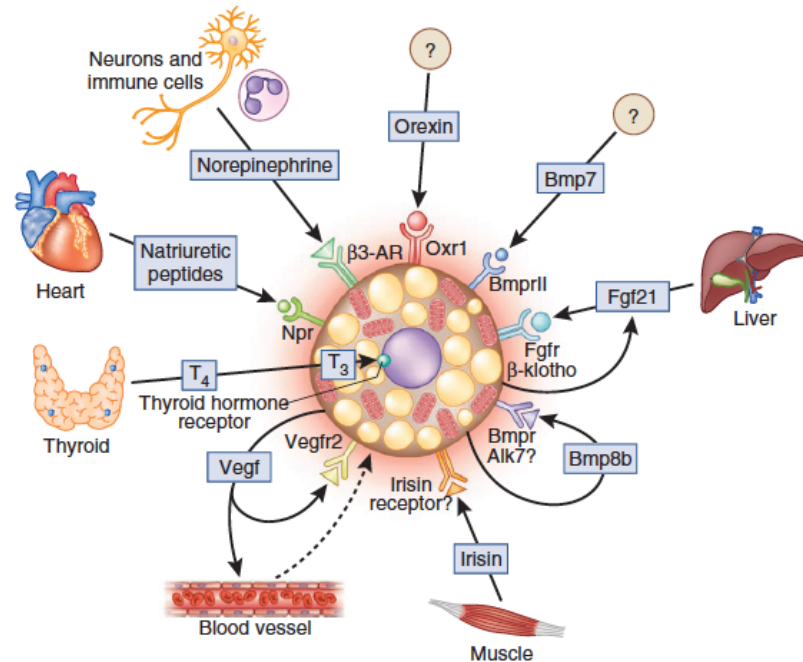
Figure 3: Secreted factors that recruit brown adipocytes, beige adipocytes or both. *From Harms and Seale, 2013 [54]*

From precursors to differentiated adipocytes

Adipocytes develop from preadipocytes, which themselves derive from precursor cells. The so-called stromal vascular fraction (SVF) is separated from mature adipocytes by collagenase digestion and low-speed centrifugation. When the SVF is cultured ex vivo, blood cells, endothelial cells, and other non-fibroblastic cells do not attach to the dish[83]. What remains can be almost completely differentiated using a hormonal cocktail that typically includes insulin, glucocorticoids, phosphodiesterase inhibitors, and often a Pparγ agonist[83]. This does not allow, however, for identification of the specific cell type within the SVF that populates the mature adipocyte fraction in vivo, and this has spurred a number of studies involving selective flow sorting using antibodies against various cell surface markers[21]. Most of these studies have shown that mesenchymal and stem cell markers such as CD34 and Sca-1 strongly enrich for adipogenic precursors[84]. More recently, other cell surface markers typical of subpopulation of stromal cells that differentiates into adipocytes have been identified, such as PDGFRα[85]. Interestingly several studies in the last decade demonstrated that brown and white adipocytes do not develop from common precursors, as previously thought. Data obtained over the last few years have shown that muscle and classical brown fat derive from the same or very similar precursors[86]. The transcriptional cofactor PRD1-BF-1-RIZ1 homologous domain-containing protein-16 (PRDM16) has been in fact identified as a dominant regulator of

the brown fat program[87]: knock down of PRDM16 in primary brown fat cultures induces a phenotypic switch to skeletal muscle, while expression of PRDM16 in myoblasts commits them to brown fat[88]. Moreover lineage-tracing studies using the muscle-selective Myf5-Cre showed that skeletal muscle and classical brown fat share a common precursor[88]. These findings helped to explain why brown preadipocytes express some myogenic genes not seen in white preadipocytes[89].

Beige adipocytes do not derive from the same Pax7+Myf5+ precursor cells that give rise to classic interscapular BAT[88]. In order to explain the origin of beige adipocytes the first theory proposed was that these cells derive from transdifferentiation of existing mature white adipocytes. More recently, however, unique precursor cells within the white fat pad have been identified using sorting and/or cloning by limiting dilution[90,91]. A lineage tracing study reported that cold exposure-induced "browning" of white fat required *de novo* adipogenesis[92]. Another study demonstrated that beige adipocytes appearing in response to an initial period of cold exposure, showed morphology and gene expression pattern similar to that of a typical white adipocyte after reintroduction to warm conditions[72]. After new exposure to the cold, many of these cells induce again the thermogenic program, suggesting that precursor cell differentiates into a beige adipocyte when conditions require it to do so, and converts back to an energy-storing ''white'' adipocyte when heat generation is no longer a priority. Collectively, these studies demonstrate that certain adipose populations show extraordinary plasticity when physiological conditions change.

At the cellular level, adipogenesis occurs in two phases: determination and terminal differentiation. During determination, possible alternate fates of an adipose precursor cell become progressively restricted such that it becomes "committed" to the adipose lineage and becomes a preadipocyte. Terminal differentiation, on the other hand, is the process by which the preadipocyte acquires the characteristics of mature adipocytes[21]. Most of the cellular models that have been employed to study adipogenesis are already committed to the adipose lineage (e.g., 3T3-L1, 3T3-F442A): for this reason we know much more about the process of terminal differentiation[93]. Nowadays other immortalized cell cultures are available, such as C3H10T1/2, an adipogenic cell line that has been isolated from bone marrow and that conserves features of early not-committed precursor. Thus this cell line is particularly useful for in-depth investigations on molecular mechanism occurring at the beginning of the adipocyte differentiation program. Some pre-adipocyte models (for example, the mouse cell lines 3T3-L1, 3T3-F442A) undergo one or two rounds of cell division prior to differentiation, whereas others (C3H10T1/2 and human pre-adipocytes) differentiate without post-confluence mitosis[94]. In order to investigate signaling pathways that regulate the adipogenic/nonadipogenic fate of multipotent cells, several studies have been performed using bone marrow-derived mesenchymal cells. For this reason the "bone-fat switch" is the most commonly described fate choice. It has been demonstrated that the Wnt and hedgehog pathways promote osteogenesis and inhibit adipogenesis in both committed and uncommitted precursor cells[93]. Even though these pathways utilize different signaling intermediates, both have been reported to converge on the

transcription factor COUP-TFII, which inhibits proadipogenic transcription factors like PPARγ and C/EBPα[95,96]. Conversely, insulin growth factor (IGF) and insulin signaling is strongly proadipogenic[97]. There are many other players that influence adipogenic program, and some of them exerts their action on specifics ligand, cell type, stage of differentiation, or other experimental conditions[21]. The transforming growth factor β and bone morphogenic protein (TGFβ/BMP) is a superfamily of proteins that participate in the regulation of adipocyte differentiation. TGFβ and its downstream effector Smad3 have been shown to exert both pro- and anti-adipogenic actions in different *in vitro* and *ex vivo* models[98,99]. Among the BMPs, BMP2 and BMP4 increase both osteogenesis and adipogenesis, depending upon other components of the differentiation cocktail, whereas BMP7 promotes brown adipogenesis specifically[100]. Also other members of the superfamily, like the activins, have disparate effects on adipogenesis and adiposity[101]. Similarly, the fibroblast growth factor (FGF) and Notch-signaling pathways have been reported to have complex effects on adipogenesis: Notch signalling seems to be required for 3T3-L1 differentiation as suppression of Notch expression or activity blocks differentiation in these cells[102]. Moreover, in 3T3-L1 cells, loss of HES1, a bHLH transcription factor that mediates some of the effects of Notch, impairs adipogenesis and induces expression of a known inhibitor of differentiation, DLK1/PREF1[103]. However, adipocyte differentiation *in vitro* is also blocked when Notch signalling is activated by Jagged or by constitutively active HES1[93].

The "master regulator" of fat cell formation is PPARγ, as it is both necessary and sufficient for adipogenesis; PPARγ is so potent as adipogenic factor that it can drive nonadipogenic cells like fibroblasts and myoblasts to become adipocytes[104,105]. It has been reported that humans with rare loss-of-function mutations in PPARγ have lipodystrophy and severe insulin resistance, confirming the crucial role of this nuclear receptor in adipogenesis, as suggested by murine studies. The bZIP factors CCAAT-enhancer-binding proteins C/EBPα, C/EBPβ, and C/EBPδ are also important inducers of adipogenesis, with C/EBPβ and C/EBPδ acting early in terminal differentiation (Figure 4). Differentiation is promoted by a positive feedback loop between PPARγ and C/EBPα[106,107]; then a second positive feedback loop between PPARγ and C/EBPβ reinforces the decision to differentiate[108]. Many of these factors bind at common genomic "hot spots," with early factors establishing chromatin accessibility at the same locations that will later be bound by downstream factors[109]. Recently, many other transcription factors have been identified that promote or inhibit adipogenesis; most of these induce or repress PPARγ expression[110]. PPARγ, in turn, directly binds to and regulates a huge number of genes that control all aspects of adipocyte metabolism[21]. There has been recent progress in identifying transcription factors involved in adipose determination: an expression screen in embryonic fibroblasts with and without adipogenic potential identified zinc-finger protein Zfp423 as a transcriptional determinant of the adipose lineage[111]. Zfp423 amplifies the effects of BMPs via a SMAD interaction domain inducing adipose lineage commitment. Zfp423 expression in the developing adipocyte is

repressed by the highly related factor Zfp521, which promotes osteogenesis and inhibits adipogenesis through interactions with Ebf1, a transcription factor required for early adipose commitment[112,113]. Another player in the regulation of adipogenic lineage commitment is Tcf7l1, although it acts in a very different manner by responding to confluency and mediating changes in structural proteins that regulate differentiation[114]. The elements of the adipogenic transcriptional cascade are common for most adipose depots, but they differ in some details. For example, mice lacking C/EBPα are generally lipodystrophic but still have mammary fat and brown adipose tissue[115].
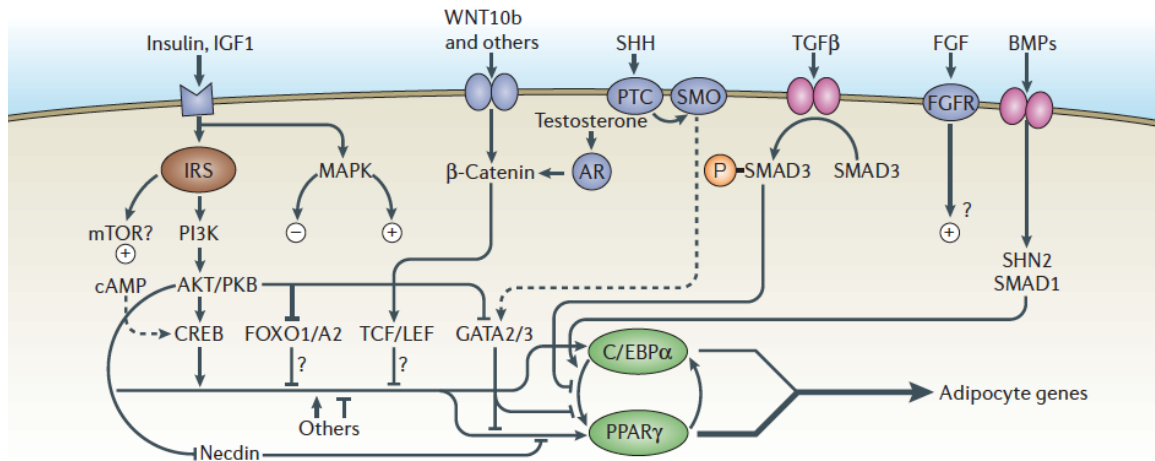
Figure 4: Signals from activators and repressors of adipogenesis are integrated in the nucleus by transcription factors that directly or indirectly regulate expression of peroxisome proliferator-activated receptor γ (PPARγ) and CCAAT-enhancer-binding protein α (C/EBPα). *From Rosen and MacDougald, 2006[93]*

Regarding brown adipose tissue, Ebf2 seems to be particularly important for development of this fat depot, as it recruits PPARγ to unique sites that determine brown adipocyte identity[116]. Interestingly, much of the specialized function of brown adipocytes is controlled by transcriptional cofactors, which do not bind DNA directly but they determine which targets are bound and activated by transcription factors. The most important of these is PGC-1α, a dominant regulator of mitochondrial biogenesis, oxidative metabolism, and thermogenesis in brown fat[117]. PGC-1α exerts its actions on mitochondria and oxidation via interactions with transcription factors like ERRα[118], Nrf-2, PPARα, and PPARγ[119]. Transcription factor partners of PGC-1α that control thermogenesis are still unknown; in fact ablation of PGC-1α reduces the expression of many thermogenic genes, but do not affect the expression of another set of brown fat-selective genes. The necessity to determine other key player in brown fat identity, led to the identification of PRDM16[87]. PRDM16 binds C/EBPβ (and presumably other transcription factors) and recruits the corepressor proteins C-terminal-binding protein 1 and 2, CtBP1 and CtBP2, to prevent gene expression associated with either white fat or muscle[120,121]. Another interesting cofactor is transducin-like enhancer protein 3 (TLE3) because it competes with PRDM16 for PPARγ binding, blocking thermogenesis in favor

of genes more indicative of white adipose tissue. Overexpression of TLE3 in fat impairs brown fat function, while adipose-specific knockouts have the opposite phenotype[122].
The role of noncoding RNAs in adipose differentiation has emerged from recent studies. MicroRNA (miRNA) in particular have been studied in this regard and at least 20 miRNA species have now been shown to affect adipogenesis, though some are not specific for fat and appear to be required for mesenchymal cell differentiation in general[123]. Some miRNAs affect directly adipogenic transcription factors like PPARγ and C/EBPα, whereas others regulate important signaling pathways like insulin-Akt, TGFβ, and Wnt[124]. Other miRNAs have a preferential effect on brown and/or beige adipocyte formation and function, including some that target PRDM16 and C/EBPβ[125].

Oxidative potential of adipose tissues: a mitochondrial issue

The oxidative capacity of organs and tissues is related to their content in mitochondria, the organelles generating the majority of cellular ATP via oxidative phosphorylation (OXPHOS). The role of mitochondria in adipose tissue is most apparent in brown adipose tissue, where flux through the electron transport chain (ETC) generates heat in the process of thermogenesis, a potentially important mechanism regulating systemic metabolism even in adult humans[126-129]. In brown fat, electron transport is greatly accelerated due to tissue-specific expression of the mitochondrial UCP1. UCP1 partly dissipates the proton gradient reducing but not completely abolishing the synthetic activity of the mitochondrial ATPase[127,130-132], thus driving continuous accelerated electron transport to meet ATP demands. UCP1-mediated uncoupling alone, however, can not fully account for the large thermogenic capacity of brown adipocytes in the absence of mechanisms that ensure continuous substrate delivery to the ETC. Thus, brown adipocyte mitochondria also contain high levels of CPT1b, which is critical for the entry of fatty acids into the mitochondria. β-Oxidation, in turn, generates large amounts of reducing equivalents for the ETC.
In contrast, white adipocytes have been described to contain less mitochondria compared with brown adipocytes or muscle. However, mitochondrial density increases dramatically, and mitochondrial remodeling occurs during white adipocyte differentiation[133-135], suggesting that mitochondrial functions are required to support the multiple biological roles of mature white adipocytes. Interestingly, a recent compendium of mitochondrial proteins from 14 different mouse tissues indicates that white adipocyte mitochondria contain a more diverse protein repertoire than mitochondria from heart, skeletal muscle, or brain[136]. Thus, white adipocyte mitochondria appear to be equipped for a broader array of functions compared with mitochondria in tissues that must sustain rapid bursts of energy-requiring processes. Among the mitochondrial functions that may be relevant for white adipose tissue function are the anaplerotic generation of metabolic intermediates for fatty acid synthesis and esterification[137], the maintenance of a robust pathway for the folding and secretion of high abundance circulating proteins such as adiponectin[138], and

interactions between mitochondrial function and components of the insulin signaling pathway[138].

Other contributors to energy metabolism

Skeletal muscle

Skeletal muscle is a high-energy demand tissue, rich in mitochondria that sustain the high oxidative request imposed on this tissue by contraction. Mitochondria play a critical role in providing sufficient levels of ATP needed; this high-level requirement for ATP by sarcomeres has likely contributed to the distinct subsarcolemmal and sarcomere-associated populations of mitochondria in muscle. Moreover, muscle cells must maintain metabolic flexibility, defined as the ability to rapidly modulate substrate oxidation as a function of ambient hormonal and energetic conditions. For example, healthy muscle tissue predominantly oxidizes lipid in the fasting state, as evidenced by low respiratory quotient (RQ), with subsequent transition to carbohydrate oxidation (increased RQ) during the fed state. Availability of fuels, particularly lipids, and capacity to oxidize them in the mitochondria are also critical for sustained exercise. Thus, mitochondrial functional capacity is likely to directly affect muscle metabolic function and, because of its large contribution to total body mass, to have a significant impact on whole-body metabolism. Skeletal muscle is the largest insulin-sensitive organ in humans, accounting for more than 80% of insulin-stimulated glucose disposal. Thus, insulin resistance in this tissue has a major impact on whole-body glucose homeostasis. Indeed, multiple metabolic defects have been observed in muscle from insulin-resistant but normoglycemic subjects at high risk for diabetes development, including reduced insulin-stimulated glycogen synthesis[139-141], alterations in insulin signal transduction[142]; and increased muscle lipid accumulation[143]. Although it remains unclear whether any of these defects plays a causal role in insulin resistance, intramuscular lipid excess strongly correlates with the severity of insulin resistance, even after correction for the degree of obesity[143], and has been observed in muscles of multiple fiber types[144]. Moreover, lipid excess has been linked experimentally to induction of insulin resistance[145] and alterations in insulin signal transduction[146-148].

Thus, one possible mechanism by which impaired mitochondrial function might contribute to insulin resistance is through altered metabolism of fatty acids. Increased tissue lipid load, as observed in obesity, and/or sustained inactivity, may lead to the accumulation of fatty acyl coenzyme A (CoA), diacylglycerols, ceramides, products of incomplete oxidation, and ROS, all of which have been linked experimentally to reduced insulin signaling and action[145-151]. Additional mechanisms potentially linking impaired mitochondrial oxidative function to insulin resistance include reduced ATP synthesis for energy-requiring functions such as insulin-stimulated glucose uptake, abnormalities in calcium homeostasis (necessary for exercise-induced glucose uptake)[152-154] and reduced ATP production during exercise[155], potentially contributing to reduced aerobic capacity, muscle weakness, and decreased voluntary exercise.

Liver

The liver plays a central, unique role in carbohydrate, protein, and fat metabolism. It is critical for maintaining glucose homeostasis during fuel availability, via storage of glucose as glycogen or conversion to lipid for export and storage in adipose tissue, and in the fasting state, via catabolism of glycogen, synthesis of glucose and ketogenesis. In turn, these responses are regulated by the key hormones, insulin and glucagon, which modulate signaling pathways and gene expression, leading to inhibition or stimulation of glucose production, respectively.

Recent studies in humans have highlighted the importance of disordered hepatic metabolism, including inappropriately increased hepatic glucose production, hyperlipidemia, and lipid accumulation, in both obesity and type 2 DM[156]. Similarly, data generated in rodent models also support an important role for the liver in diabetes pathogenesis. Liver-specific insulin receptor knockout (LIRKO) mice develop insulin resistance, glucose intolerance, impaired insulin suppression of hepatic glucose production, and altered patterns of hepatic gene expression[157]. Interestingly, these mice are also dyslipidemic and susceptible to atherosclerosis[158]. Given the diverse array of unique metabolic functions centered in the liver, it is not surprising that ultrastructure and function of hepatic mitochondria are distinct from that of muscle. Electron microscopy demonstrates that mitochondrial area is 44% lower in liver than in heart[159], with smaller size, fewer cristae, and lower matrix density. Protein expression of multiple OXPHOS components and Tfam and citrate synthase activity are also lower in liver (i.e., 7% that of cardiac muscle)[160]. Despite lower OXPHOS capacity, state 3 respiration and respiratory control ratio are equivalent in liver and muscle. By contrast, the content of mtDNA is actually higher in the liver than in other tissues. Impairments in mitochondrial number and/or oxidative function could potentially affect multiple cellular functions within hepatocytes, both directly (e.g., reduced ATP generation, alterations in oxidative stress, reduced capacity for fatty acid oxidation) and indirectly, via effects on energy-requiring processes, including gluconeogenesis, synthesis of urea, bile acids, cholesterol, proteins and detoxification.

Hepatic lipid accumulation may result when adipose lipid storage capacity is exceeded, as in obesity or adipocyte dysfunction (e.g., lipodystrophy)[161]. Alternatively, lipid accumulation may reflect an additional imbalance between *de novo* hepatic lipogenesis and mitochondrial oxidative metabolism. Interestingly, hepatic lipid accumulation is also a robust predictor of, not only hepatic, but also muscle and adipose insulin sensitivity[162,163]. Conversely, modest weight loss (about 8 kg) normalizes intrahepatic lipids in subjects with type 2 DM, in parallel with normalization of hepatic insulin sensitivity, even in the absence of changes in intramyocellular lipid accumulation or circulating adipocytokines[164]. Although these data highlight an intimate relationship between obesity, intrahepatic lipid metabolism, and insulin sensitivity in humans, mechanisms responsible for these links remain unclear. One possibility is that excessive hepatic lipid accumulation may play a central, pathogenic role in insulin resistance. This hypothesis comes from experimental

lipid loading, which can induce hepatic insulin resistance. Transgenic mice expressing lipoprotein lipase in the liver have a 2-fold increase in hepatic triglyceride content and are insulin resistant[165]. A second possibility is that hepatic insulin resistance itself contributes to alterations in mitochondrial oxidative capacity. Indeed, a recent paper demonstrated that mice with hepatic insulin resistance due to deletions of the major insulin receptor substrates (IRS-1 and IRS-2) have impaired mitochondrial function and biogenesis, as demonstrated by reduced NADH oxidation, reduced ATP production rates, reduced numbers of mitochondria per cell, reduced fatty acid oxidation, and increased hepatic triglyceride accumulation[166]. Mitochondrial dysfunction was reversed by deletion of Foxo1. These data indicate that normal insulin signaling, which inhibits Foxo1, is required for maintenance of normal mitochondrial function in this model. Finally, these data indicate that hepatic lipid accumulation and insulin resistance are intimately linked with mitochondrial oxidative dysfunction.

Epigenetics

In recent years the scientific community has witnessed a growing interest in epigenetics, as demonstrate by the increasing number of publications on this topic. Epigenetic modifications play a role in many DNA-related processes including transcription, recombination, DNA repair and replication[167]. Epigenetic modifications also regulate several important physiological and pathological processes such as embryonic development[168], aging[169] and cancer[170]. However nowadays, the importance of epigenetics has been recognized in many other fields relevant to human health, such as inflammation[171], obesity[172], insulin resistance, type 2 diabetes mellitus[173], cardiovascular[174], neurodegenerativ[175] and autoimmune diseases[176]. Epigenetics can be defined as a set of processes and mechanisms that regulate gene activity, by modifying chromatin structure without changes in DNA sequence. Nucleosomes, the typical structure formed by histones in which the genomic DNA is folded in eukaryotic cells, are building blocks of the dynamic structure called chromatin[177]. During activation of gene transcription, chromatin adopts a locally accessible and transcriptionally active form referred to as euchromatin, while highly condensed and transcriptionally less active genetic material is known as heterochromatin[178]. The main epigenetic modifications include DNA methylation and histone modifications[179]. Amino acid residues on the histone tails are modified by post-translational acetylation, methylation, ADP-ribosylation and phosphorylation leading to significant changes in the chemical structure of the histone protein tails: acetylation of lysine residues of histone tails carried out by histone acetyltransferases (HATs) increases the distance between DNA and histones and the accessibility of transcription factors to gene promoter regions, while deacetylation by histone deacetylases (HDACs) induces chromatin packaging and reduces the accessibility of transcription factors to local chromatin regions[180] (Figure 5).
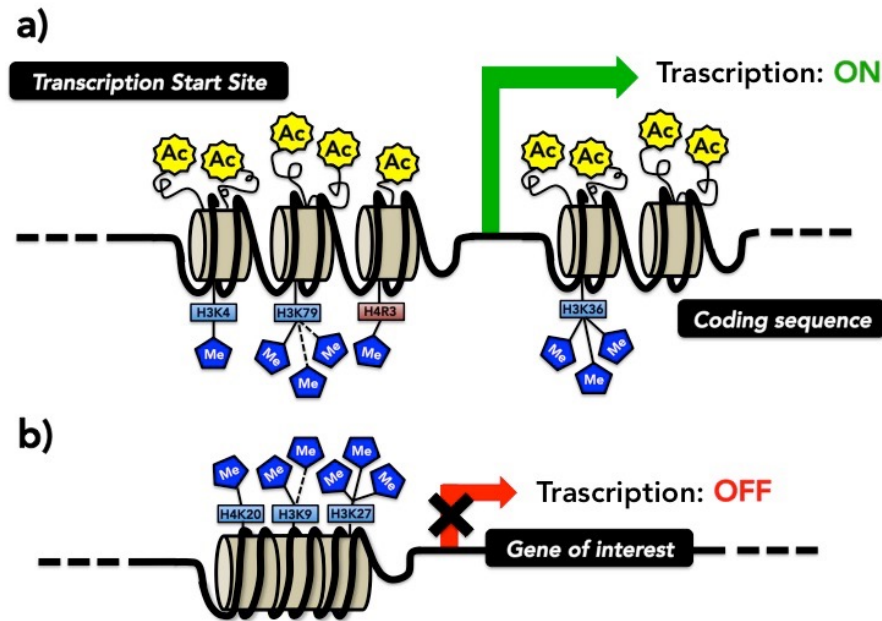
Figure 5: Epigenetic regulators control chromatin remodeling, a) Histone acetylation and methylation at specific lysine or arginine residues (H3K4, H3K79, H3K36 and H4R3) opens chromatin and activates gene transcription, b) Histone methylation at H4K20, H3K9 and H3K27 silences gene transcription.

Histone deacetylases

Mammalian HDACs are listed into four classes based on their homology with yeast HDACs (Figure 6)[181]. Class I HDACs are ubiquitously expressed and are mainly localized in the nuclear compartment where they exert the most relevant histone deacetylase activity. Class II HDACs localize in the cytoplasm, shuttling into the nucleus in response to specific cellular signals. Class IIa HDACs are characterized by post-translational regulation such as phosphorylation that determines their cytosolic localization, whereas dephosphorylation of Class IIa HDACs enables their translocation to the nucleus[182-185]. Class IIa HDACs feature only minimal histone deacetylase activity due to a swap of a key tyrosine residue in the catalytic domain with a histidine[186]; nonetheless, they act as scaffold molecules to recruit class I HDACs. Class IIb HDACs are localized in the cytoplasm and act mainly on non-histone substrates such as cytoskeletal and transmembrane proteins[181]. Class III HDACs, also known as sirtuins, are sensitive to changes in the intracellular NAD+/NADH ratio and they rely upon NAD+ hydrolysis for their deacetylase activity. In mammals, sirtuins regulate several functions, ranging from the control of cellular stress to energy metabolism[187]. Rodgers and collaborators[188] investigated the molecular mechanisms responsible for the adaptive metabolic response to fasting and found that SIRT1 is involved in the metabolic control in mammals. These authors showed that in the fasted state, SIRT1 is induced in the liver and deacetylates PPARγ coactivator 1α (PGC-1α) at specific lysine residues in a NAD+-

dependent manner: deacetylated PGC-1α is more active and transactivates the transcription of genes encoding enzymes of fatty acid b-oxidation and gluconeogenesis. In fact, knock-down of SIRT1 in the liver leads to reduced glucose production and fatty acid oxidation in the liver, under fasting conditions[189]. These studies demonstrate that SIRT1 regulates metabolic adaptation and that PGC-1α mediates most of SIRT1 effects. Finally, HDAC11 is the only member of class IV HDACs but its function is still poorly understood.

Class	Protein domain	Members
Class I	Deacetylase catalytic domain Phosphorylation sites (serine residues) at C terminus	HDAC1 HDAC2 HDAC3 HDAC8
Class IIa	Deacetylase catalytic domain Phosphorylation sites (serine residues) at N terminus Myocyte enhancer factor binding sites Binding sites for 14-3-3 chaperone protein	HDAC4 HDAC5 HDAC7 HDAC9
Class IIb	Deacetylase catalytic domain Zinc finger domain or leucine rich region	HDAC6 HDAC10
Class III (Sirtuins)	Deacetylase catalytic domain, requiring NAD^+ as cofactor	SIRT1 SIRT2 SIRT3 SIRT4 SIRT5 SIRT6 SIRT7
Class IV	Deacetylase catalytic domain	HDAC11

Figure 6: Classification of mammalian HDACs. *Adapted from Ferrari, 2012[167]*

Histone deacetylases regulate energy metabolism

In recent years it has become clear that epigenetic changes, consequent to disruption of HAT or HDAC activity, are associated to several pathological conditions, such as cancer[190], insulin resistance and diabetes. One of the first evidences of the involvement of HDACs in the pathogenesis of diabetes is a genome wide analysis showing significant linkage of HDAC2 located in the region 6q21 with both type 1 and type 2 diabetes loci[191-193]. No other mutations of HDACs have been so far reported, also for other diseases like cancer[194] in which epigenetic regulation has been extensively studied in the last decade. Furthermore, several studies revealed that HDACs, in particular HDAC4 and HDAC5, regulate the expression of metabolic genes in skeletal muscle[195-197]. Interestingly, a recent study by Gao and colleagues[198] emphasized the involvement of HDACs in energy expenditure. They reported that sodium butyrate, a short chain fatty acid often found in the diet that inhibits class I and class II HDAC activity, improves metabolic dysfunction in diet-induced obese mice. These authors observed that supplementation with sodium butyrate increased energy expenditure and fatty acid

oxidation, and protected mice from high fat diet-induced insulin resistance. Sodium butyrate also enhanced thermogenic function and reduced fat accumulation and size of brown adipocytes. In skeletal muscles sodium butyrate increased the number of oxidative fibers and enhanced mitochondrial function. Indeed, in vivo butyrate is an activator of PGC-1α, the master regulator of mitochondrial biogenesis. Based on these results, the hypothesis is that butyrate, by inhibiting histone deacetylases, opens chromatin in the PGC-1α gene promoter thus inducing the transcription of this gene. However, butyrate is known to affect energy metabolism via other mechanisms[199], as it has been shown to affect adipogenesis via HDAC-independent mechanisms[181]. Therefore it will be necessary to perform ad hoc studies with more specific inhibitors to better address the role of HDACs in energy metabolism in the context of obesity and type 2 diabetes.

Another strong evidence demonstrating that epigenetic modifications regulate energy metabolism arises from a recent study by Yamamoto et al[200], in which the authors showed that nuclear receptor corepressor 1 (NCoR1) is a regulator of muscle mass and its oxidative capacity. NCoR1 is a transcriptional corepressor that participates in the formation of repressive complexes, together with several HDACs, in particular HDAC3, HDAC4, 5, 7 and 9[201]. These authors demonstrated that muscle-specific loss of NCoR1 in mice (NCoR1skm-/-) increase muscle mass, locomotor activity (i.e., mice run for a significantly longer time and distance) and oxygen consumption, with a reduction in the respiratory exchange ratio (RER), suggesting that they preferentially use fat as energy source. In line with these observations, they detected increased mitochondrial content and activity in the gastrocnemius of NCoR1skm-/-, with concomitant reduction of the number of glycolytic MyHC2b-positive fibers and increased number of oxidative MyHC2x- and 2a- positive fibers. Interestingly, these authors showed that the expression of MEF2 family members increases in skeletal muscle of NCoR1skm-/- mice and negatively correlates with NCoR1 levels. It should be mentioned that MEF2 could be acetylated and activated by the acetyltransferases p300/CBP, whereas HDAC3[202], HDAC4, 5, 7 and 9[181,203] and SIRT1[204] interact with MEF2 and prevent its activation. Thus the absence of NCoR1 induces acetylation and activation of MEF2, leading to induction of MEF2 targets and to increased muscle mass. Moreover, NCoR1skm-/- mice show higher expression of genes related to mitochondrial respiration and fatty acid catabolism, whose expression in muscle is controlled by PPAR and estrogen related receptor (ERR) families[205]. It should be noted that NCoR1 is recruited to PPAR responsive elements (PPREs) in the Ucp3 promoter and to the extended nuclear receptor half-sites (NR1/2) that binds members of ERR family in the pyruvate dehydrogenase kinase 4 (Pdk4) promoter (Figure 5). In addition, histone 4 is hyperacetylated on these promoters in the absence of NCoR1, suggesting that under this condition the coactivator PGC-1α activates the transcription of these genes[206]. For this reason, loss of NCoR1 phenocopies PGC-1α overexpression, in that both models show induction of mitochondrial fatty acid b-oxidation and improvement of exercise capacity[207]. A recent study by Li and collaborators[208] demonstrated that NCoR1 also plays a key role in adipose tissue. PPARγ is highly expressed in this tissue and is a determinant of adipocyte

differentiation, as well as a regulator of insulin sensitivity and adipokine secretion[209-212]. However, the transcriptional regulation exerted by PPARγ depends on the multi-protein coregulatory complexes recruited on target gene promoters and NCoR1 is one of the most important corepressors also in this tissue. In the same study, they found that adipocyte-specific NCoR1 knockout (NCoR1 AKO) mice become more obese than control mice when fed with high fat diet, due to increased subcutaneous and visceral adipose tissue mass. In epididymal white adipose tissue of NCoR1 AKO mice they detected increased expression of typical adipogenic genes such as *Fas*, *Acc*, *Srebp1c*, *Scd1* and *Scd2*. Nonetheless, inflammation of adipose tissue is reduced, indicating improved functionality of this tissue and enhanced systemic insulin sensitivity. In adipose tissue, insulin promotes storage of free fatty acids into triglycerides and, consistently, authors observed reduced circulating levels of free fatty acids in NCoR1 AKO mice, suggesting a reduction of lipolysis in adipose tissue. Since it has been demonstrated that down-regulation of NCoR1 expression in 3T3-L1 cells enhances adipocyte differentiation in part by increasing PPARγ transcriptional activity[213], Li and collaborators focused on the repressive effect of NCoR1 on PPARγ[208]. In this regard it should be mentioned that Choi et al.[214] showed that high fat diet induces phosphorylation of PPARγ at serine 273, which dysregulates the expression of many genes of the adipogenic program. On the contrary, PPARγ agonists prevent phosphorylation at this site and allow the functional transcriptional cascade in adipose tissue. Consistently, in adipose tissue from NCoR1 AKO mice serine 273 phosphorylation decreases, leading to increased expression of typical markers of adipocyte functionality.
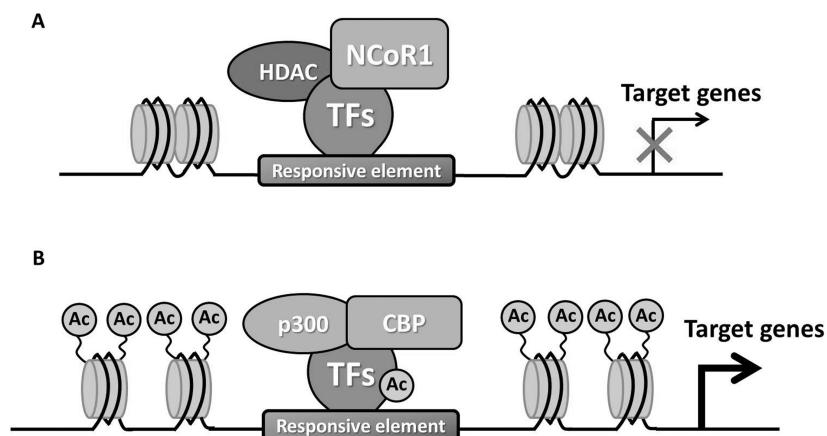
Figure 7: NCoR1 modulates transcription of oxidative genes in skeletal muscle; a) NCoR1 is recruited on the responsive element in the promoter of PPAR and ERR target genes forming a repressive complex and inhibiting the expression of these genes; (b) The ablation of NCoR1 leads to HDACs dissociation and to the recruitment of the acetyltransferases p300/CBP with the consequent derepression of target gene transcription. *From Ferrari, 2012*[167]

A recent paper by Weems and coworkers[215] demonstrated that class II HDACs regulate gene expression in adipocytes as a result of adrenergic activation. The authors observed that HDAC5 plays a central role in repression of the insulin-dependent glucose

transporter GLUT4 transcription in preadipocytes. Since it is known that repression of GLUT4 expression is correlated with insulin resistance in adipose tissue, this paper underlines the importance of HDACs in metabolic regulation and adipose tissue functionality. These authors also detected that, in the absence of HDAC5, other class II HDACs, including HDAC4 and HDAC9, may exert a redundant function. Moreover they demonstrated that cAMP-dependent down-regulation of GLUT4 mRNA expression in vivo is mediated by nuclear localization of HDAC4 and HDAC5: The Glut4 promoter contains an LXRE-binding site, and the cAMP signalling increases the recruitment of class II HDACs in this region, ultimately reducing Glut4 expression. HDACs also play a role in cardiac lipid metabolism and function. Recent evidence suggests that HDACs are important metabolic regulators in the heart. Postnatal inactivation of HDAC3 in both cardiac and skeletal muscle do not show cardiac dysfunction of mice fed with normal chow diet, whereas mice fed with high fed diet develop hypertrophic cardiomyopathy and heart failure. The reduced expression of genes encoding enzymes involved in fatty acid oxidation and lipid metabolism, typically observed in these mice, do not make them able to cope with the dietary lipid overload. These results demonstrate that efficient lipid catabolism is needed to maintain myocardial metabolic homeostasis and physiology, especially when fatty acids are the main fuel sources[216]. These results demonstrate that HDAC3 is required for cardiac metabolic regulation in response to a lipid enriched diet and that loss of HDAC3 compromises the ability of cardiac mitochondria to respond to nutritional changes and lipid overload.

Histone deacetylases inhibitors

Nowadays several HDAC inhibitors have been described; usually they are classified according to their chemical structure as short-chain fatty acids, hydroxamic acids, benzamides, ketones, and cyclic peptides with a pendant functional group. Unfortunately, most HDAC inhibitors, such as suberoylanilide hydroxamic acid (SAHA) and trichostatin A (TSA), inhibit HDAC isoforms non-specifically. Others, such as the benzamide MS-275, are more selective for class I HDACs. The therapeutic applications of HDAC inhibitors are multiple: in 2006, the US FDA approved SAHA for cutaneous manifestations of T-cell lymphoma. Many evidences suggest that HDAC inhibitors can be considered an interesting approach in cancer therapy. The DNA damage response is in fact modulated by the acetylation status of histone and non-histone proteins and HDACs protect cancer cells from genotoxic insults. Thus, HDAC inhibitors can silence DNA repair pathways, inactivate nonhistone proteins that are required for DNA stability and induce reactive oxygen species and DNA doublestrand breaks[217]. Recently, since HDACs play an important role in control of several cardiac events such as hypertrophy[218], autophagy[219], contractility[220] HDAC inhibitors could represent a novel and promising therapy in patients with heart failure[221]. Moreover, other recent evidences underline the importance of tubulin acetylation mediated by HDAC6 in the development of Huntington[222] and Parkinson diseases[223]. Based on these results, the HDAC class II

selective inhibitors have been theorized as new avenues for therapeutic intervention in some neurodegenerative disorders[224]. Given the role of different HDACs in metabolic regulation, it is possible that in the future some specific inhibitors may find some clinical applications in lipid metabolic disorders.

Histone deacetylases and adipocyte differentiation

Lately, researchers have been trying to define the HDAC modification events regulating white pre-adipocyte proliferation and differentiation[225,226]. HDACs function in the related gene regulation signal pathways and networks of adipogenesis[226-228]. However, the actual role of some HDACs in adipogenesis is still unclear, since published literature provided evidences for both activating and repressing effect of HDACs in adipocyte differentiation. In a recent study, the canonical Class I HDACs 1 and 2 were shown to have a novel and unexpected role in the control of adipogenesis[226]. In this study, the authors used genetic deletion of both Hdac1 and Hdac2 in mouse embryonic fibroblasts and demonstrated a decrease in lipid accumulation following adipogenic induction of MEFs. Notably, deletion of each individual class I HDAC did not have an effect on the differentiation process, supporting the notion that HDAC1 and HDAC2 have redundant functions in this cellular process. Moreover the authors reported that treatment of 3T3-L1 preadipocytes with the pan-HDAC inhibitors TSA, suberoylanilide hydroxamic acid (SAHA), or Scriptaid, led to a block in differentiation and adipogenesis, following induction[226]. Conversely treating 3T3-L1 cells with HDACs inhibitors sodium butyrate and valproic acid increased adipocyte differentiation[227,229]. The Class IIa specific inhibitor MC1568 was also recently shown to attenuate PPARγ-induced adipogenesis in 3T3-L1 cells, while the Class I-selective inhibitor MS275 blocked adipogenesis completely in this cellular model[230], consistent with other findings with TSA, SAHA and other HDAC inhibitors[231-233]. Interestingly a study by Chatterjee and coworkers demonstrated that class IIa HDAC9 has been implicated as a negative regulator in the control of adipogenesis[225]. In this study, out of the eleven HDACs examined, only HDAC9 mRNA was down-regulated during adipocyte differentiation. Downregulation of HDAC9 occurs relatively early and precedes the increase of expression of adipogenic genes during differentiation, suggesting that perhaps HDAC9 activity must decreased in order for adipogenesis to proceed. Pre-adipocytes from HDAC9 gene knock out mice exhibited accelerated adipogenic differentiation, whereas HDAC9 overexpression in 3T3-L1 pre-adipocytes suppressed adipogenic differentiation, demonstrating the direct role of HDAC9 as a negative regulator of adipogenesis.

Literature suggested also HDAC3 as potential regulator of adipogenesis. It is in fact known that HDAC3 binds the NCoR1/SMRT co-repressor complex[234]. Moreover Yu and colleagues demonstrate that NCoR1 and SMRT decrease Pparγ transcriptional activity and repress 3T3-L1 adipogenesis, while Fajas and collaborators[235] reported that HDAC3 by interacting with retinoblastoma forms a complex that inhibits Pparγ and adipocyte differentiation. These evidences suggested HDAC3 as a relevant regulator of

adipogenic program. In support of this idea, it has recently been reported that selective inhibition of HDAC3 promotes ligand-independent Pparγ activation by protein acetylation[236].

Aim of the study

Obesity is a severe metabolic disease, strictly associated to insulin resistance and type 2 diabetes. Maintenance of glucose homeostasis depends on a complex interplay between the insulin responsiveness of skeletal muscle, liver, adipose tissue and glucose-stimulated insulin secretion by pancreatic beta cells. Defects in these organs are responsible for insulin resistance and progression to hyperglycemia. The westernization of the diet and sedentary lifestyle in the last decades increased incidence of obesity, characterized by uncontrolled expansion of an inflamed and not functional adipose tissue. As a consequence of this dis-metabolic state, the whole body homeostasis is disrupted, leading to several changes in the systemic milieu including the onset of hyperinsulinemia, elevated circulating free fatty acids and triglycerides, hyperglycemia, and the activation of systemic immune system, typical symptoms of type 2 diabetes. Thus the development of this pathological state compromised the functionality of all the important metabolic organs, such as liver, adipose tissues and skeletal muscle. In recent years, several studies highlighted the importance of epigenetics in metabolic regulation and in the pathophysiology of metabolic disorders. There is increasing evidence that epigenetic modifications are sensitive to environmental and nutritional cues. In fact, abnormalities in epigenetic regulation have been associated with multiple metabolic disorders, such as cardiovascular disease, obesity, and type 2 diabetes. These conditions are generally associated with defective lipid metabolism and decreased oxidative gene expression in key metabolic tissues.

Epigenetic modifications allow cells to acquire heritable changes in gene function without inherent changes in the underlying coding sequence. In concert with differential transcription, epigenetic regulation enables identical cells to adopt multiple phenotypes.

Acetylation of histone tails is one of the most common forms of chromatin modification. It is a dynamic process controlled by two families of enzymes. On the one hand, histone acetyltransferases (HATs) acetylate lysine residues of histones, thereby relaxing chromatin and enhancing entry of transcriptional complexes. On the other hand, histone deacetylases (HDACs) regulate gene transcription by removing the acetyl group from these lysine residues, thus compacting chromatin and making it less accessible to transcriptional activators. HDACs can also act upon transcription factors and cofactors to regulate their activity and they are recruited along with transcriptional coregulators to form repressive complexes that assemble at the promoters of target genes. Eighteen mammalian HDACs have been described; they are divided into four classes based on their homology to yeast HDACs.

It has been demonstrated that HDACs play a role in the development and in the physiology of skeletal muscle, adipose tissue and liver. Furthermore, preliminary results obtained in our laboratory showed that in db/db mice, a genetic model of type 2 diabetes and obesity, class I HDAC inhibitor MS275 promotes oxidative metabolism, reduces body weight, increases energy expenditure, and enhances insulin sensitivity (data not shown). These effects are due to enhanced mitochondrial biogenesis in skeletal muscle, consistent with upregulation of *Pgc-1α*, the master regulator of mitochondrial biogenesis (Figure 8a), and increased functionality and oxidative capacity of adipose tissues as result

of activation of a Pgc-1α-Pparγ axis (Figure 8b). Moreover class I HDAC inhibitor MS275 causes a dramatic "browning" of white adipose tissue, as shown by higher expression of *Ucp1* in visceral fat (Figure 8c).
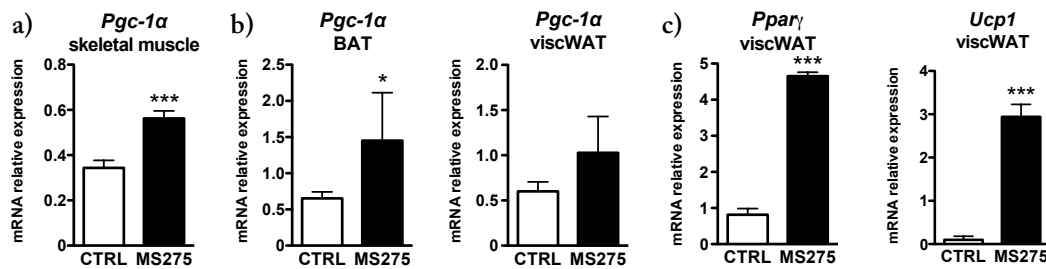

Figure 8: a) Class I HDAC inhibitor induces *Pgc-1α* expression in skeletal muscle and adipose tissues; **b)** Class I HDAC inhibitor upregulates the master regulator of adipocyte differentiation *Pparγ* in visceral WAT and activates "browning" of this fat depot, by inducing *Ucp1* expression. Statistical analysis: Student's t test, *p<0.05, ***p<0.001.

We used a cellular model of skeletal muscle, C2C12 myotubes, as a tool to understand the molecular events triggered by treatment with the class I HDAC inhibitor. We confirmed also in this cellular model that MS275 upregulates *Pgc-1α* expression (Figure 9a, white bars). Since we detected upregulation of Pgc-1α in cells and mice treated with the class I selective HDAC inhibitor, we hypothesized that this transcriptional coactivator may play a role in the effects exerted by MS275. In fact Pgc-1α silencing leads to a loss of responsiveness to the class I HDAC inhibitor in term of expression of Pgc-1α-regulated genes (Figure 9b).
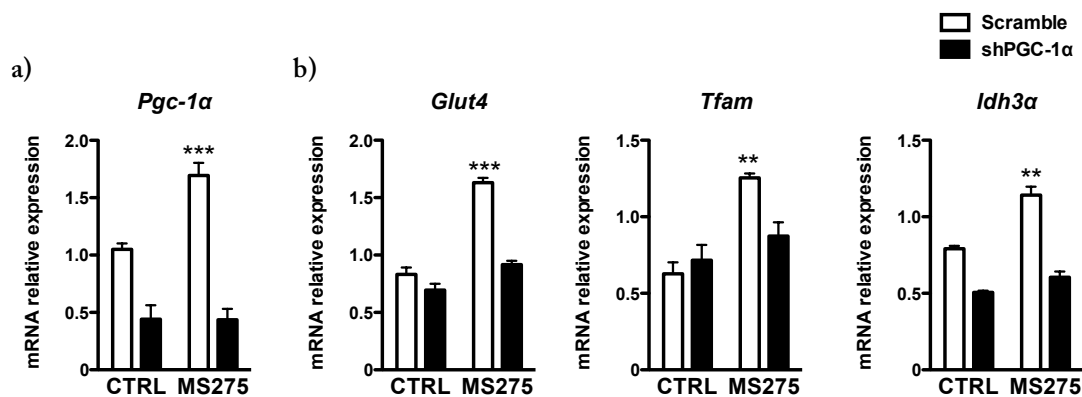
Figure 9: a) MS275 upregulates *Pgc-1α* and its main targets in C2C12 myotubes; **b)** Silencing of Pgc-1α determine a loss of responsiveness to MS275 treatment. Statistical analysis: Student's t test, **p<0.01, ***p<0.001.

It is known that *Pgc-1α* expression is regulated by HDAC1 and HDAC3, via CREB [237]and MEF2[202] binding sites, respectively, located in the Pgc-1α promoter. However, we found that only Hdac3 silencing in C2C12 cells mimics the effects of MS275 (Figure 10), suggesting this HDAC isoform as key player in the mechanism of the class I selective HDAC inhibitor.

Figure 10: Silencing of Hdac3 but not of Hdac1 mimic the effects of the class I selective HDAC inhibition. Statistical analysis: Student's t test, *p<0.05.

Based on these preliminary results and on the published literature the goals of my PhD project were the investigation of the molecular mecha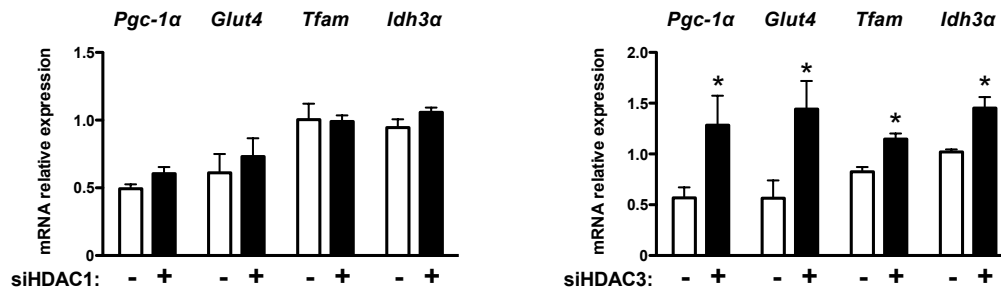nisms of class I selective HDAC inhibitor in skeletal muscle and adipose tissues, and the assessment of the contribution of these two organs to the phenotype induced by class I HDAC inhibition. To solve these open questions I used both *in vivo* and *in vitro* approaches: I have investigated the effect of MS275 in a mouse model of diet-induced obesity that recapitulates the classical features of human obesity. In parallel I have examined in depth MS275 effect in different cellular models, including C2C12 myotubes and several adipose cell lines (primary brown adipocytes, 3T3-L1 preadipocytes and C3H10T1/2 mesenchymal stem cells). These approaches, integrated with preliminary results, lead us toward the hypothesis that HDAC3 could act as a key metabolic regulator in both skeletal muscle and adipose tissue. For this reason I also have generated two tissue-specific knock out models: skeletal muscle Hdac3 knock out (H3smKO) and adipose tissue Hdac3 knock out (H3atKO). By feeding these mice high fat diet I will characterize the metabolic effect of tissue specific deletion of HDAC3. Our study will improve the knowledge about the epigenetic regulation of metabolism in the context of diabetes and obesity.

Materials and Methods

Cell cultures

C2C12 myotubes

C2C12 myoblast are a subclone (produced by H. Blau, et al) of the mouse myoblast cell line established by D. Yaffe and O. Saxel. The C2C12 cell line differentiates rapidly, forming contractile myotubes and producing characteristic muscle proteins.
Manteinance medium: Dulbecco's Modified Eagle's Medium. To make the complete growth medium, add fetal bovine serum to a final concentration of 10%, 1% L-Glutamine (Life Technologies) and 1% Pen/Strep (Life Technologies).
Differentiation medium: Dulbecco's Modified Eagle's Medium. To make the complete growth medium, add horse serum to a final concentration of 2%, 1% L-Glutamine and 1% Pen/Strep.
Temperature: 37.0°C

Subculturing protocol: remove and discard culture medium. Briefly rinse the cell layer with 0.25% (w/v) Trypsin- 0.53mM EDTA solution (Life technologies) to remove all traces of serum containing trypsin inhibitor. Add 3.0 ml of Trypsin-EDTA solution to flask and observe cells under an inverted microscope until cell layer is dispersed (usually within 5-7 minutes). Note: To avoid clumping do not agitate the cells by hitting or shaking the flask while waiting for the cells to detach. Cells that are difficult to detach may be placed at 37°C to facilitate dispersal. Add 7.0 ml of complete growth medium and aspirate cells by gently pipetting. Add appropriate aliquots of the cell suspension to new culture vessels. Inoculate at a cell concentration between 1.5×10^5 and 1.0×10^6 viable cells/75 cm2. Incubate cultures at 37°C.
Medium Renewal: Every two days.

Differentiation protocol: Plate cells at the final concentration of 70000 cells/ml in 24, 12- or 6-well plates. Two days after plating, cells become confluent. Switch the medium with the differentiation medium and renew it every two days for 4 days. At the fifth day cells are completely differentiated.

Treatment with HDAC inhibitor: After 5 days from the beginning of differentiation cells treated for 24 hours (ChIP assay) or for 48 hours (protein expression analysis) with vehicle DMSO or with 5µM MS275 (provided by professor Antonello Mai, Univeristà di Roma "La Sapienza").

Primary brown adipocytes

Primary brown adipocytes were isolated from the stromal vascular fraction (SVF) of brown adipose tissue from 0-3 days old pups (C57BL6/J). From 1 pup is possible to obtain a suitable number of cells to cover 6 wells of a 12-well plate.
Growth medium: Dulbecco's Modified Eagle's Medium. To make the complete growth medium, add fetal bovine serum to a final concentration of 20%, 1% L-Glutamine, 1% Pen/Strep, 20mM Hepes.

Induction medium: Dulbecco's Modified Eagle's Medium. To make the complete growth medium, add fetal bovine serum to a final concentration of 10%, 1% L-Glutamine, 1% Pen/Strep, 20mM Hepes, 1nM triiodotyronine, 5 µg/ml insulin, 5mM 3-isobutyl-1-methylxanthine (IBMX, Sigma Aldrich), 2 µg/ml dexamethasone (Sigma Aldrich), 0.25mM indomethacin (Sigma Aldrich).

Differentiation medium: Dulbecco's Modified Eagle's Medium. To make the complete growth medium, add fetal bovine serum to a final concentration of 10%, 1% L-Glutamine, 1% Pen/Strep, 20mM Hepes, 1nM triiodotyronine, 5 µg/ml insulin (insulin sodium salt, Sigma Aldrich).

Isolation buffer: 3M NaCl, 0.154M KCl, 100mM CaCl2, 50mM Glucose, 1M HEPES, 1% Pen/Strep, 4% Bovin Serum Albumin (BSA, Sigma Aldrich)

Collagenase A (Roche): dissolved in isolation buffer.

Isolation protocol: Remove brown adipose tissue (BAT) from the inter-scapular region of 0-3 days old pups and put it a sterile plate, containing 500ul of sterile PBS 1X. Cut the tissue with sterile blade and collect the material from 2-3 mice in a 2ml eppendorf tube. Add 500ul of collagenase A (1.5 mg/ml). Vortex the tube and put in agitation for 40 min at 37°C. While cells are digesting, put 1ml/well of growth medium in 12-well plates. Filter the cellular suspension with 70µm cell strainer (BD Biosciences). Adjust the volume, based on the number of wells to plate. Aliquot 1ml/well of cellular suspension in 12-well plates previously prepared. Incubate at 37°C.

Differentiation protocol
After 24 hours renew growth medium in order to eliminate debris. When cells reach 75-80% of confluence, replace medium with induction medium for 48 hours. Replace medium with differentiation medium, and renew it every 48 hours till the cells are fully differentiated to mature brown adipocytes.

Treatment with HDAC inhibitor: After 7 days from the beginning of differentiation cells were treated for 24 hours (mRNA expression analysis), for 48 hours (oxygen consumption analysis) or for 60 hours (mitochondrial DNA quantification) with vehicle DMSO or with 1µM MS275.

C3H10T1/2 mesenchymal stem cells

C3H/10T1/2, Clone 8 was isolated by C. Reznikoff, D. Brankow and C. Heidelberger in 1972 from a line of C3H mouse embryo cells.

Manteinance medium: Dulbecco's Modified Eagle's Medium. To make the complete growth medium, add fetal bovine serum to a final concentration of 10%, 1% L-Glutamine (Life Technologies) and 1% Pen/Strep (Life Technologies).

Induction medium: Manteinance medium supplemented with 5 µg/ml insulin, 5mM 3-isobutyl-1-methylxanthine (IBMX, Sigma Aldrich), 2 µg/ml dexamethasone (Sigma Aldrich), 5µM rosiglitazone (Cayman Chemicals).

Differentiation medium: Manteinance medium supplemented with 5 µg/ml insulin.

Temperature: 37.0°C

Subculturing protocol: remove and discard culture medium. Briefly rinse the cell layer with 0.25% (w/v) Trypsin- 0.53mM EDTA solution (Life technologies) to remove all traces of serum which contains trypsin inhibitor. Add 3.0 ml of Trypsin-EDTA solution to flask and observe cells under an inverted microscope until cell layer is dispersed (usually within 5-7 minutes). Note: To avoid clumping do not agitate the cells by hitting or shaking the flask while waiting for the cells to detach. Cells that are difficult to detach may be placed at 37°C to facilitate dispersal. Add 7.0 ml of complete growth medium and aspirate cells by gently pipetting. Add appropriate aliquots of the cell suspension to new culture vessels. Inoculate at a cell concentration between 1.5 X 10 exp5 and 1.0 X 10 exp6 viable cells/75 cm2. Incubate cultures at 37°C.
Medium Renewal: Every two days.

Differentiation protocol: Plate cells at the final concentration of 70000 cells/ml in 12-well plates. Two days after plating, cells become confluent. Leave cells at confluence for 24 hours; then switch the medium to induction medium for 3 days. Maintain cells in differentiation medium, renewing every other day, till the cells are completely differentiated.

Treatment with HDAC inhibitor: C3H10T1/2 cells were treated with vehicle or with 1μM MS275 from the beginning of differentiation, and all along the differentiation program (DMSO ind, MS275 ind), or were differentiated with the classic protocol and treated for 24 hours at the end of differentiation (DMSO p.d., MS275 p.d.).
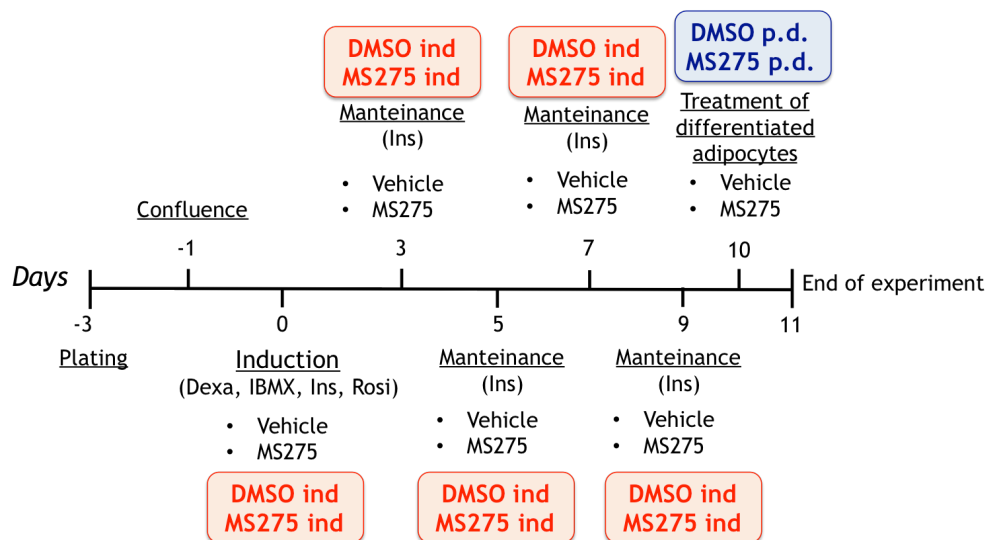

Figure 11: Experimental protocol for differentiation of C3H10T1/2 cells

3T3-L1 preadipocytes

L1 is a continuous substrain of 3T3 (Swiss albino) developed throh clonal isolation.

Manteinance medium: Dulbecco's Modified Eagle's Medium. To make the complete growth medium, add fetal bovine serum to a final concentration of 10%, 1% L-Glutamine (Life Technologies) and 1% Pen/Strep (Life Technologies).

Induction medium: Manteinance medium supplemented with 5 µg/ml insulin, 5mM 3-isobutyl-1-methylxanthine (IBMX, Sigma Aldrich), 2 µg/ml dexamethasone (Sigma Aldrich).

Differentiation medium: Manteinance medium supplemented with 5µg/ml insulin.

Temperature: 37.0°C

Subculturing protocol: remove and discard culture medium. Briefly rinse the cell layer with 0.25% (w/v) Trypsin- 0.53mM EDTA solution (Life technologies) to remove all traces of serum which contains trypsin inhibitor. Add 3.0 ml of Trypsin-EDTA solution to flask and observe cells under an inverted microscope until cell layer is dispersed (usually within 5-7 minutes). Note: To avoid clumping do not agitate the cells by hitting or shaking the flask while waiting for the cells to detach. Cells that are difficult to detach may be placed at 37°C to facilitate dispersal. Add 7.0 ml of complete growth medium and aspirate cells by gently pipetting. Add appropriate aliquots of the cell suspension to new culture vessels. Inoculate at a cell concentration between 1.5 X 10 exp5 and 1.0 X 10 exp6 viable cells/75 cm2. Incubate cultures at 37°C.

Medium Renewal: Every two days.

Differentiation protocol: Plate cells at the final concentration of 70000 cells/ml in 12-well plates. Two days after plating, cells become confluent. Leave cells at confluence for 48 hours; then switch the medium to induction medium for 2 days. Maintain cells in differentiation medium, renewing every other day, till the cells are completely differentiated.

Treatment with HDAC inhibitor: 3T3-L1 cells were treated with vehicle or with 1µM MS275 from the beginning of differentiation, and all along the differentiation program (DMSO ind, MS275 ind), or were differentiated with the classic protocol and treated for 24 hours at the end of differentiation (DMSO p.d., MS275 p.d.).
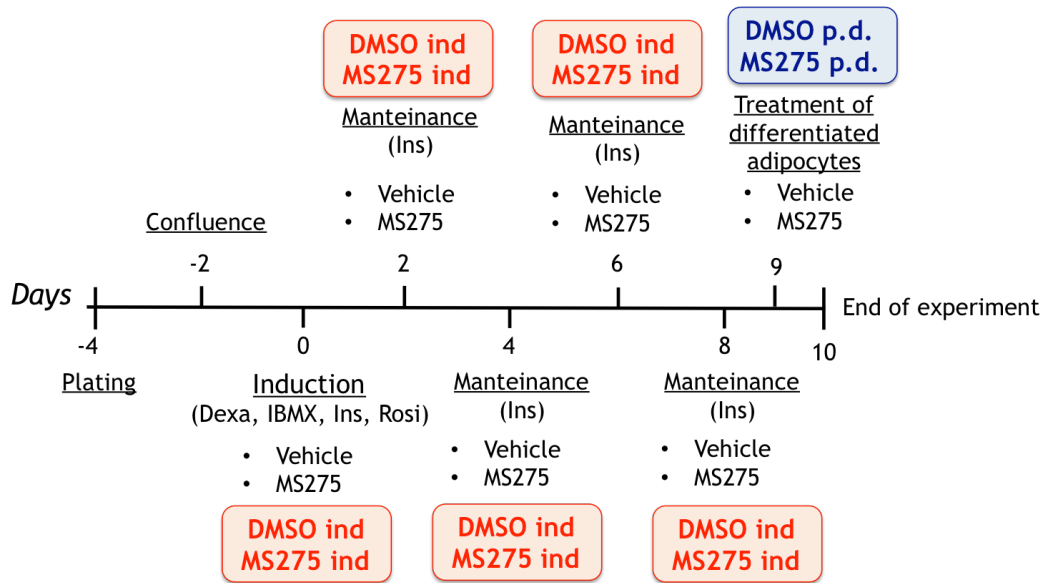
Figure 12: Experimental protocol for differentiation of 3T3-L1 cells

Electron microscopy in C2C12 cells

Samples were fixed in 3% (wt/vol) glutaraldheyde in 0.1 M Sorensen phosphate buffer (pH 7.4) for 60 min at room temperature, rinsed and postfixed in 1% osmium tetroxide in 0.1M Sorensen phosphate buffer, dehydrated through an ascending series of ethanols, and embedded in Durcupan (Sigma-Aldrich). Ultrathin sections were obtained with an Ultracut ultramicrotome (Reichert-Jung) and stained with uranyl acetate and lead citrate before undergoing examination with a JEOL JEM 1010 transmission electron microscope.were processed as previously described (14). Ultrathin sections (200 nm) were evaluated using a JEM 1010 TEM (Jeol). Bioptic fragments from gastrocnemius (2 3 2 mm) were fixed in 3% glutaraldehyde in 0.1 mol/L Sorensen buffer, pH 7.4, overnight at 4°C and Araldite embedded. Two micron semithin sections were stained with toluidine blue. Ultrathin sections (60 nm) were stained with lead citrate and uranyl acetate and examined with a Jeol CX100 TEM (Jeol).

Oxygen consumption in primary brown adipocytes

Cells (5×10^5) were detached (250µl Trypsin- 0.53mM EDTA solution/well); resuspended in PBS containing 25 mmol/L glucose, 1 mmol/L sodium pyruvate, and 2% fatty acidfree BSA; and transferred to a Clark-type oxygen electrode chamber at 37°C. After recording of basal respiration, uncoupled respiration was determined with oligomycin (2.5 mg/mL), and maximal respiration was induced with 2.4mmol/L carbonyl cyanide 4–(trifluoromethoxy)phenylhydrazone. Data were normalized to protein content.

RNA extraction and real-time qPCR

Total RNA from primary brown adipocytes, C3H10T1/2 adipocytes and 3T3-L1 adipocytes was double extracted with TRIzol Reagent® (Invitrogen), purified with commercial kit (Macherey-Nagel, Milano, Italia), and quantitated with Nanodrop (Thermo Scientific, Wilmington, DE). Total RNA from brown adipose tissue, white subcutaneous adipose tissue and white visceral adipose tissue was double extracted with Qiazol Reagent® (Qiagen), purified with commercial kit (RNeasy Lipid Tissue Mini kit, Qiagn), and quantitated with Nanodrop (Thermo Scientific, Wilmington, DE). Specific mRNA was amplified and quantitated by real time PCR, using iScriptTM One Step RT-PCR for Probes (Bio-Rad, Milano, Italia), following the manufacturer's instructions. Primer sequences are available on request. Data were normalized to 36B4 mRNA and quantitated setting up a standard curve.

Experiments were performed in triplicate and repeated at least twice with different cell preparations. Primers for real-time PCRs were designed by IDT software avilable on line optimized to work in a one-step protocol (10 min at 50°C for reverse transcription, 40 cycles of amplifications each consisting of a denaturation step at 95° C for 10 s and an annealing/extension step at 60° C for 30 s). The oligonucleotides used for real-time PCR were synthesized by or Eurofin MWG Operon (Ebersberg, Germany). Sequences were reported in table 1.

Primers and probes for Pparγ, Adrb3 and Prdm16 were from Applied Byosistems (unkown sequences).

Gene		Sequences
Pgc-1α	Forward	CATTTGATGCACTGACAGATGGA
	Reverse	GTCAGGCATGGAGGAAGGAC
	Probe	CCGTGACCACTGACA ACGAGGCC
Tfam	Forward	CACCCAGATGCAAAACTTTCAG
	Reverse	CTGCTCTTTATACTTGCTCACAG
	Probe	CCACAGGGCTGCAATTTTCCTAACC
CytC	Forward	GAAAAGGGAGGCAAGCAT
	Reverse	ACTCCATCAGGGTATCCTCT
	Probe	AACAAGAACAAAGGCATCACCTGGG
Cox6a1	Forward	GTTCGTTGCCTACCCTCAC
	Reverse	TCTCTTTACTCATCTTCATAGCCG
	Probe	ACCATACCCTCTTCCACAACCCTCA
Idh3α	Forward	ACGGAAGGAGAATACAGTGG
	Reverse	GTACTCGAAGGCAAACTCTG
	Probe	ACCCCATCAACGATCACATGCTCA

Suclg1	Forward	AATGATCCAGCCACAGAAGG
	Reverse	AGCAATGAAGGACACTACAGG
	Probe	AGCATAACTCAGGTCCAAAGGCCAA
Ucp1	Forward	GAGCTGGTAACATATGACCTC
	Reverse	GAGCTGACAGTAAATGGCA
	Probe	ACAAAATACTGGCAGATGACGTCCC
Dio2	Forward	CTGTGTCTGGAACAGCTT
	Reverse	CACTGGAATTGGGAGCAT
	Probe	CTAGATGCCTACAAACAGGTTAAACTGGGT
Elovl3	Forward	TGCTTTGCCATCTACACG
	Reverse	CAGTGGACAAAGATGAGTGG
	Probe	TGAACTGGGAGACACGGCCTT
Cidea	Forward	CACGCATTTCATGATCTTGG
	Reverse	CCTGTATAGGTCGAAGGTGA
	Probe	TTACTACCCGGTGTCCATTTCTGTCC
Glut4	Forward	TGTCGCTGGTTTCTCCAACTG
	Reverse	CCATACGATCCGCAACATACTG
	Probe	ACCTGTAACTTCATTGTCGGCATGGGTTT
Acrp30	Forward	AGGCATCCCAGGACATC
	Reverse	CCTGTCATTCCAACATCTCC
	Probe	CCTTAGGACCAAGAAGACCTGCATCTC
Fabp4	Forward	GGCGTGGAATTCGATGAA
	Reverse	GCTTGTCACCATCTCGTT
	Probe	TGATGCTCTTCACCTTCCTGTCGT
Pepck	Forward	TTGAACTGACAGACTCGCCCT
	Reverse	TGCCCATCCGAGTCATGA
	Probe	CCGCATGCTGGCCACCACA
Plin	Forward	ACAGACACAGAGGGAGAGG
	Reverse	AGTGTTCTGCACGGTGTG
	Probe	AGGAGGAAGAAGAGTCCGAGGCT
C/EBPα	Forward	AGAGCCGAGATAAAGCCAAAC
	Reverse	TCATTGTCACTGGTCAACTCC
	Probe	AGCACCTTCTGTTGCGTCTCCA
C/EBPβ	Forward	CCCCGCGTTCATGCA
	Reverse	CAGTCGGGCTCGTAGT
	Probe	ACTTCCATGGGTCTAAAGGCG
Cpt1b	Forward	GATGCAGTTCCAGAGAATCC
	Reverse	CTTGTTCTTGCCAGAGCT
	Probe	TCTGCCCACTCTACCCTTCCTC
Acadl	Forward	GAAACCAGGAACTACGTGAAG
	Reverse	GCTGTCCACAAAAGCTCT
	Probe	CACACATACAGACGGTGCAGCATA
CD36	Forward	GCGACATGATTAATGGCACAG
	Reverse	GATCCGAACACAGCGTAGATAG
	Probe	CAACAAAAGGTGGAAAGGAGGCTGC

Hsl	Forward	GCTCCCTTTCCCCGA
	Reverse	ATGCAGAGATTCCCACCT
	Probe	CACTGTGACCTGCTTGGTTCAACT
Atgl	Forward	TCGTGTTTCAGACGGAGA
	Reverse	CACATAGCGCACCCCT
	Probe	TGCAGACATTGGCCTGGATGAG
Fasn	Forward	TCGTGATGAACGTGTACCGG
	Reverse	CGGGTGAGGACGTTTACAAAG
	Probe	TGCCTTCCGTCACTTCCAGTTAGAGCA
36b4	Forward	AGATGCAGCAGATCCGCAT
	Reverse	GTTCTTGCCCATCAGCACC
	Probe	CGCTCCGAGGGAAGGCCG

Table 1: Primers and probes sequences

Chromatin immunoprecipitation assay

In vitro chromatin immunoprecipitation

C2C12 myotubes (6 wells plate, 3 wells for each condition) were fixed with fixation buffer (500mM Hepes/KOH pH 7.9, 0.1M NaCl, 1mM EDTA pH 8, 0.5mM EGTA pH 8, 11% Formaldehyde) and incubate 10 minutes. Wells were washed with PBS and collected using cell scraper. Pool cells from 3 wells in a 15 ml falcon and centrifuge 1000rpm, 5 min at 4°C. Pellets were lysed with 300μl of lysis buffer (50mM Tris pH 8.0, 5mM EDTA, 1% SDS, protein inhibitor), and sonicated. DNA was quantified by using NanoDrop (Thermo scientific). 150μg of sample were immunoprecipitated with Anti-HDAC3 o Anti IgG antibody overnight. After the immunoprecipitation protein-antibody complexes were precipitated with Dynabeads (Invitrogen), washed twice with WB I (20mM Tris pH 7.4, 150mM NaCl, 0.1% SDS, 1% Triton-X100, 2mM EDTA), once with WB II (20mM Tris pH 7.4, 250mM NaCl, 0.1% SDS, 1% Triton-X100, 2mM EDTA), twicw with Tris-EDTA buffer and eluted with elution buffer (0.1M NaHCO3, 1% SDS). Cross link reversion was carried out by overnight incubation at 65°C. Samples were incubated with proteinase K (0.1 mg/ml) for 1 hour at 55 °C. DNA was purified with Quiaquick spin columns (Qiagen). HDAC3 recruitment on Pgc-1a promoter was quantified by SyberGreen (BioRad) real time qPCR.

In vivo chromatin immunoprecipitation

Skeletal muscle and brown adipose tissue from db/db mice were dissected and fragmented in small pieces, and fixed in 0.5% paraformaldehyde for 10 minutes. Fixing was blocked by 125mM glycine. Samples were centrifuged 1000rpm, 5 min at 4°C. Pellets were lysed in lysis buffer (50mM Tris pH 8.0, 5mM EDTA, 1% SDS, pritein inhibitor), and

sonicated. The protocol of *in vitro* chromatin immunoprecipitation was followed also for tissue samples.

Protein extraction and Western Blot analysis

Lysis

C2C12 myotubes and C3H10T1/2 adipocytes cultured in 6-well plate were lysed with 300 µl of SDS sample buffer (62.5 mM Tris- HCl pH 6.8, 2% w/v SDS, 10% glycerol, 50 mM DTT, 0.01% w/v bromophenol blue).
Brown adipose tissue (50 mg) was lysed in 500 µl of SDS sample buffer.

Solutions and Reagents

Running buffer: 25 mM Tris base, 192 mM glycine, 3.5mM SDS
Transfer Buffer: 25 mM Tris base, 192 mM glycine, 20% methanol (pH 8.5).
Tris Buffered Saline (TBS): 20mM Tris ph 7.5, 150 mM Nacl.
Blocking Buffer: 1X TBS, 0.1% Tween-20 with 5% w/v nonfat dry milk
Wash Buffer: 1X TBS, 0.1% Tween-20 (TBS/T).
Antibody Dilution Buffer: 1X TBS, 0.1% Tween-20 with 5% nonfat dry milk as indicated on primary antibody datasheet

Electrophoresis and protein Blotting

Proteins are run for 2 hours at a constant voltage (90 V) in polyacrylamide gel (10% or 15% polyacrylamide).
Protein are electro-transferred (300 mA for 2 hours) on nitrocellulose or PVDF membrane.
Membrane blocking and antibody incubations: incubate membrane in 25 ml of blocking buffer for one hour at room temperature. Wash three times with 15 ml of TBS/T.
Primary antibody incubation: incubate membrane and primary antibody (at the appropriate dilution as recommended in the product datasheet) in 10 ml primary antibody dilution buffer with gentle agitation overnight at 4°C.
Wash three times with TBS/T.
Incubate membrane with the species appropriate HRP-conjugated secondary antibody for 1h at room temperature with gentle agitation.
Wash three with TBS/T.
Detection of proteins: incubate membrane with appropriate volume of SuperSignal West Pico Chemiluminescent Substrate (Pierce Thermo Scientific) for 5 minutes.
Drain membrane of excess developing solution, wrap in plastic wrap and expose to x-ray film.

<u>**Primary antibodies**</u>

Cocktail OXPHOS (MitoSciences), 1:250 in 5% nonfat dry milk
Ucp1 antibody (Abcam), 1:1000 in 5% nonfat dry milk
Pparγ antibody (Santa Cruz), 1:200 in 5% nonfat dry milk

<u>**Secondary antibodies**</u>

Anti Mouse, 1:4000 in 5% nonfat dry milk for OXPHOS
Anti Mouse, 1:5000 in 5% nonfat dry milk for Ucp1
Anti Rabbit, 1:5000 in 5% nonfat dry milk for Pparγ

Glycerol release

At the end of experiment, cell culture medium from C3H10T1/2 cells grown and differentiated in 12-well plates was collected. Glycerol release in cell medium, as an index of fatty acids beta-oxidation, was measured with Triglyceride Dosage Kit (Sentinel).

Oil red O staining

Medium was aspirated from wells and they were washed with 1 ml of 1X PBS.
Cells were fixed with 1ml of 10% formalin for at least 1 hour and then washed with 1ml of water. 1ml 60% isopropanol was added to cover the bottom of each well and let sit for 2-5 minutes. Cells were then stained with Oil Red O solution; after 10 minutes incubation wells were washed 3 times with 1 ml of water. Pictures were taken at 20X magnification using Axiovert Microscope (Zeiss).
For Oil Red O quantification, staining was eluted from wells with 1.5ml of 100% isopropanol (10 minutes incubation) and absorbance was measured (500 nm, 0.5 sec reading).

Animal studies

<u>Diet induced obese wild type mice</u>

C57BL6/J male mice were purchased from The Jackson Laboratory. Six-week-old male mice were randomized into two groups according to glucose levels and body weight and fed high fat diet (HFD, 60% calories from fat, Research Diet, D12492) for 17 weeks, monitoring body weight and fasting glycemia. From week 18 mice were treated for 23 days every other day with intraperitoneal (i.p.) injection of vehicle (DMSO) or of MS275 (10mpk).

MS275 was dissolved in DMSO and stored at +4°C. Prior to use, the solutions were warmed in a 42°C water bath with agitation. For blood analysis, db/db mice were fasted for 16 hr and blood was collected from the tail vein. Glucose levels were determined using an Accu-Chek Active glucometer (Roche). Triglyceride and cholesterol levels were determined by the Plasma Triglyceride Kit (Sentinel) and by the Plasma Cholesterol Kit (Sentinel). Insulin levels were determined using an AlphaLISA® Human Insulin Research Immunoassay Kit (Perkin Elmer). Adiponectin and Leptin levels were determined using ELISA assay Kits (Genway).

For glucose tolerance tests, mice were fasted for 16 hours, and glucose levels from tail-vein blood were determined before and 30, 60, 90, and 120 min after i.p. injection of glucose (2 g/kg). At the end of treatments, brown and white fat (subcutaneous and visceral), liver and blood samples were collected from individual animals.

For cold challenge tests, basal rectal temperature was measured at 24°C. Then mice were housed for 140 minutes at 4°C and rectal temperature was measured every 20 minutes.

Diet induced obese knock out mice

Eight-weeks-old weeksHdac3 skeletal muscle knock out (H3smKO) mice and their Cre-/- littermates (Floxed), and eight-weeks-old Hdac3 adipose tissue knock out (H3atKO) mice and their Cre-/- littermates (Floxed), were fed high fat high sucrose diet (HFHSD, 45% calories form fat, Research Diet, D12451) for 16 weeks. Body weight was measured every 2 weeks.

Animal studies were conducted strictly following regulations of European Community (Directive 2010/63/EU) and local regulations for animal care (Decreto Legislativo 4 marzo 2014, n. 26).

Magnetic resonance imaging

At day 18 of treatment, mice were anesthetized and analyzed in a 4.7 Tesla Avance II magnetic resonance imaging (MRI) scanner (Bruker Corporation). After a gradient-echo scout, 16 axial 1-mm-thick T1-weighted slices were placed in the abdominal region spanning from kidneys to bladder inclusive. The field of view was 30 X 30 mm^2 with a matrix of 128 X 128 pixels. Four averages of a spin echo sequence with time to echo 10 ms and time of repetition 400 ms were acquired in 3'25". The slice immediately frontal with respect to the ilium bone was chosen for visceral fat estimation and was computed as follows: (fat area)/(slice area). Areas were measured with Photoshop (Adobe Systems).

Histological analysis of adipose tissues

Brown adipose tissue, subcutaneous white adipose tissue, visceral white adipose tissue and liver were fixed with Carnoy solution (6 parts 100% Ethanol, 3 parts chloroform 1 part

glacial acetic acid) for 24 hours at 4°C. Tissues were then transferred in 100% ethanol. Tissues were embedded in paraffin and 8µm sections were stained with hematoxylin-eosin. Images were taken at X20 magnification. Cell size of adipocytes from white adipose tissues sections were quantified using the software Photoshop CS6 (Adobe Systems Inc., San Jose, California), by converting pixel number in surface units, and correcting for magnification.

Liver fatty acids quantification by mass spectrometry analysis

Liver from diet induced obese mice treated with vehicle or with MS275 were homogenized in methanol with tissue lyser (Qiagen). For the quantitative analysis of fatty acids, aliquots of methanolic extracts after addition of internal standards (heneicosanoic acid, Sigma-Aldrich), were subjected to acidic hydrolysis. Extracts were resuspended in chloroform-MeOH 1:2, v/v. 1N HCl:MeOH (1:2, v/v) was added to the total lipid extract and centrifuged at 150 rpm for 30 minutes. chloroform-water (1:1, v/v) was added, and the extracts were shaken. The lower organic phase was collected, split, transferred into tubes and dried under nitrogen flow. For fatty acids quantification the aliquot was suspended in 500ul of MeOH, diluted and transferred into 96-well plate and placed in an auto-sampler for LC-MS/MS analysis. Quantitative analysis was performed with calibration curves prepared and analyzed daily by electrospray ionization (ESI) using an API 4000 triple quadrupole instrument (AB Sciex, USA). The LC mobile phases were: water/10 mM isopropylethylamine/15mM acetic acid (phase A) and MeOH (phase B). The gradient (flow rate 0.5 ml/min) was as follows: T 0: 20% A, T 20: 1% A, T 25:1% A, T 25.1: 20% A, T 30: 20% A. The Hypersil GOLD C8 column (100 mm × 3 mm, 3m) was maintained at 40∘C. The API4000 was operated in negative electrospray mode and the compounds were detected in single ion monitoring (SIM).

Generation of Hdac3 tissue specific knock-out

To generate tissue specific knock out it has been used Cre-LoxP technology. To obtain specific deletion of Hdca3 in skeletal muscle, we crossed Hdac3 floxed mice in BL6 background (provided by dr. Hiebert, Vanderbilt Univesity) with B6.Cg-Tg(ACTA1-cre)79Jme/J (The Jackson Laboratory), expressing Cre under the control of promoter of the gene encoding for alpha skeletal muscle actin. To obtain specifc deletion of Hdac3 in adipose tissues we crossed Hdac3 floxed mice with B6;FVB-Tg(Adipoq-cre)1Evdr/J (The Jackson Laboratory), expressing Cre under the control of the promoter of the gene encoding for adiponectin. Breeding strategy is reported in Figure…
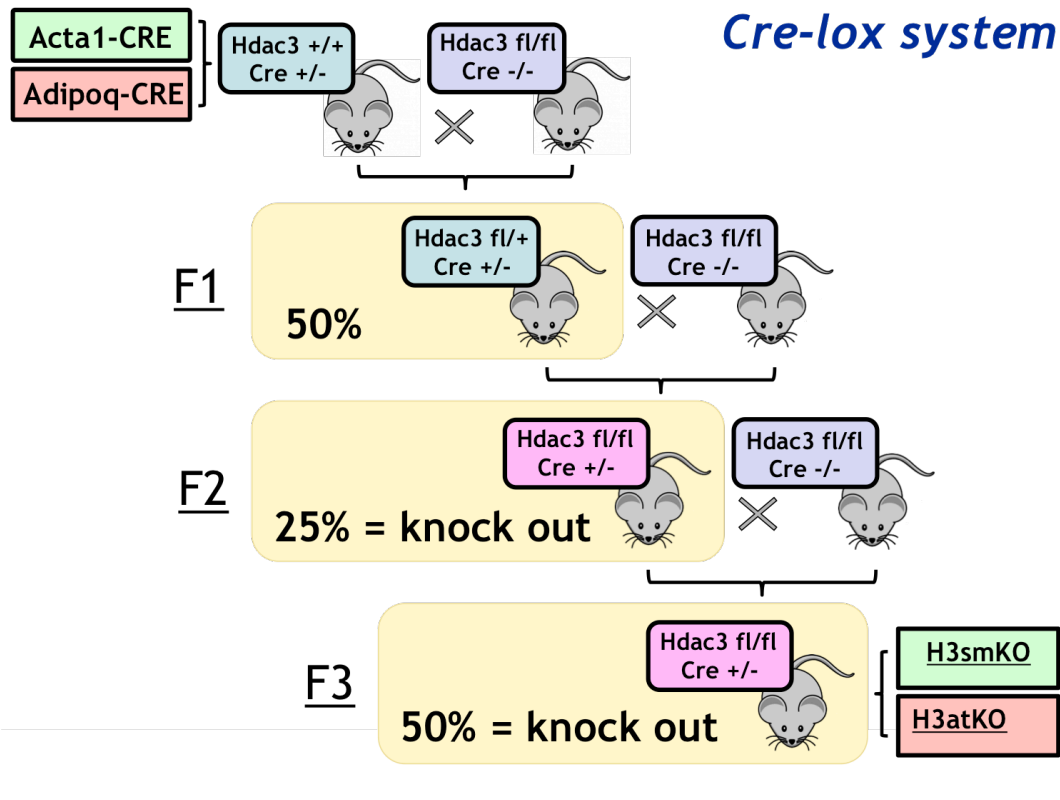
Figure 13: Breeding strategy to generate Hdac3 tissue specific knock out

Genotyping

Tail samples were digested in proteinase K 56°C overnight. Tail DNA was extracted with NucleoSpin Tissue kit (Macherey Nagel).

Primers for Cre amplification:
Transgene Forward: GCGGTCTGGCAGTAAAAACTATC
Transgene Reverse: GTGAAACAGCATTGCTGTCAC TT
Internal Positive Control Forward: CTAGGCCACAGAATTGAAAGATCT
Internal Positive Control Reverse: GTAGGTGGAAATTCTAGCATCATCC
Primers for LoxP amplification:
Forward: CTCTGGCTTCTGCTATGTCAATG
Reverse: GGACACAGTCATGACCCGGTC

Thermal protocol for Cre PCR:
→ 1 cycle: 94°C for 3minutes
→ 35 cycles: 94°C for 30 seconds
      55°C for 30 seconds
      72°C for 45 seconds
→ 1 cycle: 72°C for 2 minutes
After PCR amplification, samples were run on 3% TAE gel.
Thermal protocol for LoxP PCR:
→ 1 cycle: 94°C for 5 minutes

<div align="right">

55°C for 1 minute

72°C for 1.5 minutes

</div>

→ 35 cycles: 94°C for 1 minute

<div align="right">

55°C for 45 seconds

72°C for 1.5 minutes

</div>

→ 1 cycle: 72°C for 10 minute

After PCR amplification, samples were run on 2% TAE gel.

Expected bands:

Cre: positive ctrl band = 324 bp

    Cre positive band = 100 bp

LoxP: floxed band = 504 bp

    Wild type band = 464 bp

Statistical Analysis

Statistical analyses were performed by Student's t test for the comparison of two different experimental groups or one-way ANOVA with the indicated post-test for multiple testing comparisons. All statistical analyses were performed using GraphPad (GraphPad Software).

Results

Class I HDAC inhibitor MS275 promotes mitochondrial biogenesis in a cellular model of skeletal muscle

It has been reported that HDACs are involved in the conversion of glycolytic to oxidative fibers that differ in the number of mitochondria. Our preliminary results showed in cells and mice increased expression of the master regulator of mitochondrial biogenesis Pgc-1a upon MS275 treatment. In order to investigate further how class I HDAC inhibition affects mitochondrial morphology and function, in collaboration with Dr. Donetti (Dip. Morfolgia Umana, Università degli Studi di Milano) we performed transmission electron microscopy analysis in C2C12 myotubes treated with vehicle or with the class I HDAC inhibitor. The ultrastructural appearance of mitochondria in vehicle treated cells was characterized by a dense matrix and well-organized cristae with dilated intracristae spaces. MS275 treated cells showed increased mitochondrial density and greater electron opacity of the matrix typical of metabolically active cells (Figure 14).
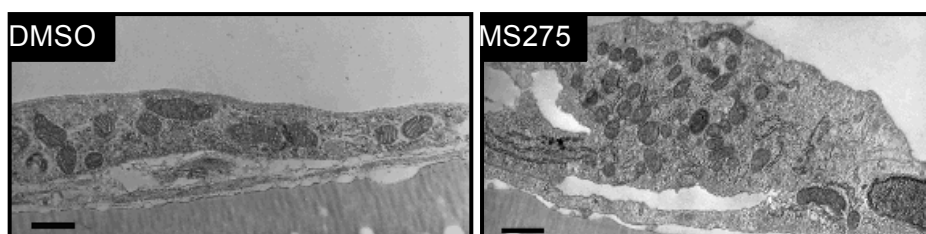

Figure 14: Representative electron microphotographs of ultrathin sections of C2C12 monolayers. Treatment with MS275 resulted in an increase in mitochondrial density and greater electron opacity of the matrix to the detriment of the development and organization of cristae. (Bar: 500nm).

These changes were paralleled by increased expression of the protein complexes of the electron transport chain (Figure 15).
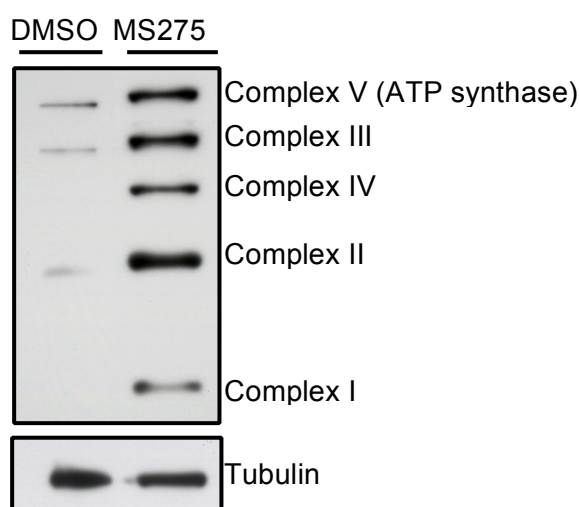
Figure 15: Western blot analysis of mitochondrial complexes I–V of the electron transport chain in C2C12 myotubes treated with HDAC inhibitor for 48 h.

Class I HDAC selective inhibitor reduces Hdac3 recruitment on Pgc-1α promoter in muscle

Previous experiment demonstrated that Hdac3 inhibition recapitulated the effect of class I HDAC inhibitor in term of expression of *Pgc-1α* and its main targets. In order to deepen the molecular mechanism whereby MS275 by inhibiting Hdac3 remodel metabolic profile, we performed a chromatin immunoprecipitation analysis. Interestingly I found a reduced Hdac3 recruitment in MEF region in Pgc-1α promoter, in C2C12 myotubes and in skeletal muscle gastrocnemius from *db/db* mice treated with the class I selective inhibitor (Figure 16).
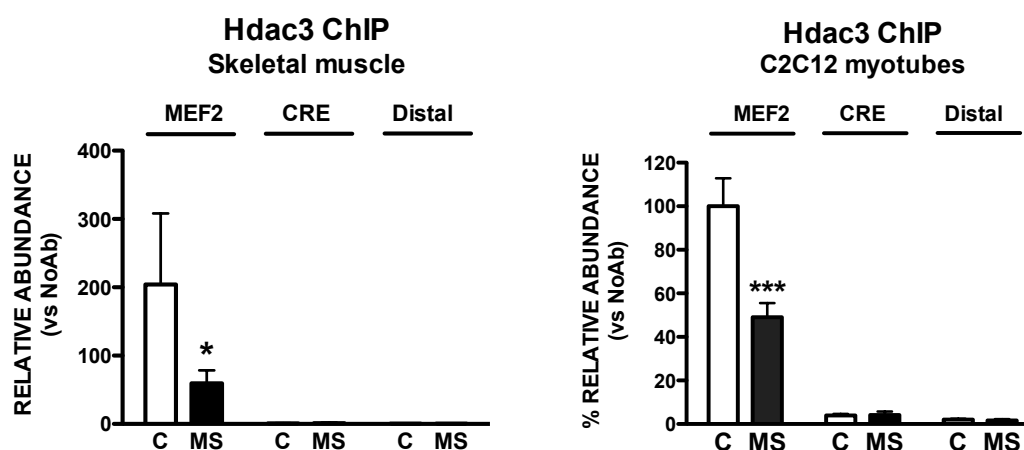

Figure 16: Treatment with MS275 reduced Hdac3 recruitment in Pgc-1α promoter leading to the transcriptional de-repression of this gene. Statistical analysis: Student's t test, *p<0.05, ***p<0.001.

Class I HDAC inhibition in primary brown adipocytes activates mitochondrial biogenesis and mitochondrial function

Previous experiment performed in our laboratory showed that *db/db* mice treated with MS275 were able to better counteract the reduction of body temperature during an acute cold exposure (data not shown). The tissue mostly involved in the regulation of body temperature via non-shivering thermogenesis is brown adipose tissue (BAT). We hypothesized that the class I HDAC inhibitor potentiates oxidative metabolism, along with increased mitochondrial thermogenesis, as a result of the uncoupling of electron transport chain to oxidative phosphorylation in this tissue. To test this hypothesis we isolated primary brown adipocytes and we treated them with vehicle DMSO or with MS275: class I selective inhibitor increased gene expression of the gene encoding for

uncoupling protein 1 (*Ucp1*), the most important marker of BAT, and of the beta 3 adrenergic receptor (*Adrb3*), key player in the activation of thermogenesis in response to SNS adrenergic stimulation (Figure 17). Moreover, upon MS275 treatment, we detected a significant increase of the expression of typical markers of mitochondrial biogenesis (*Pgc-1α, Tfam*), and adipose tissue functionality such as the master regulator of adipocyte differentiation *Pparγ*. In this cell line MS275 also upregulated genes involved in oxidative metabolism, such as the dehydrogenase for the long-chain acyl-CoA *Acadl*, the fatty acid transporter *Cd36*, the α subunit of isocitrate dehydrogenase *Idh3α* and subunit VIa of the cytochrome C oxidase *Cox6a1* (Figure 17).
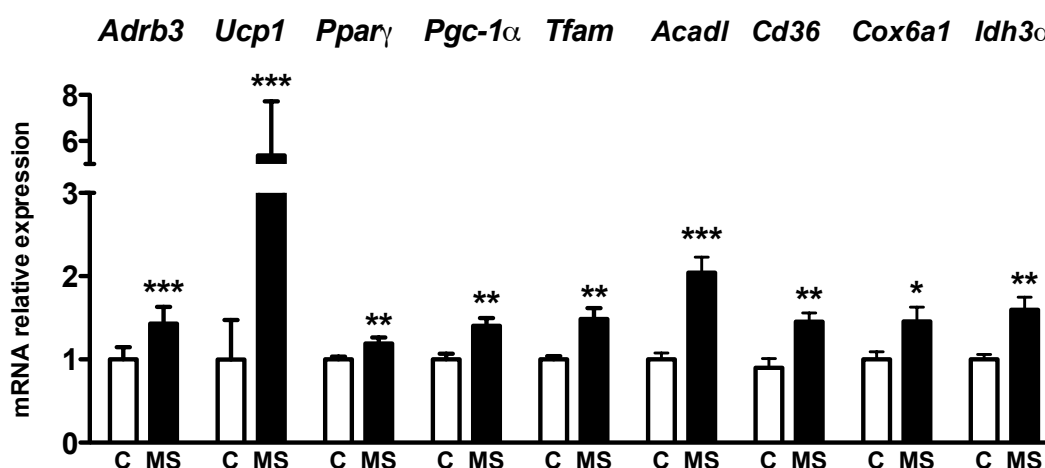

Figure 17: Gene expression profile in primary brown adipocytes treated with vehicle or MS275 1uM for 24 hours. Statistical analysis: Student's t test, *p<0.05, ***p<0.001.

To prove that class I HDAC inhibition promotes mitochondrial biogenesis in BAT, we analyzed mitochondrial DNA content in primary brown adipocytes and we detected a significant increase in MS275 treated cells. Moreover we analyzed oxygen consumption in cultured cells and we found that the class I HDAC inhibitor MS275 significantly increased basal, uncoupled and maximal respiration (Figure 18).
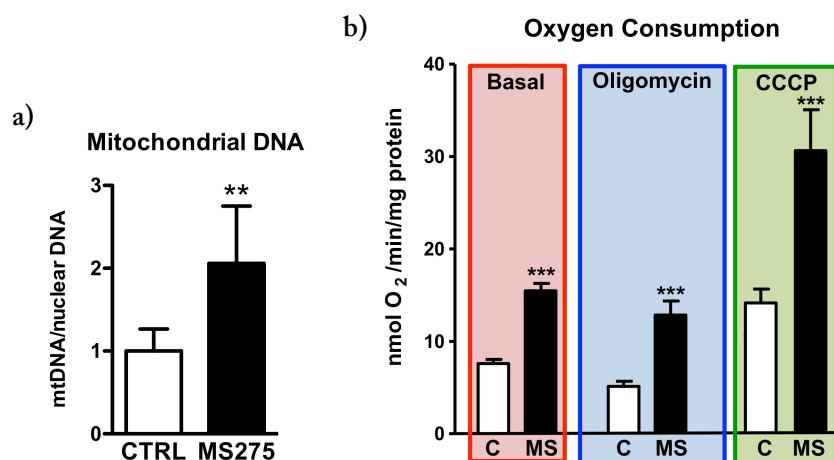

Figure 18: a) Mitochondrial DNA content in primary brown adipocytes treated with vehicle or with MS275. b) Oxygen consumption measured in basal, uncoupled (2.5 uM oligomycin),

maximal (2.5 uM CCCP) condition in primary brown adipocytes treated with MS275 for 24 hours. Statistical analysis: Student's t test, **p<0.01, ***p<0.001.

Class I HDAC inhibition reduces Hdac3 recruitment on Pgc-1α promoter in brown adipose tissue

Having identified Hdac3 at the crossroad of the effects of class I HDAC selective inhibitor in skeletal muscle, we hypothesized that HDAC3 also plays a key role in brown adipose tissue. Chromatin immunoprecipitation of Hdac3 in brown adipose tissue from *db/db* mice revealed in fact a reduced recruitment of Hdac3 in PPRE region in Pgc-1α promoter (Figure 19). This result explained the upregulation of *Pgc-1α* expression detected in BAT of *db/db* mice treated with MS275 (see preliminary data). Pgc-1α along with Pparγ and other transcriptional coactivators are recruited on the PPRE in the Ucp1 promoter, leading to transcription activation of this gene. Accordingly, we detected higher expression of Ucp1 (both at mRNA and protein level) in BAT from MS275-treated mice (Figure 16).
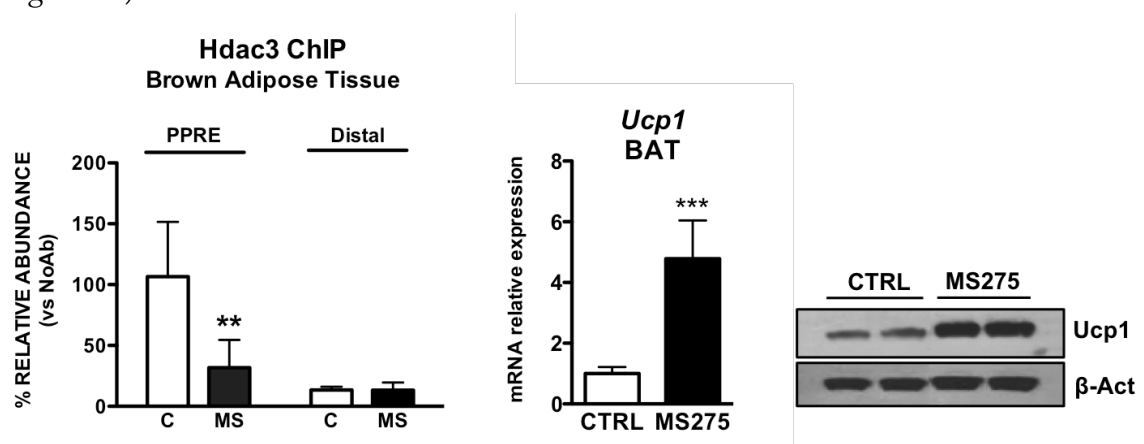

Figure 19: ChIP assay on BAT from db/db mice showed a reduced recruitment of Hdac3 on Pgc-1α promoter in response to MS275 treatment. Consequently we detected increased expression of Ucp1 at mRNA and protein level. Statistical analysis: Student's t test, **p<0.01, ***p<0.001.

Hdac3: key regulator of oxidative metabolism?

Results obtained in *db/db* mice and cells treated with the class I selective inhibitor demonstrated that class I HDACs strongly influence energy metabolism in skeletal muscle and adipose tissue, suggesting Hdac3 as key metabolic regulator. To assess the contribution of skeletal muscle and adipose tissues to the phenotype induced by class I selective HDAC inhibitor and to investigate further the metabolic role of Hdac3, during my doctorate I have generated two mouse models: Hdac3 selective knock out in skeletal muscle and in adipose tissue. The purpose is to investigate the metabolic effect of Hdac3 deletion in obesity.To this end, treatment of tissue specific Hdac3 ko mice with a high fat diet (60% calories from fat) to make knock out mice obese and insulin resistant are

currently under way. The results in knock out mice will be compared with results obtained upon a biochemical inhibition of class I HDACs with MS275.

Inhibition of class I HDACs improves obese phenotype

We investigated whether inhibition of class I HDACs could counteract obesity and insulin resistance in a mouse model of diet-induced obesity (DIO mice). We fed 6-week-old male C57BL/6 mice a high fat diet (HFD, 60% kcal). After 16 weeks on HFD mice were randomized in two groups, without statistically significant difference in weight and glycemia. Mice were treated for 22 days, every other day, with vehicle DMSO or with the class I selective HDAC inhibitor MS275 10mg/kg/d, since our previous results demonstrated that at this dose the compound retained its class-selective inhibitory activity[238]. Starting from day 16 of treatment, MS275 treated mice showed lower body weight (Figure 20a), reaching 10% reduction at day 22 (Figure 20b), with no changes in daily food consumption (Figure 20c).
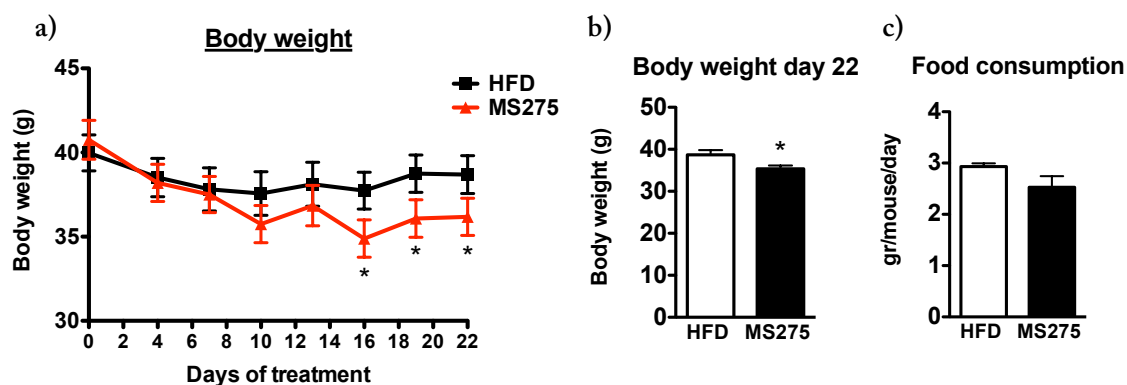
Figure 20: a) Body weight loss in DIO mice treated with MS275 for 22 days, **b)** Body weight at day 22 in vehicle- and MS275-treated mic,e **c)** Food consumption 22 in vehicle- and MS275-treated mice. Statistical analysis: Student's t test, *p<0.05.

Glucose tolerance test showed that treatment with MS275 improved glucose clearance in diet induced obese mice (Figure 21a). Plasma insulin and adiponectin levels at the end of the experiment did not show differences in two groups of mice (Figure 21b). However, we detected decreased level of circulating leptin (Figure 21b), suggesting amelioration of leptin resistance.

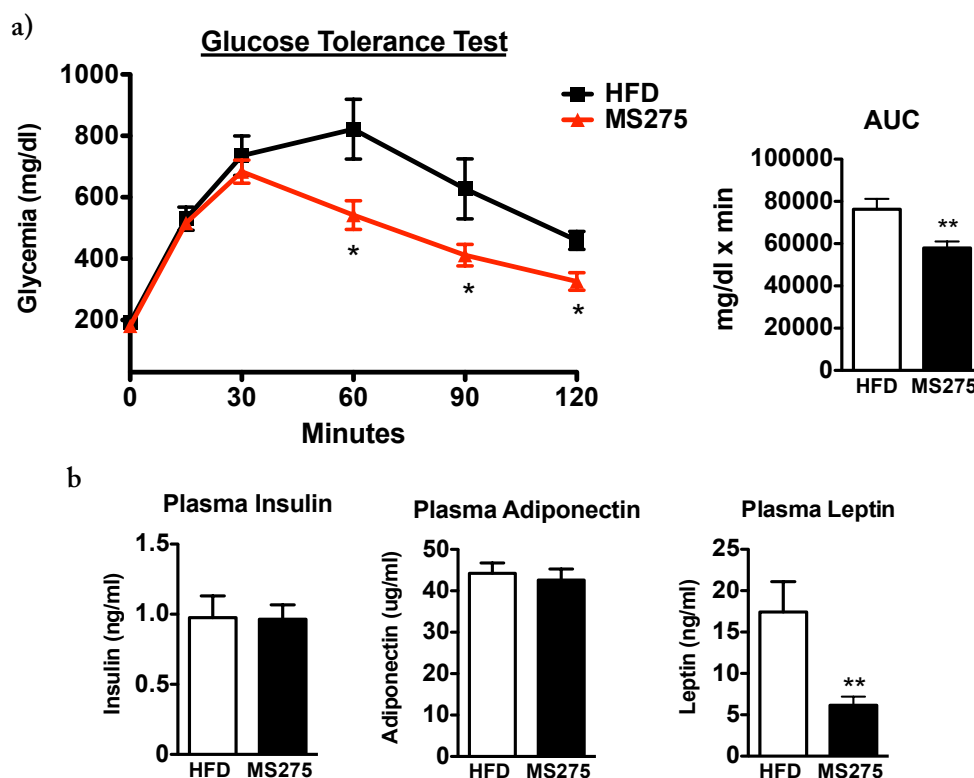**Figure 21: a) Glucose tolerance test in DIO mice treated with vehicle or MS275 performed after 16 days of treatment, b) Plasma levels of insulin, adiponectin and leptin in the two groups of mice. Statistical analysis: Student's t test, *p<0.05, **p<0.01.**

Surprisingly, we observed no changes of circulating levels of triglycerides and cholesterol (Figure 22a). Hematoxylin and eosin staining highlighted reduced lipid accumulation in liver of MS275-treated mice (Figure 22b), confirmed by mass spectrometry analysis showing a reduction of total hepatic fatty acids (Figure 22c). In particular it has been found a significant decrease of oleic acid, stearic acid, docosahexanoic acid and arachidonic acid. This last one particularly correlates with hepatic inflammation, thus my results suggested an amelioration of liver phenotype in MS275 treated mice.
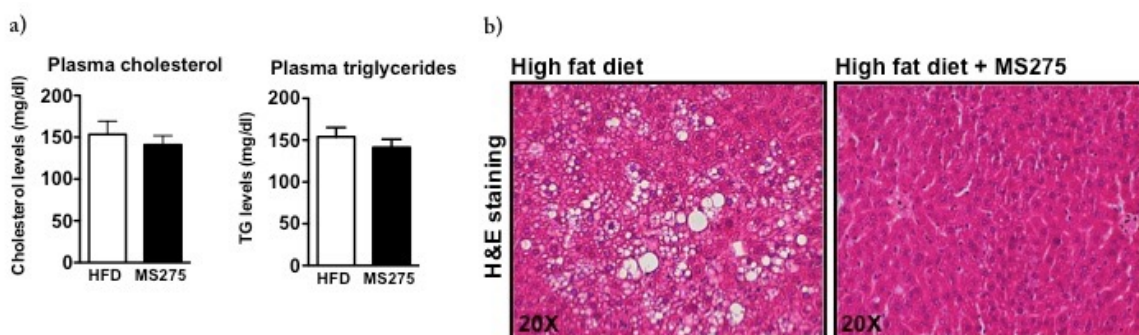
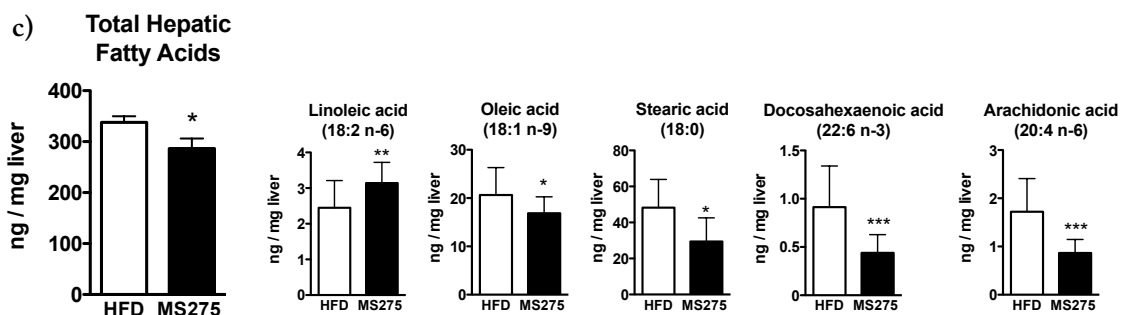Figure 22: a) Cholesterol and triglycerides levels in plasma from vehicle- and MS275-treated mice, b) Hematoxylin and eosin staining in liver from the groups of mice, c) Hepatic fatty acids measured by mass spectrometry. Statistical analysis: Student's t test, *p<0.05, **p<0.01, ***p<0.001

Class I HDAC inhibition improves brown adipose tissue functionality

Since previous results in *db/db* mice have demonstrated that class I HDAC inhibition increased heat production[238], we tested whether treatment with MS275 could affect thermogenic capacity in diet induced obese mice: after an acute exposure to 4°C MS275-treated mice could better cope the cold challenge (Figure 23a). Brown adipose tissue (BAT) controls body temperature via non-shivering thermogenesis. Magnetic resonance imaging (MRI) of interscapular area showed that BAT mass was not affected by treatment (Figure 23b).
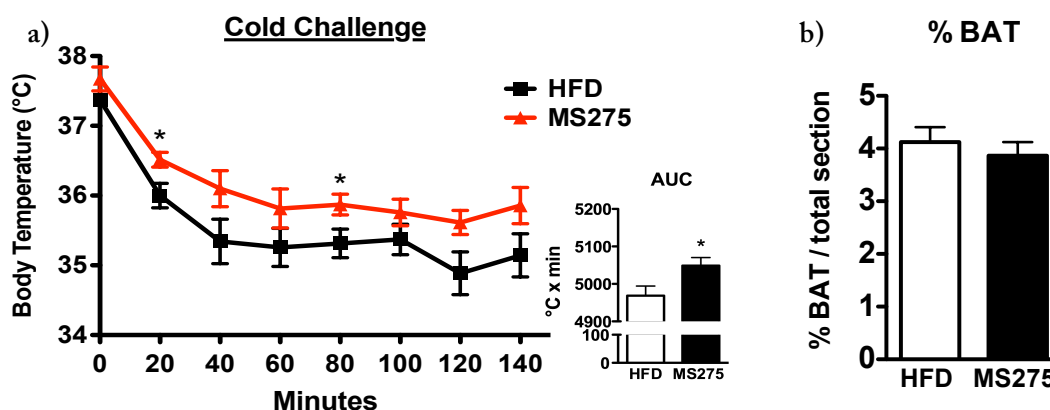
Figure 23: a) Cold challenge showed that MS275 stimulated thermogenesis, b) MRI analysis showing that BAT mass was not significantly different in two groups of mice. Statistical analysis: Student's t test, *p<0.05.

Nevertheless, hematoxylin and eosin staining showed that in control mice brown adipocytes were large, with big lipid droplets, typical of BAT from obese mice, which becomes less functional. In MS275-treated mice brown adipocytes were smaller and multilocular (Figure 24a), suggesting that even though BAT mass was not increased, the global phenotype of this tissue improved. Accordingly we detected increased expression of typical BAT markers *Dio2* and *Elovl3*. Interestingly MS275 did not induce expression of *Ucp1*, which plays a key role in the thermogenic program (Figure 24b).
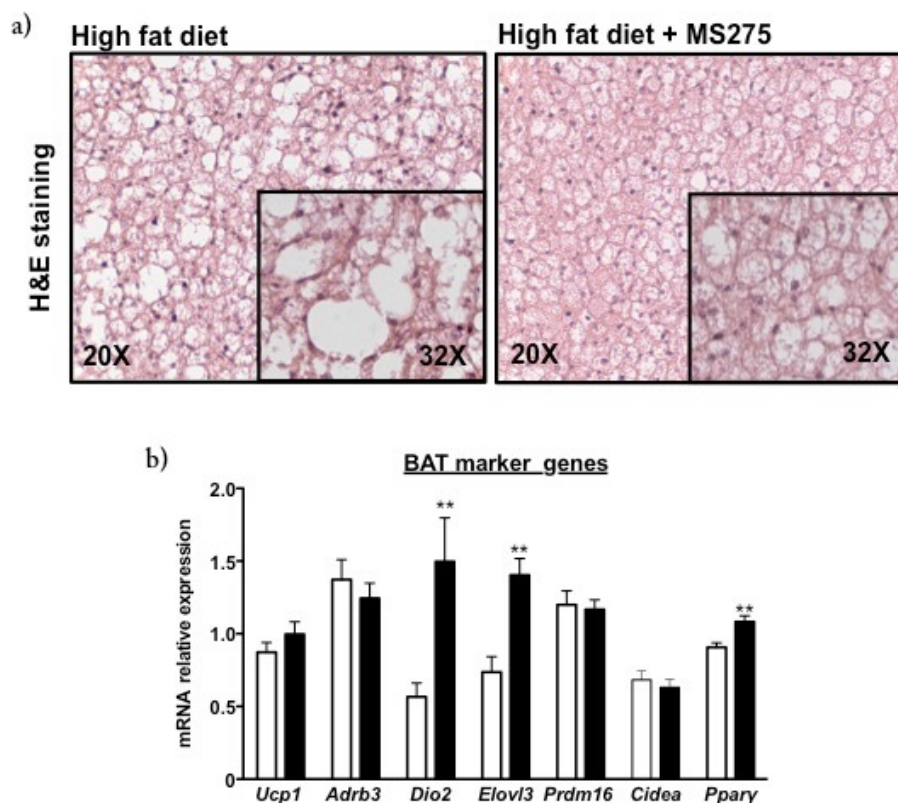
Figure 24: a) Hematoxylin and eosin staining of BAT from DIO mice treated with vehicle or MS275, b) Gene expression of brown adipose tissue markers. Statistical analysis: Student's t test, **p<0.01.

MS275 reduces white adipose tissue mass and adipocyte size

Magnetic resonance imaging (Figure 25a) of abdominal section of vehicle- and MS275-treated mice showed 22% reduction of total white adipose tissue (WAT) mass as an effect of MS275 treatment (data not shown). The reduction detected in WAT mass was mostly due to reduced area of subcutaneous WAT (subWAT) since there was mild but not significant decrease of visceral WAT (viscWAT) (Figure 25b). Staining of inguinal subWAT (Figure 25c) and mesenteric viscWAT (Figure 25d) indicated that MS275 significantly reduced both subcutaneous and visceral adipocyte size.
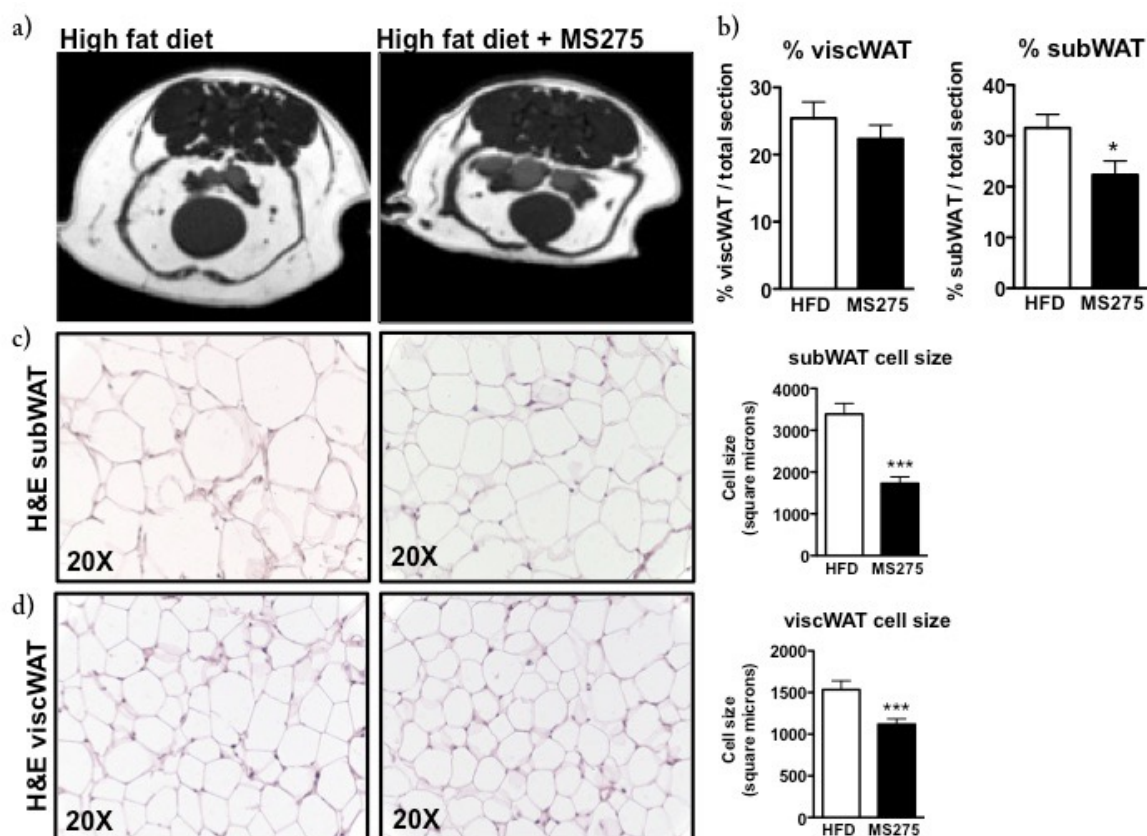
Figure 25: a) Representative images from MRI analysis, b) Quantification of visceral and subcutaneous WAT area normalized on total section area, c) H&E staining and cell size measurement of subcutaneous WAT sections d) H&E staining and cell size measurement of visceral WAT sections. Statistical analysis: Student's t test, *p<0.05, ***p<0.001, n=5.

Inhibition of class I HDACs promotes lipid oxidation and a brown like phenotype in white fat

Gene expression analysis of WAT showed that MS275 upregulated the expression of typical adipocyte markers, such as *Pparγ*, *Glut4*, *Fabp4* and *Acrp30* (Figure 26a, b) in both subWAT and viscWAT, suggesting improvement of white fat functionality. In addition in WAT from MS275-treated mice we noticed higher expression of genes involved in triglycerides catabolism (*Cd36*, *Hsl*, *Atgl*) and significant upregulation of β-oxidation genes (*Cpt1b*, *Acadl*) (Figure 26a, b). Concomitantly, MS275 reprogrammed WAT toward brown-like phenotype, as genes highly expressed in brown fat (*Adrb3*, *Cidea*) were strongly upregulated in both WAT (Figure 26a, b). Furthermore, gene expression analysis of viscWAT showed dramatic increase of the expression of *Ucp1* (Figure 26b). These findings may indicate a role of "brown-like" WAT in thermogenic process, suggesting that the improved thermogenic capacity of MS275-treated mice (Figure 23a) could be due not only to the enhanced functionality of brown fat but also to the increased oxidative potential of visceral WAT.
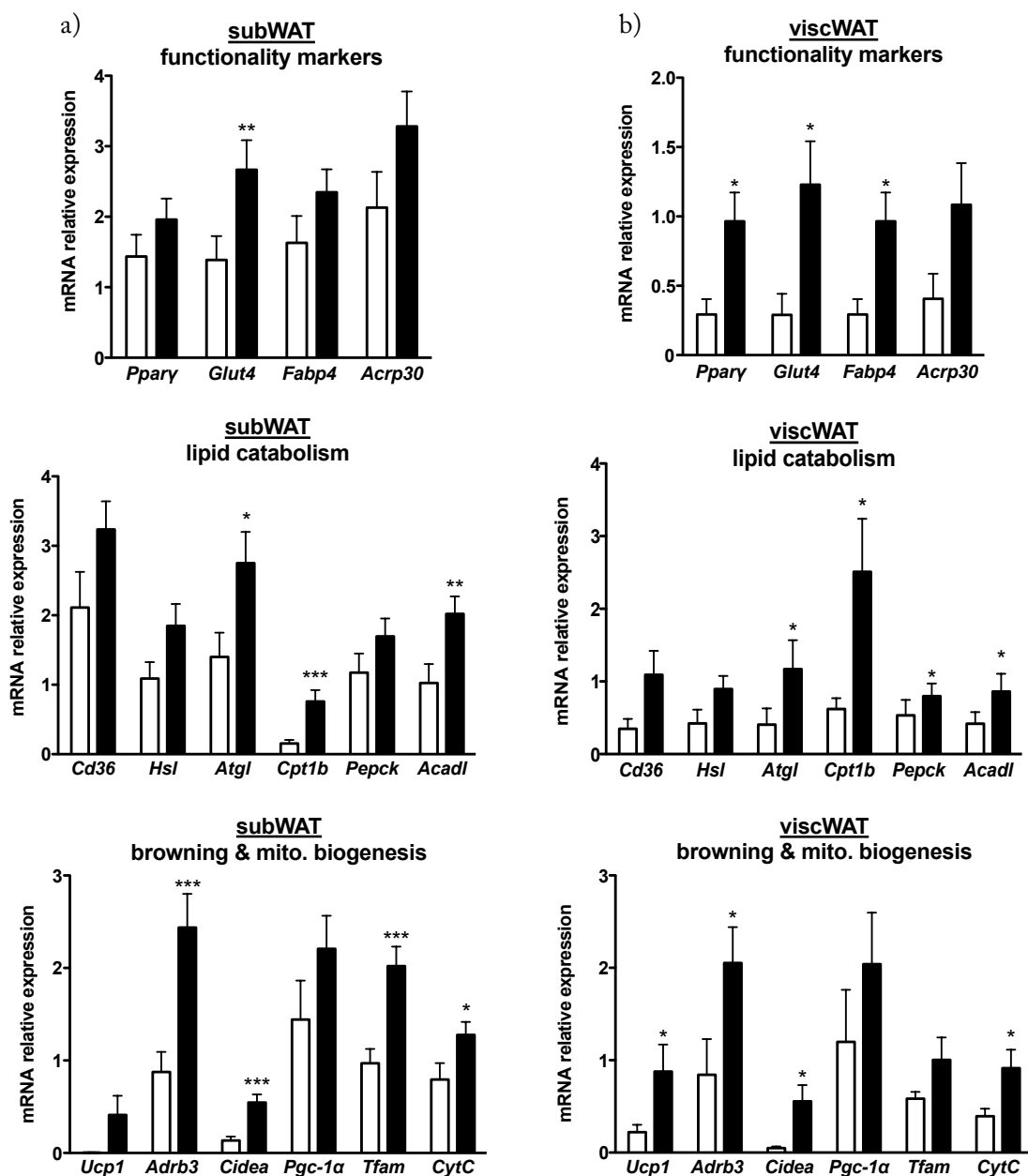
Figure 26: a) Gene expression analysis of functionality markers, genes involved in lipid catabolism, "browning" and mitochondrial biogenesis in subcutaneous WAT, **b)** Gene expression analysis of functionality markers, genes involved in lipid catabolism, "browning" and mitochondrial biogenesis in visceral WAT. Statistical analysis: Student's t test, *$p < 0.05$, **$p < 0.01$, ***$p < 0.001$.

Class I histone deacetylases regulate adipocyte precursor differentiation fate

Our findings in DIO mice suggested the role of class I HDACs in the regulation of adipose tissue functionality. To investigate the molecular mechanism underlying the effect of MS275 in WAT, we performed further *in vitro* experiments. In both subcutaneous and visceral WAT there are different cell populations: among them preadipocytes and mature

adipocytes. The question we asked was whether MS275 exerts its effect on differentiated adipocytes or whether it affects adipocyte precursor cell fate. To this end we chose C3H10T1/2 cells, a mesenchymal stem cell line that in addition to classical hormonal inducers requires further stimuli (i.e. BMP4/7, Rosiglitazone) to differentiate to adipocytes[239,240].

Class I HDAC inhibition induces morphological changes in differentiating C3H10T1/2 mesenchymal stem cells

We treated C3H10T1/2 preadipocytes with vehicle or with 1μM MS275 at induction of the differentiation program (ind) or after differentiation (p.d.). We found that only cells treated with the class I HDAC inhibitor at the beginning of differentiation showed different morphology (smaller cells, with smaller lipid droplets) (Figure 27), while treatment in differentiated adipocytes had no effect.
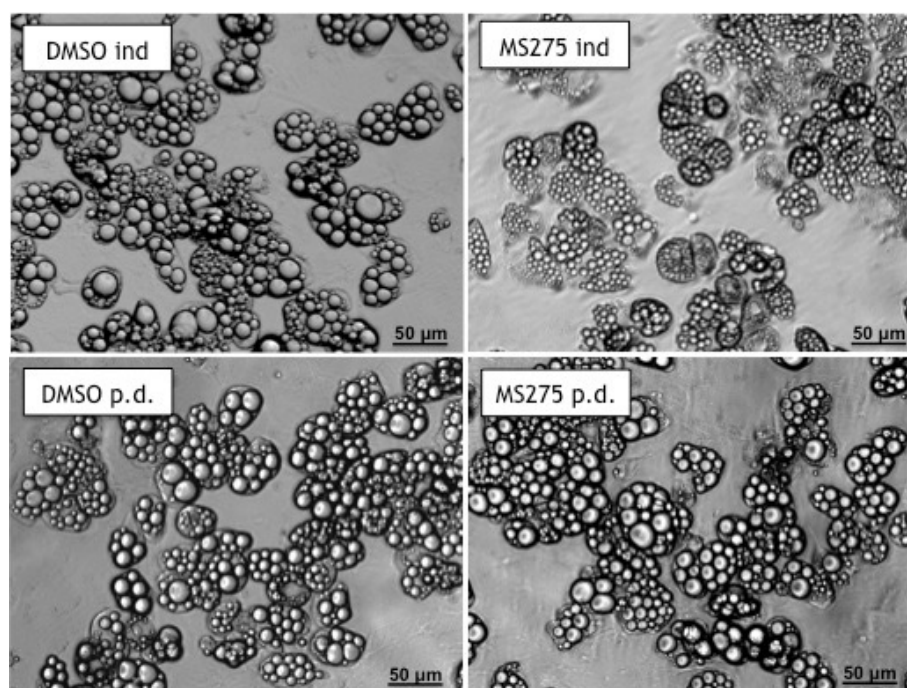
Figure 27: C3H10T1/2 cells differentiated in presence of MS275 were smaller after 9 days of differentiation (upper panel on the right).

Class I HDAC inhibition enhances oxidative capacity in C3H10T1/2 mesenchymal stem cells

Based on these morphological changes we hypothesized that MS275 treatment activated the oxidative program, leading to reduced lipid accumulation and consequently to smaller lipid droplets. In addition, we found that treatment with MS275 both at the end of differentiation (Figure 28a) or during differentiation program (Figure 28b) upregulated the expression of gene encoding dehydrogenase of long chain acyl-CoA (*Acadl*), a key enzyme of fatty acid β-oxidation and of the gene encoding isocitrate dehydrogenase 3α

(*Idh3a*), an enzyme of Krebs cycle. The effect of MS275 on the expression of *Acadl* was more pronounced in cells treated with the inhibitor from the beginning of differentiation (3.5 fold increase). Consistently, we detected higher glycerol release in the medium of cells differentiated in the presence of MS275, an index of fatty acid β-oxidation, only in cells exposed to inhibitor from day 1 of differentiation (Figure 28c).
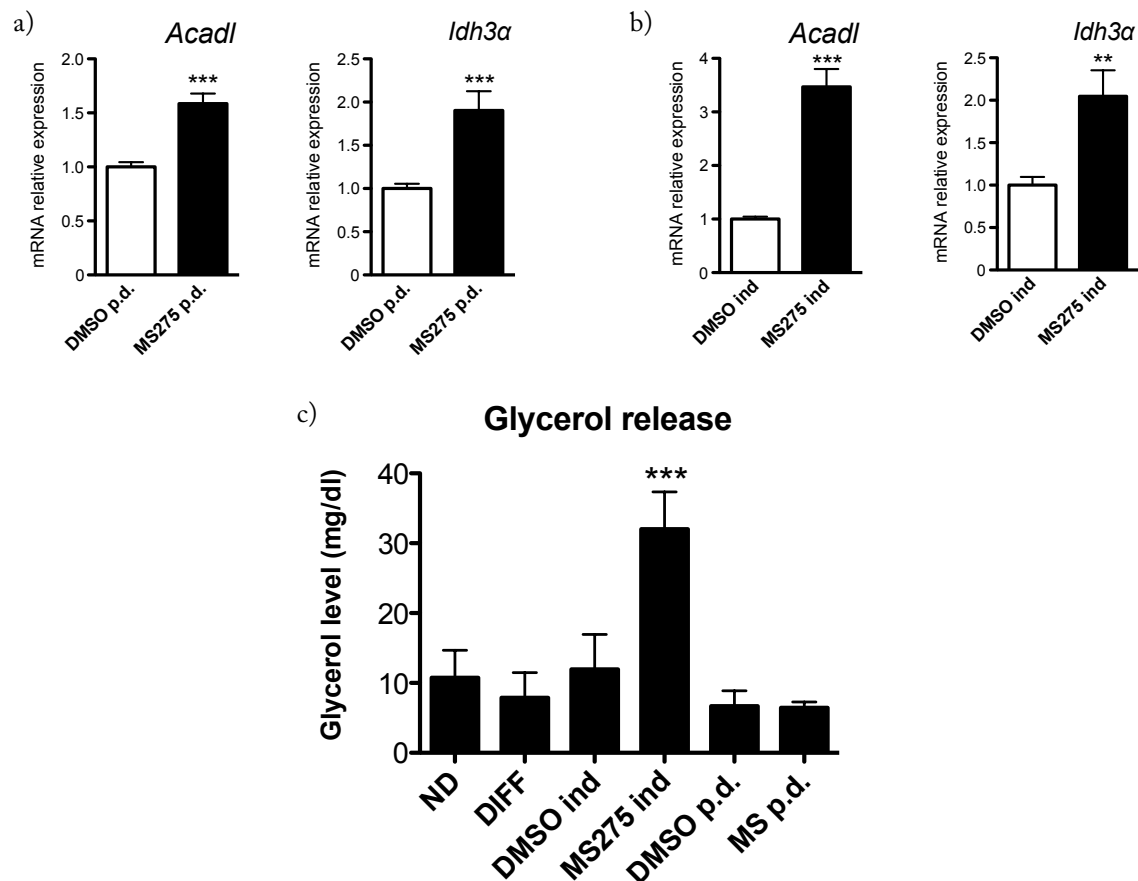
Figure 28: a) Gene expression analysis of markers of fatty acid beta oxidation and Krebs cycle in cells differentiated and exposed to vehicle or to MS275 in the last 24 hours; b) Gene expression analysis of markers of fatty acid beta oxidation and Krebs cycle in cells differentiated in presence of vehicle or MS275. Statistical analysis: Student's t test, $**p<0.01$, $***p<0.001$; c) Measurement of glycerol release in medium of differentiated cells in all the cited conditions. ND: cells not differentiated, DIFF: cells differentiated with classic cocktail. Statistical analysis: One way ANOVA, Tukey as post hoc test, $***p<0.001$.

Class I HDAC inhibition does not affect lipid accumulation in C3H10T1/2 mesenchymal stem cells

The observation of enhanced fatty acid β-oxidation in C3H10T1/2 cells exposed to MS275 from the beginning of differentiation suggested reduction of lipid accumulation in these cells. Surprisingly Oil Red O staining reveled that, in spite of the drastic change of cellular morphology, lipid accumulation in cells treated with the class I selective inhibitor during differentiation (Figure 29) did not differ from that of control cells.
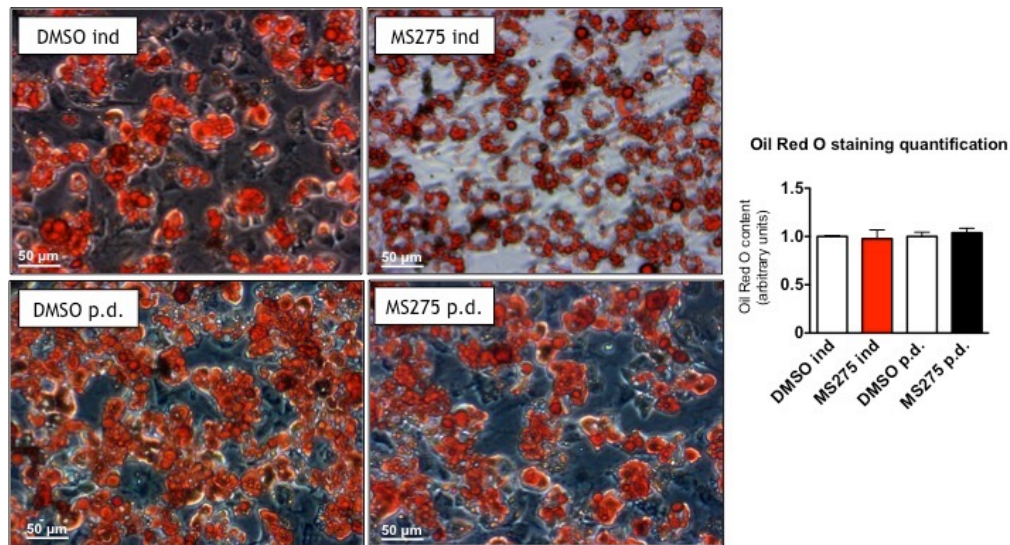
Figure 29: a) Oil Red O staining in C3H10T1/2 cells differentiated in presence of vehicle or MS275 (top panels) or differentiated with classic cocktail and treated with vehicle or MS275 in the last 24 hours (bottom panels); **b)** Oil Red O spectrophotometric quantification.

Class I HDAC inhibition increases adipocyte functionality marker expression in differentiating C3H10T1/2 mesenchymal stem cells

To gain more insights on the effect of class I HDAC inhibition on adipocyte differentiation and functionality we performed gene expression analysis on C3H10T1/2 cells terminally differentiated and treated with MS275: the class I HDAC inhibitor did not affect the expression of the master regulator of adipocyte functionality *Pparγ* and it decreased the expression of *Acrp30* and *Glut4*, whose expression correlates with insulin sensitivity. On the other hand, MS275 increased the expression of *Fabp4*, a key mediator of intracellular transport and metabolism of fatty acids in adipose tissues. The expression of other important markers of adipose tissue functionality, such as the transcriptional factors *C/EBPα, C/EBPβ*, perilipin (*Plin*), a protein that coats lipid droplets in adipocytes, and the scavenger receptor Cd36 (*Cd36*) was not affected by MS275 treatment at the end of differentiation (Figure 30).

Conversely in C3H10T1/2 cells differentiated in the presence of MS275 we detected significant increase of Pparγ expression (both at mRNA and protein level), and its main targets (*Acrp30, Glut4, Fabp4*) and others adipocyte functionality markers (*C/EBPα, Plin, Cd36*) (Figure 31).

A kinetic study of gene expression analysis in C3H10T1/2 cells exposed to vehicle or MS275 from the beginning of differentiation reveled that the class I HDAC inhibitor induced a significant increase of all markers from day 5 of differentiation, reaching the maximum effect at day 9 of differentiation (Figure 32).

Interestingly, we detected the same kinetic gene expression profile in cells incubated with MS275 only for the first 72 hours of differentiation program, suggesting that early inhibition of class I HDACs is sufficient to "imprint" preadipocytes cell fate and commit them to adipocytes (Figure 33).

Figure 30: Gene expression analysis of adipocyte markers in C3H10T1/2 cells not differentiated (ND), differentiated with classic cocktail (DIFF), or differentiated with classic cocktail and treated with vehicle (DMSO p.d.) or MS275 (MS275 p.d.) for the last 24 hours. Statistical analysis: Student's t test, *p<0.05.
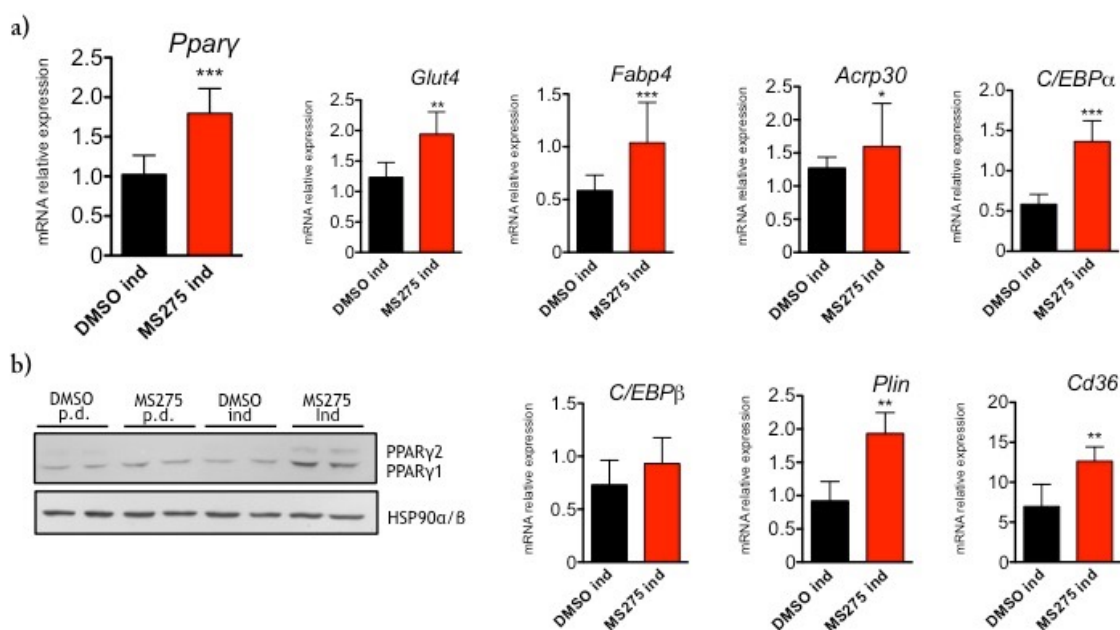
Figure 31: a) Gene expression analysis of adipocyte markers in C3H10T1/2 cells differentiated in presence of vehicle (DMSO ind) or MS275 (MS275 ind). Statistical analysis: Student's t test, *p<0.05, **p<0.01, ***p<0.001; b) Western blot analysis showing Pparγ expression in cells differentiated with classic cocktail and treated with vehicle (DMSO p.d.) or MS275 (MS275 p.d.) for the last 24 hours, and in cells differentiated in presence of vehicle (DMSO ind) or MS275 (MS275 ind). Student's t test, *p<0.05, **p<0.01, ***p<0.001.
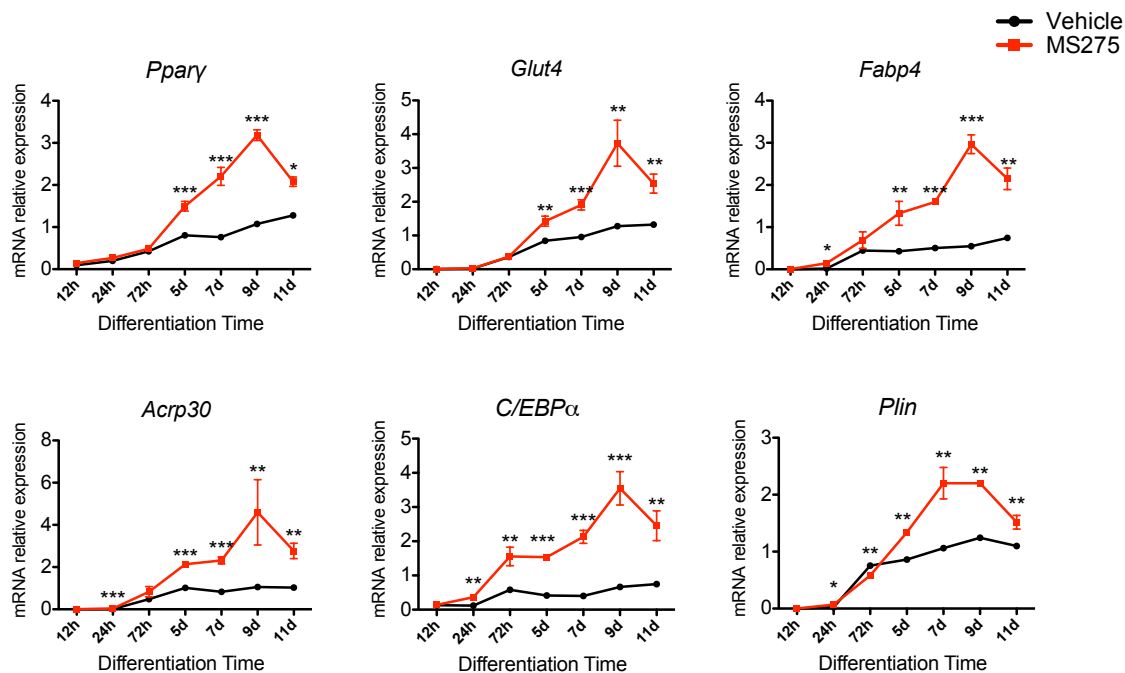
Figure 32: Kinetic study of gene expression of adipocyte markers in C3H10T1/2 cells exposed to vehicle or with MS275 from the induction to the end of the experiment (day 11). Statistical analysis: Student's t test, *p<0.05, **p<0.01, ***p<0.001.
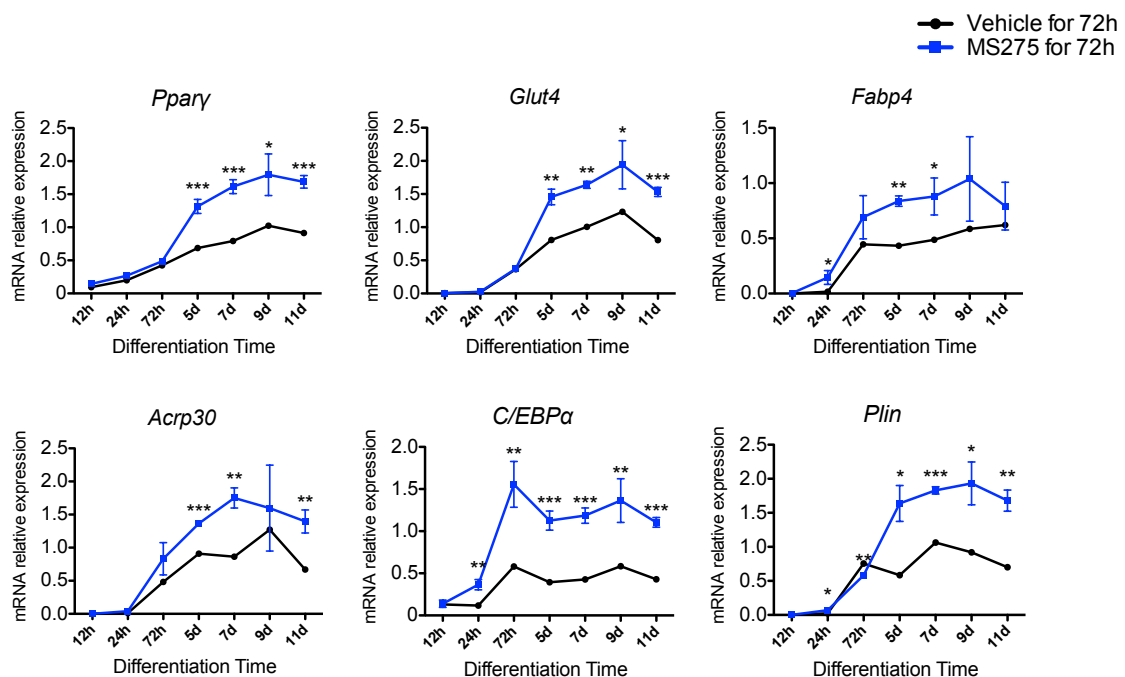
Figure 33: Kinetic study of gene expression of adipocyte markers in C3H10T1/2 cells exposed to vehicle or with MS275 for 72 hours at the beginning of differentiation. Statistical analysis: Student's t test, *p<0.05, **p<0.01, ***p<0.001.

Class I HDAC inhibition promotes lipid turnover in differentiating C3H10T1/2 cells

We next wanted to investigate whether treatment with the class I HDAC inhibitor affects lipid turnover. To this end, we measured the expression of typical markers of lipogenesis, such as the gene encoding fatty acid synthase (*Fasn*), and of lipolysis (e.g., hormone sensitive lipase *Hsl* and the adipose TG lipase *Atgl*). Interestingly, we found that only cells exposed to MS275 from the beginning of differentiation showed statistically significant increase of the expression of markers of lipogenesis and lipolysis (Figure 34), suggesting that early inhibition of class I HDAC in differentiation program promotes greater lipid turnover in this cell line.
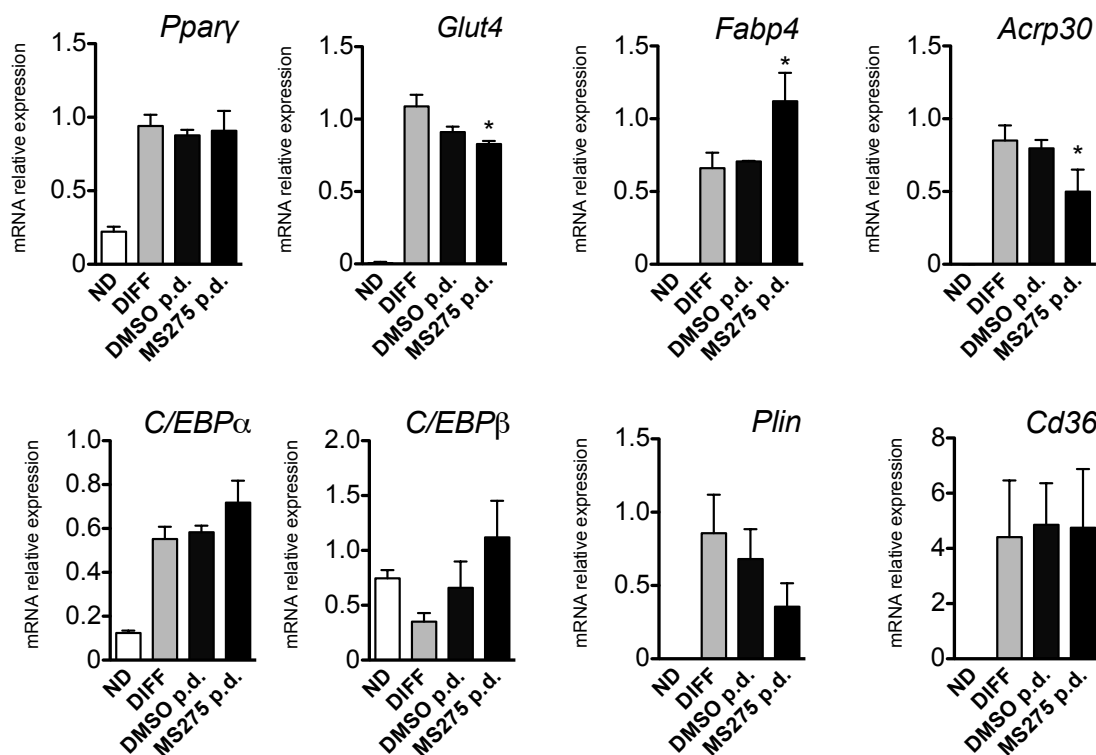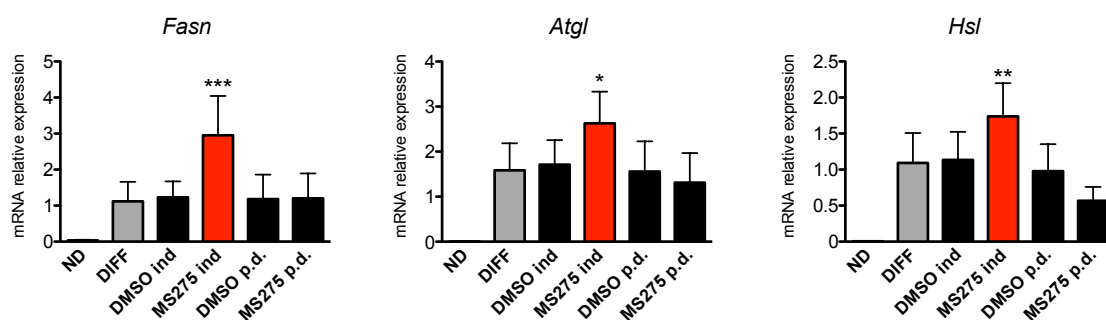

Figure 34: Gene expression analysis of lipogenesis/lipolysis markers in C3H10T1/2 cells not differentiated (ND), differentiated with classic cocktail (DIFF), differentiated in presence of vehicle (DMSO ind) or MS275 (MS275 ind), and differentiated with classic cocktail and treated with vehicle (DMSO p.d.) or MS275 (MS275 p.d.) for the last 24 hours. Statistical analysis: One way ANOVA, Tukey as post hoc test, **p<0.01, ***p<0.001.

Inhibition of class I histone deacetylases hampers differentiation in adipose-committed preadipocyte

Surprisingly, in a different cell model of adipocyte precursor, committed preadipocytes 3T3-L1, treatment with MS275 at the beginning of differentiation completely blocks differentiation program. In cells exposed to the class I HDAC inhibitor from day 1 of differentiation we detected significant reduction of adipocyte marker *Ppary*, *Glut4*, *Fabp4* and *Acrp30* (Figure 35).
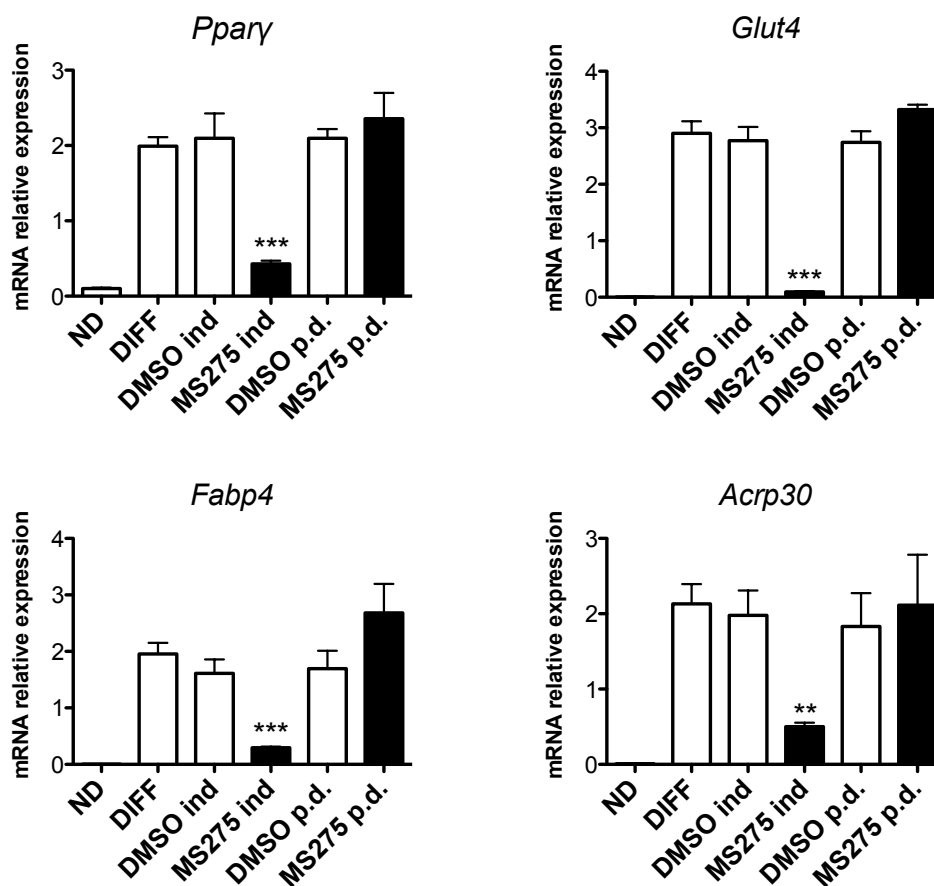
Figure 35: Gene expression analysis of adipocyte markers in 3T3-L1 cells not differentiated (ND), differentiated with classic cocktail (DIFF), differentiated in presence of vehicle (DMSO ind) or MS275 (MS275 ind), and differentiated with classic cocktail and treated with vehicle (DMSO p.d.) or MS275 (MS275 p.d.) for the last 24 hours. Statistical analysis: One way ANOVA, Tukey as post hoc test, **p<0.01, ***p<0.001.

Effect of tissue specific deletion of Hdac3 on body weight

Our previous studies with RNAi and ChIP analyses suggested HDAC3 as a candidate target for the metabolic effects of MS275 on energy metabolism in skeletal muscle and adipose tissue. Therefore, to investigate the role of Hdac3 in skeletal muscle and adipose tissue in a setting of obesity, we generated the tissue specific knock out mouse models of Hdac3 in skeletal muscle Hdac3 (H3smKO) and adipose tissue (H3atKO). At 8 weeks of age we fed male knock out mice and male littermates control mice (Floxed) with a high fat high sucrose (HFHS) diet. After 16 weeks on HFHS diet, H3smKO showed significant reduction of body weight when compared to floxed mice, while no differences were detected in H3atKO mice compared to control mice (Figure 36). These preliminary observations with tissue specific knock out mice, suggest that Hdac3 may be involved in the determination of body mass and pave the way to further investigations in these animal models to unravel the underlying mechanisms.
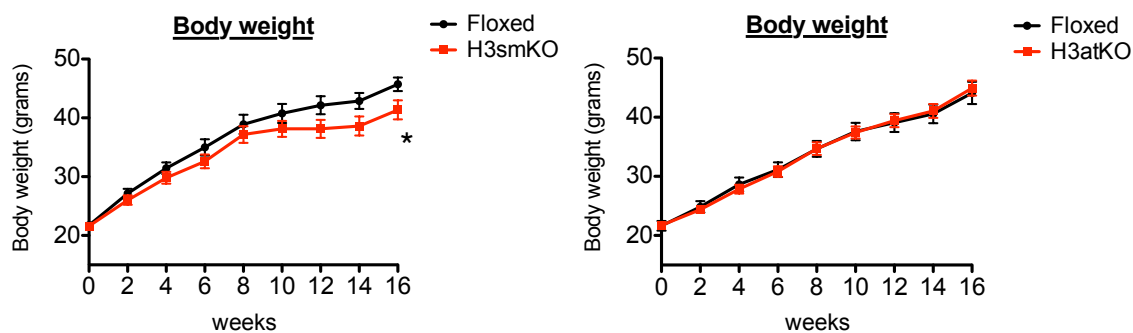
Figure 36: Increase in body weight in knock out and wild type mice fed HFHS diet for 16 weeks. Statistical analysis: Student's t test, *p<0.05.

Discussion

Class I histone deacetylases enhance mitochondrial function of skeletal muscle and brown adipose tissue

Skeletal muscle plays an important role in energy metabolism and recent studies showed that HDACs participate in metabolic regulation in this organ[241]. A study by Potthoff and colleagues demonstrated the involvement of different HDACs in differentiation and remodeling of skeletal muscle through transcriptional modulation of key genes of mitochondrial biogenesis and oxidative metabolism[242]. Accordingly, inhibition of class I HDACs increased oxidation of substrates in the electron transport chain in skeletal muscle gastrocnemius of *db/db* mice[238]. Here we demonstrated that this is the result of a mitochondrial re-organization: MS275 treated myotubes showed a higher density of small mitochondria, that are metabolically active, and characterized by strong oxidative potential.

MS275 is known to inhibit both HDAC1 and HDAC3, although only HDAC3 inhibition recapitulated the effect of class I HDAC inhibitor, as it up-regulated the expression of *Pgc-1α* and of its main targets[238]. In fact we have shown that the class I HDAC selective inhibitor *in vitro* and *in vivo* induced Pgc-1α transcription by blunting HDAC3 recruitment to MEF binding site in the Pgc-1α promoter, thus driving oxidative gene expression in skeletal muscle. HDAC3 is a crucial player also in the regulation of brown adipose tissue oxidative potential, as *in vivo* ChIP from BAT of *db/db* mice showed that MS275 reduced recruitment of this HDAC isoform to PPRE in Pgc-1α promoter. Accordingly, the class I HDAC inhibitor increased mitochondrial biogenesis and activity in isolated primary brown adipocytes, pinpointing a crucial role of HDAC3 in the regulation of oxidative capacity of brown fat.

Class I HDAC inhibition as a strategy to cope diet induced obesity

In the last decades the interest about the study of human obesity and its co-morbidities increased exponentially. Since western obesity is strictly related to a diet enriched in fat and carbohydrates, in this study we used a murine model of diet-induced obesity (DIO) to investigate the role of HDACs in the developing of this pathological condition.

Class I HDACs emerged as important regulators of energy homeostasis: inhibition of this class of enzymes by MS275 reduced body weight, enhanced glucose tolerance and improved thermogenic capacity. Interestingly, unlike the effects described in *db/db* mice, in DIO mice inhibition of class I HDACs did not significantly affect skeletal muscle functionality. *db/db* mice are in fact profoundly compromised at the metabolic level and develop diabetes and insulin resistance at early stages of life. The link between diabetes mellitus and impaired muscle mitochondrial oxidative function has been established[243] and it has been proposed that it might be associated to lower mitochondrial density[244]. However, in a model of diet-induced obesity, lipid infiltration and disruption of

mitochondrial functionality in skeletal muscle are probably some of the late stage complications of the pathological status. Thus is difficult to appreciate the beneficial effect of MS275 treatment on mitochondrial biogenesis in skeletal muscles in DIO mice. Since we did not detect relevant changes in skeletal muscle, we focused our attention to other important insulin-sensitive organs. The increased thermogenic capacity consequent to treatment with MS275 suggested us to investigate further the effects of class I HDAC inhibitor in BAT. Although BAT mass did not change, we found that BAT phenotype was improved in MS275 treated mice, which showed higher number of smaller multilocular brown adipocytes, expressing BAT markers such as *Dio2* and *Elovl3*. Interestingly no significant changes were found in the expression of *Ucp1* and *Adrb3*. The two proteins encoded by these genes, uncoupling protein 1 and β3 adrenergic receptor, are considered the key activators of the thermogenic program. A possible explanation for the increased thermogenic activation in response to cold in MS275 treated mice came from the analysis of white fat. Interestingly in both subcutaneous and visceral WAT from MS275 treated mice we observed upregulation of *Adrb3*, while a significant increase of *Ucp1* was detected only in viscWAT. "Browning" of white adipose tissue consequent to inhibition of class I HDACs in DIO mice highlighted a different behavior of subcutaneous and visceral WAT. Accordingly, expression of WAT functionality markers, of genes involved in triglycerides and fatty acid catabolism and of mitochondrial biogenesis markers were upregulated in both types of white fat, but at a greater extent in viscWAT. To date, browning of WAT has been obtained by pharmacological treatment or by genetic manipulation[54,76,245] in inguinal WAT or on epidydimal WAT. Our data, showing browning in visceral mesenteric WAT indicate that class I HDAC selective inhibition induces deep reprogramming in adipocyte differentiation pathway, resulting in more functional visceral adipocytes. White adipocytes of MS275 treated mice could, in fact, better internalize lipids, efficiently store them as triglycerides and used them as a metabolic fuel as a result of increased expression of β-oxidation genes (i.e. *Acadl*, *Cpt1b*). The finding of improved functionality of mesenteric white adipose tissue is particularly relevant when considering the link between the intra-abdominal fat accumulation typical of obesity and other related severe complications, such as cardiovascular events[235]. In spite of these considerations the MRI analysis revealed a significant reduction of adipose mass in subcutaneous WAT whereas in visceral WAT the trend did not reach statistical significance. This could depend on different features of viscWAT and subWAT: subcutaneous fat, which is less susceptible to inflammation[246], is characterized by larger adipocytes than those of visceral fat. MS275 reduced the size of both subcutaneous and visceral adipocytes, however the effect was more pronounced in subWAT. This dramatic reduction of subcutaneous adipocytes hypertrophy can explain the reduced subWAT mass, as detected by MRI analysis. Conversely, gene expression analysis of functionality markers showed that MS275 is more efficient in visceral fat: visceral adipocytes are smaller than subcutaneous adipocytes yet more susceptible to inflammation because of their lower critical size. Thus, even though the reduction in adipocyte size is not as evident as in subWAT, the decrease of adipocyte hypertrophy is sufficient to rescue

adipocyte functionality, as assessed by gene expression analysis. On the contrary, subcutaneous adipocytes in obesity feature greater expandability that does not impair their functionality. Thus, the effects of MS275 on the expression of functionality markers are less pronounced in subWAT as compared to the effects observed in viscWAT.

In the liver of DIO mice treated with MS275 we found reduced lipid steatosis, as assessed by histological analysis and by mass spectrometry analysis of total fatty acids. The reduction of hepatic steatosis contrasts with the accumulation of liver lipids seen in mice with specific deletion of HDAC3 in liver[247,248]. This difference may be ascribed to the effect of global versus local HDAC3 inhibition: in diabetic mice, systemic HDAC3 inhibition (i.e., MS275 treatment) increases oxidative metabolism and energy expenditure in other tissues such as adipose tissue, thus preventing hepatic lipid buildup.

Our *in vivo* results demonstrate that inhibition of class I HDACs in a model of diet-induced obesity ameliorates obese and diabetic phenotype, as a consequence of improved functionality of adipose tissue, preventing the excessive lipid accumulation that would impair adipocyte function and lead to insulin resistance.

Class I HDACs in cell fate determination of early adipocyte precursors

The amelioration of adipose tissue functionality consequent to MS275 treatment raised new questions about the role of class I HDACs in WAT physiology. The elucidation of epigenetic pathways regulating early stages of adipocyte differentiation from precursors is still missing. Our results in mesenchymal stem cells C3H10T1/2 demonstrated that MS275 reduced cell size, as a consequence of reduction in lipid droplets size, only if added at the beginning of differentiation. Nevertheless, these cells maintained unaltered capacity to accumulate lipids. Considering that cells differentiating in the presence of MS275 accumulate similar amount of lipids compared to cells differentiated without MS275, we speculate that MS275 increased the number of differentiated cells. Considering that the onset of obesity correlates with adipocyte hypertrophy[30], which is closely linked to adipose tissue inflammation, by increasing the number of differentiated adipocytes MS275 treatment prevented excessive lipid accumulation in the already differentiated adipocytes, ultimately avoiding the activation of inflammatory pathways. The net result was higher number of smaller but more functional adipocytes.

Consistent with this interpretation, we observed that C3H10T1/2 cells differentiated in presence of MS275 showed a significant increase in the expression of markers of adipocyte functionality. On the contrary, in fully differentiated C3H10T1/2 cells treatment with the class I HDAC inhibitor MS275 did not affect the expression of adipocyte functionality marker, suggesting that inhibition of class I HDACs selectively in early precursors may influence the differentiation fate of these cells. At this regard, it is worth mentioning that adipocyte precursors exposed to MS275 only during the first 72 hours of differentiation program expressed higher levels of adipose marker genes. This

suggests that class I HDAC inhibition at early stages of adipose differentiation is sufficient to imprint preadipocyte fate toward a different adipose phenotype.

In this experimental setting we also detected increased expression of genes involved in lipogenesis, lipolysis and fatty acid β-oxidation in C3H10T1/2 cells differentiated in the presence of MS275, suggesting higher lipid turnover in cells treated with the selective class I HDAC inhibitor. This is relevant because it has been reported that healthy adipocytes are characterized by higher lipid turnover and that the balance between lipid storage and removal is important to preserve the functionality of adipose tissue, preventing severe metabolic impairment. It should be noted that high storage but low triglyceride removal promotes fat tissue accumulation and obesity, while reduction of both triglyceride storage and removal decreases lipid shunting through adipose tissue and thus promotes dyslipidaemia[249]. Interestingly we found increased expression of markers of oxidative metabolism also in fully differentiated C3H10T1/2 cells treated with MS275: this result suggests that class I HDAC inhibition in mature adipocytes induces a metabolic switch of these cells to a more oxidative phenotype, preventing further lipid accumulation in resident adipocytes.

Overall, results obtained in C3H10T1/2 showed that treatment with the selective class I HDAC inhibitor remodels adipocytes features, providing an explanation to the restored functionality of WAT detected in MS275-treated obese mice.

Interestingly, we found an opposite effect of MS275 in differentiating 3T3-L1 preadipocytes, as the inhibitor completely abolished the differentiation, by reducing the expression of adipocyte markers. This result is consistent with Nebbioso et al.[230] who demonstrated that treatment of 3T3-L1 cells with MS275 for 8 days during differentiation blocked adipogenesis. Several independent studies reported conflicting results regarding the role of HDACs in adipocyte differentiation. In 3T3-L1 preadipocytes treated with the pan-HDAC inhibitors TSA, suberoylanilide hydroxamic acid (SAHA), or Scriptaid, differentiation and adipogenesis was inhibited[250]. Conversely, the HDAC inhibitors sodium butyrate and valproic acid increased differentiation of 3T3-L1 cells to adipocyte. Some authors explained the different behavior of 3T3-L1 cells in response to HDAC inhibitors as related to the chemical identity of these compounds. Haberland and collaborators stated that the adipogenic effect of valproic acid and butyrate is due to their short chain fatty acid (SCFA) nature and not to the fact that these molecules are HDAC inhibitors[226]. We believe that the effects of MS275 observed in C3H10T1/2 cells can be explained considering the differences among the two cell lines used in our study. C3H10T1/2 cells are early adipocyte precursors; they can be differentiated to osteoblasts, chondrocytes, or adipocytes in response to appropriate signals[251]. 3T3-L1 cells are, instead, preadipocytes that are already committed toward the adipose fate. Thus, based on our results, we propose that the epigenome setting changes at different stages of adipose differentiation. Early perturbation of this setting induced by MS275 in C3H10T1/2 leads to the induction of the adipose phenotype here described. Conversely, the later perturbation of epigenome induced by MS275 in 3T3-L1 cells blocks adipocyte differentiation, as reported by other authors.

To further characterize the effect of MS275 in adipose cell lines, future experiments will focus on pathways involved in the early steps of differentiation programs (e.g., Wnt signaling and the Zfp423/Zfp521 pathway. These zinc finger proteins represent interesting targets since it has been reported that Zfp423 amplifies the effects of BMPs via a SMAD interaction domain inducing adipose lineage commitment. Zfp423 expression in the developing adipocyte is repressed by the highly related factor Zfp521, which promotes osteogenesis and inhibits adipogenesis through interactions with Ebf1, a transcription factor required for early adipose commitment[112,113]. It has been demonstrated that Zfp521 expression declines during adipogenesis in C3H10T1/2 cells; this allows the expression of Zfp423 that activates the adipose differentiation program. Moreover knockdown of Zfp521 results in increased H3K9 acetylation, an epigenetic mark of transcriptionally active chromatin, in the Zfp423 promoter region[205]. Thus Zfp423 could be a possible target of MS275 effect in the early stage of differentiation.

Furthermore, it has been reported that Zfp521 interacts with HDAC3 and that this complex regulates the osteoblastic differentiation program of progenitor cells[252]. Considering that adipocytes and osteoblasts arise from the same precursor, we theorize that, as demonstrated for other cellular models (e.g. C2C12 myotubes and primary brown adipocytes) HDAC3 could be a player in the mechanism whereby MS275 regulates preadipocyte fate. Further chromatin immunoprecipitation experiments will be required to probe this hypothesis, to cast a new light upon the role of histone deacetylases in the regulation of adipocyte commitment.

Deletion of Hdac3 in skeletal muscle prevents body weight gain

Our latest results in skeletal muscle Hdac3 knock out (H3smKO) and adipose tissue Hdac3 knock out (H3atKO) fed for 16 weeks with a diet enriched in fat and carbohydrates (HFHS) showed that only Hdac3 deletion in skeletal muscle reduced weight gain significantly. These promising results confirmed the key role of skeletal muscle in the regulation of energy homeostasis and suggested HDAC3 as an important regulator of muscle metabolism and function. Furthermore, even though we observed no change in body weight gain during challenge with HFHS diet in H3atKO, we cannot rule out that Hdac3 may play a role in adipose tissue functionality. HDAC3 in fact, along with the transcriptional corepressor NCoR1 participates in the formation of repressive complex that binds Pparγ promoter205. Recently Olefsky and collaborators demonstrated that specific adipose deletion of NCoR1 increased obesity. Nevertheless, NCoR1 adipose tissue knock out (AKO) mice showed improved glucose tolerance. Euglycemic clamp studies demonstrated enhanced insulin sensitivity in liver, muscle and fat[208]. Accordingly, we will investigate whether adipose deletion of Hdac3 will recapitulate a phenotype similar to that of the AKO mice.

Conclusions

The results reported in this thesis demonstrate the importance of class I histone deacetylases in the regulation of several aspects of energy metabolism. First, in depots enriched in mitochondria, as skeletal muscle and brown adipose tissue, the inhibition of class I HDACs stimulates mitochondrial biogenesis and mitochondrial function, potentiating the oxidative capacity of these tissues. On the other hand, inhibition of these enzymes reverts the loss of functionality of obese white adipose tissue, due to the activation of an oxidative program in differentiated adipocytes and to a reprogramming of adipocyte precursor fate toward a healthier adipose phenotype. Based on literature and on our results, our hypothesis is that these effects can be ascribed to inhibition of HDAC3. Further *in vivo* and *ex vivo* studies in skeletal muscle and adipose tissue Hdac3 specific knock out mice will be required to test this hypothesis. The full characterization of the phenotype of these mouse models will shed a new light on the role played by HDAC3 in the pathophysiology of metabolic disorders.

References

1   Froguel, P. & Boutin, P. Genetics of pathways regulating body weight in the development of obesity in humans. *Experimental biology and medicine (Maywood, N.J.)* **226**, 991-996 (2001).

2   Maillard, G. *et al.* Macronutrient energy intake and adiposity in non obese prepubertal children aged 5-11 y (the Fleurbaix Laventie Ville Sante Study). *International journal of obesity and related metabolic disorders : journal of the International Association for the Study of Obesity* **24**, 1608-1617 (2000).

3   Hedley, A. A. *et al.* Prevalence of overweight and obesity among US children, adolescents, and adults, 1999-2002. *Jama* **291**, 2847-2850, doi:10.1001/jama.291.23.2847 (2004).

4   Kopelman, P. G. Obesity as a medical problem. *Nature* **404**, 635-643 (2000).

5   Tchernof, A. & Despres, J. P. Pathophysiology of human visceral obesity: an update. *Physiol Rev* **93**, 359-404, doi:10.1152/physrev.00033.2011 (2013).

6   Cummings, D. E. & Schwartz, M. W. Genetics and pathophysiology of human obesity. *Annual review of medicine* **54**, 453-471, doi:10.1146/annurev.med.54.101601.152403 (2003).

7   Kahn, S. E., Hull, R. L. & Utzschneider, K. M. Mechanisms linking obesity to insulin resistance and type 2 diabetes. *Nature* **444**, 840-846 (2006).

8   Martins, A. R. *et al.* Mechanisms underlying skeletal muscle insulin resistance induced by fatty acids: importance of the mitochondrial function. *Lipids in health and disease* **11**, 30, doi:10.1186/1476-511x-11-30 (2012).

9   Kasuga, M. Insulin resistance and pancreatic {beta} cell failure. *J. Clin. Invest. %R 10.1172/JCI29189* **116**, 1756-1760 (2006).

10   Okada, T., Kawano, Y., Sakakibara, T., Hazeki, O. & Ui, M. Essential role of phosphatidylinositol 3-kinase in insulin-induced glucose transport and antilipolysis in rat adipocytes. Studies with a selective inhibitor wortmannin. *J Biol Chem* **269**, 3568-3573 (1994).

11   Boucher, J., Kleinridders, A. & Kahn, C. R. Insulin receptor signaling in normal and insulin-resistant states. *Cold Spring Harbor perspectives in biology* **6**, doi:10.1101/cshperspect.a009191 (2014).

12   Dresner, A. *et al.* Effects of free fatty acids on glucose transport and IRS-1-associated phosphatidylinositol 3-kinase activity. *J Clin Invest* **103**, 253-259, doi:10.1172/jci5001 (1999).

13   Petersen, K. F. & Shulman, G. I. Etiology of insulin resistance. *Am J Med* **119**, S10-16, doi:10.1016/j.amjmed.2006.01.009 (2006).

14   Jump, D. Fatty acid regulation of gene transcription. *Crit Rev Clin Lab Sci* **41**, 41-78 (2004).

15   Tchkonia, T. *et al.* Mechanisms and Metabolic Implications of Regional Differences among Fat Depots. *Cell metabolism* **17**, 644-656 (2013).

16   Nedergaard, J., Bengtsson, T. & Cannon, B. Unexpected evidence for active brown adipose tissue in adult humans. *Am J Physiol Endocrinol Metab* **293**, E444-452, doi:10.1152/ajpendo.00691.2006 (2007).

17   Pond, C. M. Adipose tissue and the immune system. *Prostaglandins, leukotrienes, and essential fatty acids* **73**, 17-30, doi:10.1016/j.plefa.2005.04.005 (2005).

18   Cannon, B. & Nedergaard, J. Brown adipose tissue: function and physiological significance. *Physiol Rev* **84**, 277-359, doi:10.1152/physrev.00015.2003 (2004).

19   Alkhouli, N. *et al.* The mechanical properties of human adipose tissues and their relationships to the structure and composition of the extracellular matrix. *Am J*

Physiol Endocrinol Metab **305**, E1427-1435, doi:10.1152/ajpendo.00111.2013 (2013).

20   Trayhurn, P. & Beattie, J. H. Physiological role of adipose tissue: white adipose tissue as an endocrine and secretory organ. *The Proceedings of the Nutrition Society* **60**, 329-339 (2001).

21   Rosen, Evan D. & Spiegelman, Bruce M. What We Talk About When We Talk About Fat. *Cell* **156**, 20-44 (2014).

22   Kershaw, E. E. & Flier, J. S. Adipose Tissue as an Endocrine Organ. *The Journal of Clinical Endocrinology & Metabolism* **89**, 2548-2556, doi:doi:10.1210/jc.2004-0395 (2004).

23   Zhang, Y. *et al.* Positional cloning of the mouse obese gene and its human homologue. *Nature* **372**, 425-432 (1994).

24   Ruan, H. & Lodish, H. F. Insulin resistance in adipose tissue: direct and indirect effects of tumor necrosis factor-α. *Cytokine & Growth Factor Reviews* **14**, 447-455 (2003).

25   Maeda, K. *et al.* cDNA Cloning and Expression of a Novel Adipose Specific Collagen-like Factor, apM1 (AdiposeMost Abundant Gene Transcript 1). *Biochemical and Biophysical Research Communications* **221**, 286-289, doi:http://dx.doi.org/10.1006/bbrc.1996.0587 (1996).

26   Banerjee, R. R. & Lazar, M. A. Resistin: molecular history and prognosis. *Journal of molecular medicine (Berlin, Germany)* **81**, 218-226, doi:10.1007/s00109-003-0428-9 (2003).

27   Mertens, I. & Gaal, L. F. V. Obesity, haemostasis and the fibrinolytic system. *Obesity Reviews* **3**, 85-101, doi:10.1046/j.1467-789X.2002.00056.x (2002).

28   Belanger, C., Luu-The, V., Dupont, P. & Tchernof, A. Adipose tissue intracrinology: potential importance of local androgen/estrogen metabolism in the regulation of adiposity. *Hormone and metabolic research = Hormon- und Stoffwechselforschung = Hormones et metabolisme* **34**, 737-745, doi:10.1055/s-2002-38265 (2002).

29   Greenberg, A. S. *et al.* Perilipin, a major hormonally regulated adipocyte-specific phosphoprotein associated with the periphery of lipid storage droplets. *J Biol Chem* **266**, 11341-11346 (1991).

30   Tchoukalova, Y. D. *et al.* Regional differences in cellular mechanisms of adipose tissue gain with overfeeding. *Proc Natl Acad Sci U S A* **107**, 18226-18231, doi:10.1073/pnas.1005259107 (2010).

31   Johnson, P. R. & Hirsch, J. Cellularity of adipose depots in six strains of genetically obese mice. *Journal of Lipid Research* **13**, 2-11 (1972).

32   Wellen, K. E. & Hotamisligil, G. S. Inflammation, stress, and diabetes. *J Clin Invest* **115**, 1111-1119, doi:10.1172/jci25102 (2005).

33   Weisberg, S. P. *et al.* Obesity is associated with macrophage accumulation in adipose tissue. *The Journal of Clinical Investigation* **112**, 1796-1808, doi:10.1172/JCI19246 (2003).

34   Clement, K. *et al.* Weight loss regulates inflammation-related genes in white adipose tissue of obese subjects. *Faseb j* **18**, 1657-1669, doi:10.1096/fj.04-2204com (2004).

35   Ramos-Nino, M. E. The role of chronic inflammation in obesity-associated cancers. *ISRN oncology* **2013**, 697521, doi:10.1155/2013/697521 (2013).

36   Green, A., Dobias, S. B., Walters, D. J. & Brasier, A. R. Tumor necrosis factor increases the rate of lipolysis in primary cultures of adipocytes without altering levels of hormone-sensitive lipase. *Endocrinology* **134**, 2581-2588, doi:10.1210/endo.134.6.8194485 (1994).

37   Guilherme, A., Virbasius, J. V., Puri, V. & Czech, M. P. Adipocyte dysfunctions linking obesity to insulin resistance and type 2 diabetes. *Nat Rev Mol Cell Biol* **9**, 367-377, doi:10.1038/nrm2391 (2008).

38   Xu, H. *et al.* Chronic inflammation in fat plays a crucial role in the development of obesity-related insulin resistance. *J Clin Invest* **112**, 1821-1830, doi:10.1172/jci19451 (2003).

39   Arkan, M. C. *et al.* IKK-beta links inflammation to obesity-induced insulin resistance. *Nat Med* **11**, 191-198, doi:10.1038/nm1185 (2005).

40   Cinti, S. *et al.* Adipocyte death defines macrophage localization and function in adipose tissue of obese mice and humans. *Journal of Lipid Research* **46**, 2347-2355, doi:10.1194/jlr.M500294-JLR200 (2005).

41   Arkan, M. C. *et al.* IKK-b links inflammation to obesity-induced insulin resistance. *Nat Med* **11**, 191 (2005).

42   Stern, J. S., Batchelor, B. R., Hollander, N., Cohn, C. K. & Hirsch, J. Adipose-cell size and immunoreactive insulin levels in obese and normal-weight adults. *Lancet* **2**, 948-951 (1972).

43   Harman-Boehm, I. *et al.* Macrophage infiltration into omental versus subcutaneous fat across different populations: effect of regional adiposity and the comorbidities of obesity. *J Clin Endocrinol Metab* **92**, 2240-2247, doi:10.1210/jc.2006-1811 (2007).

44   Hausman, D. B., DiGirolamo, M., Bartness, T. J., Hausman, G. J. & Martin, R. J. The biology of white adipocyte proliferation. *Obesity reviews : an official journal of the International Association for the Study of Obesity* **2**, 239-254 (2001).

45   Tchkonia, T. *et al.* Fat tissue, aging, and cellular senescence. *Aging Cell* **9**, 667-684, doi:10.1111/j.1474-9726.2010.00608.x (2010).

46   Hill, A. A., Reid Bolus, W. & Hasty, A. H. A decade of progress in adipose tissue macrophage biology. *Immunological reviews* **262**, 134-152, doi:10.1111/imr.12216 (2014).

47   Vieira-Potter, V. J. Inflammation and macrophage modulation in adipose tissues. *Cellular microbiology* **16**, 1484-1492, doi:10.1111/cmi.12336 (2014).

48   Lumeng, C. N., Bodzin, J. L. & Saltiel, A. R. Obesity induces a phenotypic switch in adipose tissue macrophage polarization. *J Clin Invest* **117**, 175-184, doi:10.1172/jci29881 (2007).

49   Oh, D. Y., Morinaga, H., Talukdar, S., Bae, E. J. & Olefsky, J. M. Increased macrophage migration into adipose tissue in obese mice. *Diabetes* **61**, 346-354, doi:10.2337/db11-0860 (2012).

50   Cypess, A. M. *et al.* Identification and Importance of Brown Adipose Tissue in Adult Humans. *N Engl J Med* **360**, 1509-1517, doi:10.1056/NEJMoa0810780 (2009).

51   Nicholls, D. G., Bernson, V. S. & Heaton, G. M. The identification of the component in the inner membrane of brown adipose tissue mitochondria responsible for regulating energy dissipation. *Experientia. Supplementum* **32**, 89-93 (1978).

52   Chechi, K., Carpentier, A. C. & Richard, D. Understanding the brown adipocyte as a contributor to energy homeostasis. *Trends Endocrinol Metab* **24**, 408-420, doi:10.1016/j.tem.2013.04.002 (2013).

53   Morrison, S. F., Madden, C. J. & Tupone, D. Central control of brown adipose tissue thermogenesis. *Frontiers in Endocrinology* **3**, doi:10.3389/fendo.2012.00005 (2012).

54   Harms, M. & Seale, P. Brown and beige fat: development, function and therapeutic potential. *Nat Med* **19**, 1252-1263, doi:10.1038/nm.3361 (2013).

55   Bordicchia, M. *et al.* Cardiac natriuretic peptides act via p38 MAPK to induce the brown fat thermogenic program in mouse and human adipocytes. *J Clin Invest* **122**, 1022-1036, doi:10.1172/jci59701 (2012).

56   Whittle, A. J. & Vidal-Puig, A. NPs -- heart hormones that regulate brown fat? *J Clin Invest* **122**, 804-807, doi:10.1172/jci62595 (2012).

57   Cao, W. *et al.* p38 Mitogen-Activated Protein Kinase Is the Central Regulator of Cyclic AMP-Dependent Transcription of the Brown Fat Uncoupling Protein 1 Gene. *Mol. Cell. Biol.* **24**, 3057-3067 (2004).

58   Cao, W., Medvedev, A. V., Daniel, K. W. & Collins, S. beta -Adrenergic Activation of p38 MAP Kinase in Adipocytes. cAMP induction of the uncoupling protein 1 (ucp1) gene requires p38 Map kinase. *J. Biol. Chem.* **276**, 27077-27082 (2001).

59   Puigserver, P. *et al.* A cold-inducible coactivator of nuclear receptors linked to adaptive thermogenesis. *Cell* **92**, 829-839 (1998).

60   Finck, B. N. & Kelly, D. P. PGC-1 coactivators: inducible regulators of energy metabolism in health and disease. *J. Clin. Invest. %R 10.1172/JCI27794* **116**, 615-622 (2006).

61   Mori, M., Nakagami, H., Rodriguez-Araujo, G., Nimura, K. & Kaneda, Y. Essential role for miR-196a in brown adipogenesis of white fat progenitor cells. *PLoS Biol* **10**, e1001314, doi:10.1371/journal.pbio.1001314 (2012).

62   Fedorenko, A., Lishko, P. V. & Kirichok, Y. Mechanism of fatty-acid-dependent UCP1 uncoupling in brown fat mitochondria. *Cell* **151**, 400-413, doi:10.1016/j.cell.2012.09.010 (2012).

63   Nguyen, K. D. *et al.* Alternatively activated macrophages produce catecholamines to sustain adaptive thermogenesis. *Nature* **480**, 104-108, doi:http://www.nature.com/nature/journal/v480/n7375/abs/nature10653.html - supplementary-information (2011).

64   Brito, N. A., Brito, M. N. & Bartness, T. J. Differential sympathetic drive to adipose tissues after food deprivation, cold exposure or glucoprivation. *Am J Physiol Regul Integr Comp Physiol* **294**, R1445-1452, doi:10.1152/ajpregu.00068.2008 (2008).

65   Huttunen, P., Hirvonen, J. & Kinnula, V. The occurrence of brown adipose tissue in outdoor workers. *European journal of applied physiology and occupational physiology* **46**, 339-345 (1981).

66   English, J. T., Patel, S. K. & Flanagan, M. J. Association of pheochromocytomas with brown fat tumors. *Radiology* **107**, 279-281, doi:10.1148/107.2.279 (1973).

67   van Marken Lichtenbelt, W. D. & Schrauwen, P. Implications of nonshivering thermogenesis for energy balance regulation in humans. *Am J Physiol Regul Integr Comp Physiol* **301**, R285-296, doi:10.1152/ajpregu.00652.2010 (2011).

68   Virtanen, K. A. *et al.* Functional brown adipose tissue in healthy adults. *N Engl J Med* **360**, 1518-1525, doi:10.1056/NEJMoa0808949 (2009).

69   Wu, J. *et al.* Beige adipocytes are a distinct type of thermogenic fat cell in mouse and human. *Cell* **150**, 366-376, doi:10.1016/j.cell.2012.05.016 (2012).

70   Walden, T. B., Hansen, I. R., Timmons, J. A., Cannon, B. & Nedergaard, J. Recruited vs. nonrecruited molecular signatures of brown, "brite," and white adipose tissues. *Am J Physiol Endocrinol Metab* **302**, E19-31, doi:10.1152/ajpendo.00249.2011 (2012).

71   Schulz, T. J. *et al.* Brown-fat paucity due to impaired BMP signalling induces compensatory browning of white fat. *Nature* **495**, 379-383, doi:http://www.nature.com/nature/journal/v495/n7441/abs/nature11943.html - supplementary-information (2013).

72   Rosenwald, M., Perdikari, A., Rulicke, T. & Wolfrum, C. Bi-directional interconversion of brite and white adipocytes. *Nat Cell Biol* **15**, 659-667, doi:10.1038/ncb2740 (2013).

73   Vitali, A. *et al.* The adipose organ of obesity-prone C57BL/6J mice is composed of mixed white and brown adipocytes. *J Lipid Res* **53**, 619-629, doi:10.1194/jlr.M018846 (2012).

74   Himms-Hagen, J. *et al.* Multilocular fat cells in WAT of CL-316243-treated rats derive directly from white adipocytes. *American journal of physiology. Cell physiology* **279**, C670-681 (2000).

75   Barbatelli, G. *et al.* The emergence of cold-induced brown adipocytes in mouse white fat depots is determined predominantly by white to brown adipocyte transdifferentiation. *Am J Physiol Endocrinol Metab* **298**, E1244-1253, doi:10.1152/ajpendo.00600.2009 (2010).

76   Petrovic, N. *et al.* Chronic Peroxisome Proliferator-activated Receptor γ (PPARγ) Activation of Epididymally Derived White Adipocyte Cultures Reveals a Population of Thermogenically Competent, UCP1-containing Adipocytes Molecularly Distinct from Classic Brown Adipocytes. *Journal of Biological Chemistry* **285**, 7153-7164, doi:10.1074/jbc.M109.053942 (2010).

77   Bartelt, A. & Heeren, J. Adipose tissue browning and metabolic health. *Nat Rev Endocrinol* **10**, 24-36, doi:10.1038/nrendo.2013.204 (2014).

78   Wenz, T., Rossi, S. G., Rotundo, R. L., Spiegelman, B. M. & Moraes, C. T. Increased muscle PGC-1alpha expression protects from sarcopenia and metabolic disease during aging. *Proc Natl Acad Sci U S A* **106**, 20405-20410, doi:10.1073/pnas.0911570106 (2009).

79   Bostrom, P. *et al.* A PGC1-alpha-dependent myokine that drives brown-fat-like development of white fat and thermogenesis. *Nature* **481**, 463-468, doi:10.1038/nature10777 (2012).

80   Villarroya, F. & Vidal-Puig, A. Beyond the sympathetic tone: the new brown fat activators. *Cell Metab* **17**, 638-643, doi:10.1016/j.cmet.2013.02.020 (2013).

81   Watanabe, M. *et al.* Bile acids induce energy expenditure by promoting intracellular thyroid hormone activation. *Nature* **439**, 484 (2006).

82   Whittle, A. J. *et al.* BMP8B increases brown adipose tissue thermogenesis through both central and peripheral actions. *Cell* **149**, 871-885, doi:10.1016/j.cell.2012.02.066 (2012).

83   Aune, U. L., Ruiz, L. & Kajimura, S. Isolation and differentiation of stromal vascular cells to beige/brite cells. *Journal of visualized experiments : JoVE*, doi:10.3791/50191 (2013).

84   Cawthorn, W. P., Scheller, E. L. & MacDougald, O. A. Adipose tissue stem cells meet preadipocyte commitment: going back to the future. *Journal of Lipid Research* **53**, 227-246, doi:10.1194/jlr.R021089 (2012).

85   Berry, R. & Rodeheffer, M. S. Characterization of the adipocyte cellular lineage in vivo. *Nat Cell Biol* **15**, 302-308, doi:10.1038/ncb2696 (2013).

86   Shan, T. *et al.* Distinct populations of adipogenic and myogenic Myf5-lineage progenitors in white adipose tissues. *J Lipid Res* **54**, 2214-2224, doi:10.1194/jlr.M038711 (2013).

87   Seale, P. *et al.* Transcriptional control of brown fat determination by PRDM16. *Cell Metab* **6**, 38-54, doi:10.1016/j.cmet.2007.06.001 (2007).

88   Seale, P. *et al.* PRDM16 controls a brown fat/skeletal muscle switch. *Nature* **454**, 961-967 (2008).

89   Timmons, J. A. *et al.* Myogenic gene expression signature establishes that brown and white adipocytes originate from distinct cell lineages. *Proc Natl Acad Sci U S A* **104**, 4401-4406, doi:10.1073/pnas.0610615104 (2007).

90   Lee, Y. H., Petkova, A. P., Mottillo, E. P. & Granneman, J. G. In vivo identification of bipotential adipocyte progenitors recruited by beta3-adrenoceptor activation and high-fat feeding. *Cell Metab* **15**, 480-491, doi:10.1016/j.cmet.2012.03.009 (2012).

91   Vegiopoulos, A. *et al.* Cyclooxygenase-2 controls energy homeostasis in mice by de novo recruitment of brown adipocytes. *Science* **328**, 1158-1161, doi:10.1126/science.1186034 (2010).

92   Wang, Q. A., Tao, C., Gupta, R. K. & Scherer, P. E. Tracking adipogenesis during white adipose tissue development, expansion and regeneration. *Nat Med* **19**, 1338-1344, doi:10.1038/nm.3324 (2013).

93   Rosen, E. D. & MacDougald, O. A. Adipocyte differentiation from the inside out. *Nat Rev Mol Cell Biol* **7**, 885-896 (2006).

94   Otto, T. C. & Lane, M. D. Adipose development: from stem cell to adipocyte. *Crit Rev Biochem Mol Biol* **40**, 229-242, doi:10.1080/10409230591008189 (2005).

95   Okamura, M. *et al.* COUP-TFII acts downstream of Wnt/beta-catenin signal to silence PPARgamma gene expression and repress adipogenesis. *Proc Natl Acad Sci U S A* **106**, 5819-5824, doi:10.1073/pnas.0901676106 (2009).

96   Wei, X., Sasaki, M., Huang, H., Dawson, V. L. & Dawson, T. M. The Orphan Nuclear Receptor, Steroidogenic Factor 1, Regulates Neuronal Nitric Oxide Synthase Gene Expression in Pituitary Gonadotropes. *Mol Endocrinol* **16**, 2828-2839 (2002).

97   Garten, A., Schuster, S. & Kiess, W. The insulin-like growth factors in adipogenesis and obesity. *Endocrinology and metabolism clinics of North America* **41**, 283-295, v-vi, doi:10.1016/j.ecl.2012.04.011 (2012).

98   Choy, L., Skillington, J. & Derynck, R. Roles of autocrine TGF-beta receptor and Smad signaling in adipocyte differentiation. *J Cell Biol* **149**, 667-682 (2000).

99   Yadav, H. *et al.* Protection from obesity and diabetes by blockade of TGF-beta/Smad3 signaling. *Cell Metab* **14**, 67-79, doi:10.1016/j.cmet.2011.04.013 (2011).

100   Zamani, N. & Brown, C. W. Emerging roles for the transforming growth factor-{beta} superfamily in regulating adiposity and energy expenditure. *Endocr Rev* **32**, 387-403, doi:10.1210/er.2010-0018 (2011).

101   Dani, C. Activins in adipogenesis and obesity. *International journal of obesity (2005)* **37**, 163-166, doi:10.1038/ijo.2012.28 (2013).

102   Garces, C. *et al.* Notch-1 controls the expression of fatty acid-activated transcription factors and is required for adipogenesis. *J Biol Chem* **272**, 29729-29734 (1997).

103   Ross, D. A., Rao, P. K. & Kadesch, T. Dual roles for the Notch target gene Hes-1 in the differentiation of 3T3-L1 preadipocytes. *Mol Cell Biol* **24**, 3505-3513 (2004).

104   Hu, E., Tontonoz, P. & Spiegelman, B. M. Transdifferentiation of myoblasts by the adipogenic transcription factors PPAR gamma and C/EBP alpha. *Proc Natl Acad Sci U S A* **92**, 9856-9860 (1995).

105   Tontonoz, P., Hu, E. & Spiegelman, B. M. Stimulation of adipogenesis in fibroblasts by PPAR gamma 2, a lipid-activated transcription factor. *Cell* **79**, 1147-1156 (1994).

106   Wu, Z. *et al.* Cross-regulation of C/EBP alpha and PPAR gamma controls the transcriptional pathway of adipogenesis and insulin sensitivity. *Mol Cell* **3**, 151-158 (1999).

107   Rosen, E. D. *et al.* C/EBPalpha induces adipogenesis through PPARgamma: a unified pathway. *Genes Dev* **16**, 22-26, doi:10.1101/gad.948702 (2002).

108   Park, B. O., Ahrends, R. & Teruel, M. N. Consecutive positive feedback loops create a bistable switch that controls preadipocyte-to-adipocyte conversion. *Cell Rep* **2**, 976-990, doi:10.1016/j.celrep.2012.08.038 (2012).

109   Siersbaek, R., Nielsen, R. & Mandrup, S. Transcriptional networks and chromatin remodeling controlling adipogenesis. *Trends Endocrinol Metab* **23**, 56-64, doi:10.1016/j.tem.2011.10.001 (2012).

110   Cristancho, A. G. & Lazar, M. A. Forming functional fat: a growing understanding of adipocyte differentiation. *Nat Rev Mol Cell Biol* **12**, 722-734, doi:10.1038/nrm3198 (2011).

111   Gupta, R. K. *et al.* Transcriptional control of preadipocyte determination by Zfp423. *Nature* **464**, 619-623, doi:10.1038/nature08816 (2010).

112   Festa, E. *et al.* Adipocyte lineage cells contribute to the skin stem cell niche to drive hair cycling. *Cell* **146**, 761-771, doi:10.1016/j.cell.2011.07.019 (2011).

113   Kang, S. *et al.* Regulation of early adipose commitment by Zfp521. *PLoS Biol* **10**, e1001433, doi:10.1371/journal.pbio.1001433 (2012).

114   Cristancho, A. G. *et al.* Repressor transcription factor 7-like 1 promotes adipogenic competency in precursor cells. *Proc Natl Acad Sci U S A* **108**, 16271-16276, doi:10.1073/pnas.1109409108 (2011).

115   Linhart, H. G. *et al.* C/EBPalpha is required for differentiation of white, but not brown, adipose tissue. *Proc Natl Acad Sci U S A* **98**, 12532-12537, doi:10.1073/pnas.211416898 (2001).

116   Rajakumari, S. *et al.* EBF2 determines and maintains brown adipocyte identity. *Cell Metab* **17**, 562-574, doi:10.1016/j.cmet.2013.01.015 (2013).

117   Puigserver, P. *et al.* Insulin-regulated hepatic gluconeogenesis through FOXO1-PGC-1a interaction. *Nature* **423**, 550-555 (2003).

118   Giguere, V. Transcriptional Control of Energy Homeostasis by the Estrogen-Related Receptors. *Endocr Rev* **29**, 677-696, doi:10.1210/er.2008-0017 (2008).

119   Puigserver, P. & Spiegelman, B. M. Peroxisome Proliferator-Activated Receptor-{gamma} Coactivator 1{alpha} (PGC-1{alpha}): Transcriptional Coactivator and Metabolic Regulator. *Endocr Rev* **24**, 78-90, doi:10.1210/er.2002-0012 (2003).

120   Kajimura, S. *et al.* Initiation of myoblast to brown fat switch by a PRDM16-C/EBP-β transcriptional complex. *Nature* **460**, 1154-1158 (2009).

121   Kajimura, S. *et al.* Regulation of the brown and white fat gene programs through a PRDM16/CtBP transcriptional complex. *Genes Dev.* **22**, 1397-1409, doi:10.1101/gad.1666108 (2008).

122   Villanueva, C. J. *et al.* Adipose subtype-selective recruitment of TLE3 or Prdm16 by PPARgamma specifies lipid storage versus thermogenic gene programs. *Cell Metab* **17**, 423-435, doi:10.1016/j.cmet.2013.01.016 (2013).

123   Oskowitz, A. Z. *et al.* Human multipotent stromal cells from bone marrow and microRNA: regulation of differentiation and leukemia inhibitory factor expression. *Proc Natl Acad Sci U S A* **105**, 18372-18377, doi:10.1073/pnas.0809807105 (2008).

124   Chen, L. *et al.* microRNAs regulate adipocyte differentiation. *Cell biology international* **37**, 533-546, doi:10.1002/cbin.10063 (2013).

125   Trajkovski, M. & Lodish, H. MicroRNA networks regulate development of brown adipocytes. *Trends Endocrinol Metab* **24**, 442-450, doi:10.1016/j.tem.2013.05.002 (2013).

126   Astrup, A. Thermogenesis in human brown adipose tissue and skeletal muscle induced by sympathomimetic stimulation. *Acta Endocrinol Suppl (Copenh)* **278**, 1-32 (1986).

127   Cannon, B. & Nedergaard, J. The biochemistry of an inefficient tissue: brown adipose tissue. *Essays Biochem* **20**, 110-164 (1985).

128   Cypess, A. M. *et al.* Identification and Importance of Brown Adipose Tissue in Adult Humans. *New England Journal of Medicine* **360**, 1509-1517, doi:doi:10.1056/NEJMoa0810780 (2009).

129   Weber, W. A. Brown Adipose Tissue and Nuclear Medicine Imaging. *J Nucl Med* **45**, 1101-1103 (2004).

130   Bouillaud, F., Ricquier, D., Thibault, J. & Weissenbach, J. Molecular approach to thermogenesis in brown adipose tissue: cDNA cloning of the mitochondrial uncoupling protein. *Proceedings of the National Academy of Sciences of the United States of America* **82**, 445-448 (1985).

131   Jacobsson, A., Stadler, U., Glotzer, M. A. & Kozak, L. P. Mitochondrial uncoupling protein from mouse brown fat. Molecular cloning, genetic mapping, and mRNA expression. *Journal of Biological Chemistry* **260**, 16250-16254 (1985).

132   Ricquier, D. & Bouillaud, F. The mitochondrial uncoupling protein: structural and genetic studies. *Prog Nucleic Acid Res Mol Biol* **56**, 83-108 (1997).

133   Kim, B. W., Choo, H. J., Lee, J. W., Kim, J. H. & Ko, Y. G. Extracellular ATP is generated by ATP synthase complex in adipocyte lipid rafts. *Exp Mol Med* **36**, 476-485, doi:200406301 [pii] (2004).

134   Luo, G.-F., Yu, T.-Y., Wen, X.-H., Li, Y. & Yang, G.-S. Alteration of mitochondrial oxidative capacity during porcine preadipocyte differentiation and in response to leptin. *Molecular and Cellular Biochemistry* **307**, 83-91, doi:10.1007/s11010-007-9587-2 (2008).

135   Wilson-Fritch, L. *et al.* Mitochondrial Biogenesis and Remodeling during Adipogenesis and in Response to the Insulin Sensitizer Rosiglitazone. *Mol. Cell. Biol.* **23**, 1085-1094 (2003).

136   Pagliarini, D. J. *et al.* A Mitochondrial Protein Compendium Elucidates Complex I Disease Biology. *Cell* **134**, 112-123 (2008).

137   Owen, O. E., Kalhan, S. C. & Hanson, R. W. The Key Role of Anaplerosis and Cataplerosis for Citric Acid Cycle Function. *Journal of Biological Chemistry* **277**, 30409-30412, doi:10.1074/jbc.R200006200 (2002).

138   Koh, E. H. *et al.* Essential Role of Mitochondrial Function in Adiponectin Synthesis in Adipocytes. *Diabetes* **56**, 2973-2981, doi:10.2337/db07-0510 (2007).

139   Eriksson, J. *et al.* Early Metabolic Defects in Persons at Increased Risk for Non-Insulin-Dependent Diabetes Mellitus. *New England Journal of Medicine* **321**, 337-343, doi:doi:10.1056/NEJM198908103210601 (1989).

140   Ducluzeau, P.-H. *et al.* Regulation by Insulin of Gene Expression in Human Skeletal Muscle and Adipose Tissue. *Diabetes* **50**, 1134-1142, doi:10.2337/diabetes.50.5.1134 (2001).

141   Vaag, A., Henriksen, J. E. & Beck-Nielsen, H. Decreased insulin activation of glycogen synthase in skeletal muscles in young nonobese Caucasian first-degree relatives of patients with non-insulin-dependent diabetes mellitus. *The Journal of Clinical Investigation* **89**, 782-788 (1992).

142   Pratipanawatr, W. *et al.* Skeletal Muscle Insulin Resistance in Normoglycemic Subjects With a Strong Family History of Type 2 Diabetes Is Associated With Decreased Insulin-Stimulated Insulin Receptor Substrate-1 Tyrosine Phosphorylation. *Diabetes* **50**, 2572-2578, doi:10.2337/diabetes.50.11.2572 (2001).

143   Jacob, S. *et al.* Association of increased intramyocellular lipid content with insulin resistance in lean nondiabetic offspring of type 2 diabetic subjects. *Diabetes* **48**, 1113-1119, doi:10.2337/diabetes.48.5.1113 (1999).

144   Malenfant, P. *et al.* Fat content in individual muscle fibers of lean and obese subjects. *Int J Obes Relat Metab Disord* **25**, 1316-1321, doi:10.1038/sj.ijo.0801733 (2001).

145   Dresner, A. *et al.* Effects of free fatty acids on glucose transport and IRS-1,Äìassociated phosphatidylinositol 3-kinase activity. *The Journal of Clinical Investigation* **103**, 253-259 (1999).

146   Holland, W. L. *et al.* Inhibition of Ceramide Synthesis Ameliorates Glucocorticoid-, Saturated-Fat-, and Obesity-Induced Insulin Resistance. *Cell Metabolism* **5**, 167-179 (2007).

147   Koves, T. R. *et al.* Mitochondrial Overload and Incomplete Fatty Acid Oxidation Contribute to Skeletal Muscle Insulin Resistance. *Cell Metabolism* **7**, 45-56 (2008).

148   Savage, D. B., Petersen, K. F. & Shulman, G. I. Disordered Lipid Metabolism and the Pathogenesis of Insulin Resistance. *Physiol. Rev.* **87**, 507-520, doi:10.1152/physrev.00024.2006 (2007).

149   Chibalin, A. V. *et al.* Downregulation of Diacylglycerol Kinase Delta Contributes to Hyperglycemia-Induced Insulin Resistance. *Cell* **132**, 375-386 (2008).

150   Houstis, N., Rosen, E. D. & Lander, E. S. Reactive oxygen species have a causal role in multiple forms of insulin resistance. *Nature* **440**, 944 (2006).

151 Yu, C. *et al.* Mechanism by Which Fatty Acids Inhibit Insulin Activation of Insulin Receptor Substrate-1 (IRS-1)-associated Phosphatidylinositol 3-Kinase Activity in Muscle. *Journal of Biological Chemistry* **277**, 50230-50236, doi:10.1074/jbc.M200958200 (2002).

152 Lanner, J. T., Bruton, J. D., Katz, A. & Westerblad, H. Ca2+ and insulin-mediated glucose uptake. *Current Opinion in Pharmacology* **8**, 339-345 (2008).

153 Lebeche, D., Davidoff, A. J. & Hajjar, R. J. Interplay between impaired calcium regulation and insulin signaling abnormalities in diabetic cardiomyopathy. *Nat Clin Pract Cardiovasc Med* **5**, 715-724 (2008).

154 Park, S. *et al.* Chronic elevated calcium blocks AMPK-induced GLUT-4 expression in skeletal muscle. *Am J Physiol Cell Physiol* **296**, C106-115, doi:10.1152/ajpcell.00114.2008 (2009).

155 Kacerovsky-Bielesz, G. *et al.* Short-Term Exercise Training Does Not Stimulate Skeletal Muscle ATP Synthesis in Relatives of Humans With Type 2 Diabetes. *Diabetes* **58**, 1333-1341, doi:10.2337/db08-1240 (2009).

156 Kotronen, A., Seppala-Lindroos, A., Bergholm, R. & Yki-Jarvinen, H. Tissue specificity of insulin resistance in humans: fat in the liver rather than muscle is associated with features of the metabolic syndrome. *Diabetologia* **51**, 130-138, doi:10.1007/s00125-007-0867-x (2008).

157 Michael, M. D. *et al.* Loss of insulin signaling in hepatocytes leads to severe insulin resistance and progressive hepatic dysfunction. *Mol Cell* **6**, 87-97, doi:S1097-2765(05)00015-8 [pii] (2000).

158 Biddinger, S. B. *et al.* Hepatic insulin resistance is sufficient to produce dyslipidemia and susceptibility to atherosclerosis. *Cell Metab* **7**, 125-134, doi:S1550-4131(07)00368-3 [pii]
10.1016/j.cmet.2007.11.013 (2008).

159 Veltri, K. L., Espiritu, M. & Singh, G. Distinct genomic copy number in mitochondria of different mammalian organs. *J Cell Physiol* **143**, 160-164, doi:10.1002/jcp.1041430122 (1990).

160 Benard, G. *et al.* Physiological diversity of mitochondrial oxidative phosphorylation. *Am J Physiol Cell Physiol* **291**, C1172-1182, doi:00195.2006 [pii]
10.1152/ajpcell.00195.2006 (2006).

161 Agarwal, A. K. & Garg, A. Genetic disorders of adipose tissue development, differentiation, and death. *Annu Rev Genomics Hum Genet* **7**, 175-199, doi:10.1146/annurev.genom.7.080505.115715 (2006).

162 Hwang, J. H. *et al.* Increased intrahepatic triglyceride is associated with peripheral insulin resistance: in vivo MR imaging and spectroscopy studies. *Am J Physiol Endocrinol Metab* **293**, E1663-1669, doi:00590.2006 [pii]
10.1152/ajpendo.00590.2006 (2007).

163 Korenblat, K. M., Fabbrini, E., Mohammed, B. S. & Klein, S. Liver, muscle, and adipose tissue insulin action is directly related to intrahepatic triglyceride content in obese subjects. *Gastroenterology* **134**, 1369-1375, doi:S0016-5085(08)00181-9 [pii]
10.1053/j.gastro.2008.01.075 (2008).

164 Petersen, K. F. *et al.* Reversal of nonalcoholic hepatic steatosis, hepatic insulin resistance, and hyperglycemia by moderate weight reduction in patients with type 2 diabetes. *Diabetes* **54**, 603-608, doi:54/3/603 [pii] (2005).

165   Kim, J. K. *et al.* Tissue-specific overexpression of lipoprotein lipase causes tissue-specific insulin resistance. *Proc Natl Acad Sci U S A* **98**, 7522-7527, doi:10.1073/pnas.121164498

121164498 [pii] (2001).

166   Cheng, Z. *et al.* Foxo1 integrates insulin signaling with mitochondrial function in the liver. *Nat Med* **15**, 1307-1311, doi:nm.2049 [pii]

10.1038/nm.2049 (2009).

167   Ferrari, A. *et al.* Linking epigenetics to lipid metabolism: Focus on histone deacetylases. *Molecular Membrane Biology* **29**, 257-266, doi:10.3109/09687688.2012.729094 (2012).

168   Boland, M. J., Nazor, K. L. & Loring, J. F. Epigenetic regulation of pluripotency and differentiation. *Circ Res* **115**, 311-324, doi:10.1161/circresaha.115.301517 (2014).

169   Mitteldorf, J. How does the body know how old it is? Introducing the epigenetic clock hypothesis. *Interdisciplinary topics in gerontology* **40**, 49-62, doi:10.1159/000364929 (2015).

170   Toden, S. & Goel, A. The Importance of Diets and Epigenetics in Cancer Prevention: A Hope and Promise for the Future? *Alternative therapies in health and medicine* **20**, 6-11 (2014).

171   Shanmugam, M. K. & Sethi, G. Role of epigenetics in inflammation-associated diseases. *Subcell Biochem* **61**, 627-657, doi:10.1007/978-94-007-4525-4_27 (2013).

172   Herrera, B. M., Keildson, S. & Lindgren, C. M. Genetics and epigenetics of obesity. *Maturitas* **69**, 41-49, doi:10.1016/j.maturitas.2011.02.018 (2011).

173   Ling, C. & Groop, L. Epigenetics: a molecular link between environmental factors and type 2 diabetes. *Diabetes* **58**, 2718-2725, doi:10.2337/db09-1003 (2009).

174   Webster, A. L., Yan, M. S. & Marsden, P. A. Epigenetics and cardiovascular disease. *The Canadian journal of cardiology* **29**, 46-57, doi:10.1016/j.cjca.2012.10.023 (2013).

175   Marques, S. C., Oliveira, C. R., Pereira, C. M. & Outeiro, T. F. Epigenetics in neurodegeneration: a new layer of complexity. *Progress in neuro-psychopharmacology & biological psychiatry* **35**, 348-355, doi:10.1016/j.pnpbp.2010.08.008 (2011).

176   Quintero-Ronderos, P. & Montoya-Ortiz, G. Epigenetics and autoimmune diseases. *Autoimmune diseases* **2012**, 593720, doi:10.1155/2012/593720 (2012).

177   Talbert, P. B. & Henikoff, S. Environmental responses mediated by histone variants. *Trends Cell Biol*, doi:10.1016/j.tcb.2014.07.006 (2014).

178   Richards, E. J. & Elgin, S. C. R. Epigenetic Codes for Heterochromatin Formation and Silencing: Rounding up the Usual Suspects. *Cell* **108**, 489-500, doi:http://dx.doi.org/10.1016/S0092-8674(02)00644-X (2002).

179   Vaillant, I. & Paszkowski, J. Role of histone and DNA methylation in gene regulation. *Current Opinion in Plant Biology* **10**, 528-533, doi:http://dx.doi.org/10.1016/j.pbi.2007.06.008 (2007).

180   Lopez-Rodas, G. *et al.* Histone deacetylase. A key enzyme for the binding of regulatory proteins to chromatin. *FEBS Lett* **317**, 175-180 (1993).

181   Haberland, M., Montgomery, R. L. & Olson, E. N. The many roles of histone deacetylases in development and physiology: implications for disease and therapy. *Nat Rev Genet* **10**, 32-42 (2009).

182   Lu, J., McKinsey, T. A., Nicol, R. L. & Olson, E. N. Signal-dependent activation of the MEF2 transcription factor by dissociation from histone deacetylases. *Proc Natl Acad Sci U S A* **97**, 4070-4075, doi:10.1073/pnas.080064097 (2000).

183   McKinsey, T. A., Zhang, C. L., Lu, J. & Olson, E. N. Signal-dependent nuclear export of a histone deacetylase regulates muscle differentiation. *Nature* **408**, 106-111, doi:10.1038/35040593 (2000).

184   Passier, R. *et al.* CaM kinase signaling induces cardiac hypertrophy and activates the MEF2 transcription factor in vivo. *J Clin Invest* **105**, 1395-1406, doi:10.1172/jci8551 (2000).

185   Vega, R. B. *et al.* Protein kinases C and D mediate agonist-dependent cardiac hypertrophy through nuclear export of histone deacetylase 5. *Mol Cell Biol* **24**, 8374-8385, doi:10.1128/mcb.24.19.8374-8385.2004 (2004).

186   Lahm, A. *et al.* Unraveling the hidden catalytic activity of vertebrate class IIa histone deacetylases. *Proceedings of the National Academy of Sciences* **104**, 17335-17340, doi:10.1073/pnas.0706487104 (2007).

187   Finkel, T., Deng, C. X. & Mostoslavsky, R. Recent progress in the biology and physiology of sirtuins. *Nature* **460**, 587-591, doi:10.1038/nature08197 (2009).

188   Rodgers, J. T. *et al.* Nutrient control of glucose homeostasis through a complex of PGC-1[alpha] and SIRT1. *Nature* **434**, 113 (2005).

189   Rodgers, J. T. & Puigserver, P. Fasting-dependent glucose and lipid metabolic response through hepatic sirtuin 1. *Proceedings of the National Academy of Sciences* **104**, 12861-12866, doi:10.1073/pnas.0702509104 (2007).

190   Miremadi, A., Oestergaard, M. Z., Pharoah, P. D. & Caldas, C. Cancer genetics of epigenetic genes. *Human molecular genetics* **16 Spec No 1**, R28-49, doi:10.1093/hmg/ddm021 (2007).

191   Gray, S. G. & Ekström, T. J. The Human Histone Deacetylase Family. *Experimental Cell Research* **262**, 75-83, doi:http://dx.doi.org/10.1006/excr.2000.5080 (2001).

192   Nerup, J. & Pociot, F. A genomewide scan for type 1-diabetes susceptibility in Scandinavian families: identification of new loci with evidence of interactions. *Am J Hum Genet* **69**, 1301-1313 (2001).

193   Xiang, K. *et al.* Genome-Wide Search for Type 2 Diabetes/Impaired Glucose Homeostasis Susceptibility Genes in the Chinese: Significant Linkage to Chromosome 6q21-q23 and Chromosome 1q21-q24. *Diabetes* **53**, 228-234, doi:10.2337/diabetes.53.1.228 (2004).

194   Dawson, M. A. & Kouzarides, T. Cancer epigenetics: from mechanism to therapy. *Cell* **150**, 12-27, doi:10.1016/j.cell.2012.06.013 (2012).

195   Czubryt, M. P., McAnally, J., Fishman, G. I. & Olson, E. N. Regulation of peroxisome proliferator-activated receptor g coactivator 1a (PGC-1a) and mitochondrial function by MEF2 and HDAC5. *Proc. Natl. Acad. Sci. USA* **100**, 1711-1716 (2003).

196   Potthoff, M. *et al.* Histone deacetylase degradation and MEF2 activation promote the formation of slow-twitch myofibers. *J Clin Invest* **117**, 2459-2467 (2007).

197   McGee, S. L. *et al.* AMP-activated protein kinase regulates GLUT4 transcription by phosphorylating histone deacetylase 5. *Diabetes* **57**, 860-867, doi:10.2337/db07-0843 (2008).

198   Gao, Z. *et al.* Butyrate Improves Insulin Sensitivity and Increases Energy Expenditure in Mice. *Diabetes* **58**, 1509-1517, doi:10.2337/db08-1637 (2009).

199   Donohoe, D. R. *et al.* The Microbiome and Butyrate Regulate Energy Metabolism and Autophagy in the Mammalian Colon. *Cell metabolism* **13**, 517-526 (2011).

200   Yamamoto, H. *et al.* NCoR1 is a conserved physiological modulator of muscle mass and oxidative function. *Cell* **147**, 827-839, doi:10.1016/j.cell.2011.10.017 (2011).

201   Perissi, V., Jepsen, K., Glass, C. K. & Rosenfeld, M. G. Deconstructing repression: evolving models of co-repressor action. *Nat Rev Genet* **11**, 109-123, doi:10.1038/nrg2736 (2010).

202   Gregoire, S. *et al.* Histone deacetylase 3 interacts with and deacetylates myocyte enhancer factor 2. *Mol Cell Biol* **27**, 1280-1295, doi:10.1128/mcb.00882-06 (2007).

203   McKinsey, T. A., Zhang, C. L. & Olson, E. N. Identification of a Signal-Responsive Nuclear Export Sequence in Class II Histone Deacetylases. *Mol. Cell. Biol.* **21**, 6312-6321 (2001).

204   Zhao, X., Sternsdorf, T., Bolger, T. A., Evans, R. M. & Yao, T. P. Regulation of MEF2 by histone deacetylase 4- and SIRT1 deacetylase-mediated lysine modifications. *Mol Cell Biol* **25**, 8456-8464, doi:10.1128/mcb.25.19.8456-8464.2005 (2005).

205   Addison, W. N. *et al.* Direct transcriptional repression of Zfp423 by Zfp521 mediates a bone morphogenic protein-dependent osteoblast versus adipocyte lineage commitment switch. *Mol Cell Biol* **34**, 3076-3085, doi:10.1128/mcb.00185-14 (2014).

206   Handschin, C. & Spiegelman, B. M. Peroxisome proliferator-activated receptor gamma coactivator 1 coactivators, energy homeostasis, and metabolism. *Endocr Rev* **27**, 728-735, doi:10.1210/er.2006-0037 (2006).

207   Lin, J. *et al.* Transcriptional co-activator PGC-1 alpha drives the formation of slow-twitch muscle fibres. *Nature* **418**, 797-801, doi:10.1038/nature00904 (2002).

208   Li, P. *et al.* Adipocyte NCoR knockout decreases PPARgamma phosphorylation and enhances PPARgamma activity and insulin sensitivity. *Cell* **147**, 815-826, doi:10.1016/j.cell.2011.09.050 (2011).

209   Evans, R. M., Barish, G. D. & Wang, Y. X. PPARs and the complex journey to obesity. *Nat Med* **10**, 355-361, doi:10.1038/nm1025 (2004).

210   Imai, T. *et al.* Peroxisome proliferator-activated receptor gamma is required in mature white and brown adipocytes for their survival in the mouse. *Proc Natl Acad Sci U S A* **101**, 4543-4547, doi:10.1073/pnas.0400356101 (2004).

211   Rangwala, S. M. & Lazar, M. A. Peroxisome proliferator-activated receptor gamma in diabetes and metabolism. *Trends Pharmacol Sci* **25**, 331-336, doi:10.1016/j.tips.2004.03.012 (2004).

212   Tontonoz, P. & Spiegelman, B. M. Fat and beyond: the diverse biology of PPARgamma. *Annu Rev Biochem* **77**, 289-312, doi:10.1146/annurev.biochem.77.061307.091829 (2008).

213   Yu, C. *et al.* The nuclear receptor corepressors NCoR and SMRT decrease peroxisome proliferator-activated receptor gamma transcriptional activity and repress 3T3-L1 adipogenesis. *J Biol Chem* **280**, 13600-13605, doi:10.1074/jbc.M409468200 (2005).

214   Choi, J. H. *et al.* Anti-diabetic drugs inhibit obesity-linked phosphorylation of PPARgamma by Cdk5. *Nature* **466**, 451-456, doi:10.1038/nature09291 (2010).

215   Weems, J. C., Griesel, B. A. & Olson, A. L. Class II histone deacetylases downregulate GLUT4 transcription in response to increased cAMP signaling in cultured adipocytes and fasting mice. *Diabetes* **61**, 1404-1414, doi:10.2337/db11-0737 (2012).

216   Sun, Z. *et al.* Diet-induced lethality due to deletion of the Hdac3 gene in heart and skeletal muscle. *J Biol Chem* **286**, 33301-33309, doi:10.1074/jbc.M111.277707 (2011).

217   Rajendran, P., Ho, E., Williams, D. E. & Dashwood, R. H. Dietary phytochemicals, HDAC inhibition, and DNA damage/repair defects in cancer cells. *Clinical epigenetics* **3**, 4, doi:10.1186/1868-7083-3-4 (2011).

218   Antos, C. L. *et al.* Dose-dependent blockade to cardiomyocyte hypertrophy by histone deacetylase inhibitors. *J Biol Chem* **278**, 28930-28937, doi:10.1074/jbc.M303113200 (2003).

219   Cao, D. J. *et al.* Histone deacetylase (HDAC) inhibitors attenuate cardiac hypertrophy by suppressing autophagy. *Proc Natl Acad Sci U S A* **108**, 4123-4128, doi:10.1073/pnas.1015081108 (2011).

220   Gupta, M. P., Samant, S. A., Smith, S. H. & Shroff, S. G. HDAC4 and PCAF bind to cardiac sarcomeres and play a role in regulating myofilament contractile activity. *J Biol Chem* **283**, 10135-10146, doi:10.1074/jbc.M710277200 (2008).

221   McKinsey, T. A. Therapeutic potential for HDAC inhibitors in the heart. *Annual review of pharmacology and toxicology* **52**, 303-319, doi:10.1146/annurev-pharmtox-010611-134712 (2012).

222   Dompierre, J. P. *et al.* Histone deacetylase 6 inhibition compensates for the transport deficit in Huntington's disease by increasing tubulin acetylation. *J Neurosci* **27**, 3571-3583, doi:10.1523/jneurosci.0037-07.2007 (2007).

223   Outeiro, T. F. *et al.* Sirtuin 2 inhibitors rescue alpha-synuclein-mediated toxicity in models of Parkinson's disease. *Science* **317**, 516-519, doi:10.1126/science.1143780 (2007).

224   Li, G., Jiang, H., Chang, M., Xie, H. & Hu, L. HDAC6 alpha-tubulin deacetylase: a potential therapeutic target in neurodegenerative diseases. *Journal of the neurological sciences* **304**, 1-8, doi:10.1016/j.jns.2011.02.017 (2011).

225   Chatterjee, T. K. *et al.* Histone deacetylase 9 is a negative regulator of adipogenic differentiation. *J Biol Chem* **286**, 27836-27847, doi:10.1074/jbc.M111.262964 (2011).

226   Haberland, M., Carrer, M., Mokalled, M. H., Montgomery, R. L. & Olson, E. N. Redundant Control of Adipogenesis by Histone Deacetylases 1 and 2. *Journal of Biological Chemistry* **285:**, 14663-14670., doi:10.1074/jbc.M109.081679 (2010).

227   Kim, S. N., Choi, H. Y. & Kim, Y. K. Regulation of adipocyte differentiation by histone deacetylase inhibitors. *Arch Pharm Res* **32**, 535-541, doi:10.1007/s12272-009-1409-5 (2009).

228   Li, D. *et al.* Kruppel-like factor-6 promotes preadipocyte differentiation through histone deacetylase 3-dependent repression of DLK1. *J Biol Chem* **280**, 26941-26952, doi:10.1074/jbc.M500463200 (2005).

229   Yoo, E. J., Chung, J. J., Choe, S. S., Kim, K. H. & Kim, J. B. Down-regulation of histone deacetylases stimulates adipocyte differentiation. *J Biol Chem* **281**, 6608-6615, doi:10.1074/jbc.M508982200 (2006).

230   Nebbioso, A. *et al.* HDACs class II-selective inhibition alters nuclear receptor-dependent differentiation. *J Mol Endocrinol* **45**, 219-228, doi:10.1677/jme-10-0043 (2010).

231   Burton, G. R., Nagarajan, R., Peterson, C. A. & McGehee, R. E., Jr. Microarray analysis of differentiation-specific gene expression during 3T3-L1 adipogenesis. *Gene* **329**, 167-185, doi:10.1016/j.gene.2003.12.012 (2004).

232   Lagace, D. C. & Nachtigal, M. W. Inhibition of Histone Deacetylase Activity by Valproic Acid Blocks Adipogenesis. *J. Biol. Chem.* **279**, 18851-18860 (2004).

233   Catalioto, R. M., Maggi, C. A. & Giuliani, S. Chemically distinct HDAC inhibitors prevent adipose conversion of subcutaneous human white preadipocytes at an early stage of the differentiation program. *Exp Cell Res* **315**, 3267-3280, doi:10.1016/j.yexcr.2009.09.012 (2009).

234   Li, J. *et al.* Both corepressor proteins SMRT and N-CoR exist in large protein complexes containing HDAC3. *Embo j* **19**, 4342-4350, doi:10.1093/emboj/19.16.4342 (2000).

235   Fajas, L. *et al.* The retinoblastoma-histone deacetylase 3 complex inhibits PPARgamma and adipocyte differentiation. *Dev Cell* **3**, 903-910 (2002).

236   Jiang, X., Ye, X., Guo, W., Lu, H. & Gao, Z. Inhibition of HDAC3 promotes ligand-independent PPARgamma activation by protein acetylation. *J Mol Endocrinol* **53**, 191-200, doi:10.1530/jme-14-0066 (2014).

237   Canettieri, G. *et al.* Attenuation of a phosphorylation-dependent activator by an HDAC-PP1 complex. *Nat Struct Biol* **10**, 175-181, doi:10.1038/nsb895 [doi] nsb895 [pii] (2003).

238   Galmozzi, A. *et al.* Inhibition of Class I Histone Deacetylases Unveils a Mitochondrial Signature and Enhances Oxidative Metabolism in Skeletal Muscle and Adipose Tissue. *Diabetes* **62**, 732-742, doi:10.2337/db12-0548 (2013).

239   Huang, H. *et al.* BMP signaling pathway is required for commitment of C3H10T1/2 pluripotent stem cells to the adipocyte lineage. *Proc Natl Acad Sci U S A* **106**, 12670-12675, doi:10.1073/pnas.0906266106 (2009).

240   Chappard, D., Marchand-Libouban, H., Moreau, M. F. & Basle, M. F. Thiazolidinediones cause compaction of nuclear heterochromatin in the pluripotent mesenchymal cell line C3H10T1/2 when inducing an adipogenic phenotype. *Analytical and quantitative cytopathology and histopathology* **35**, 85-94 (2013).

241   Bharathy, N., Ling, B. M. & Taneja, R. Epigenetic regulation of skeletal muscle development and differentiation. *Subcell Biochem* **61**, 139-150, doi:10.1007/978-94-007-4525-4_7 (2013).

242   Potthoff, M. J. *et al.* Histone deacetylase degradation and MEF2 activation promote the formation of slow-twitch myofibers. *J Clin Invest* **117**, 2459-2467, doi:10.1172/jci31960 (2007).

243   Kelley, D. E., He, J., Menshikova, E. V. & Ritov, V. B. Dysfunction of Mitochondria in Human Skeletal Muscle in Type 2 Diabetes. *Diabetes* **51**, 2944-2950, doi:10.2337/diabetes.51.10.2944 (2002).

244   Boushel, R. *et al.* Patients with type 2 diabetes have normal mitochondrial function in skeletal muscle. *Diabetologia* **50**, 790-796, doi:10.1007/s00125-007-0594-3 (2007).

245   Tiraby, C. *et al.* Acquirement of Brown Fat Cell Features by Human White Adipocytes. *J. Biol. Chem.* **278**, 33370-33376 (2003).

246   Murano, I. *et al.* Dead adipocytes, detected as crown-like structures, are prevalent in visceral fat depots of genetically obese mice. *Journal of Lipid Research* **49**, 1562-1568, doi:10.1194/jlr.M800019-JLR200 (2008).

247   Knutson, S. K. *et al.* Liver-specific deletion of histone deacetylase 3 disrupts metabolic transcriptional networks. *EMBO J* **27**, 1017-1028 (2008).

248   Sun, Z. *et al.* Hepatic Hdac3 promotes gluconeogenesis by repressing lipid synthesis and sequestration. *Nat Med* **18**, 934-942, doi:10.1038/nm.2744 (2012).

249   Arner, P. *et al.* Dynamics of human adipose lipid turnover in health and metabolic disease. *Nature* **478**, 110-113, doi:http://www.nature.com/nature/journal/v478/n7367/abs/nature10426.html - supplementary-information (2011).

250   Mihaylova, M. M. & Shaw, R. J. Metabolic reprogramming by class I and II histone deacetylases. *Trends Endocrinol Metab* **24**, 48-57, doi:10.1016/j.tem.2012.09.003 (2013).

251   Tang, Q. Q., Otto, T. C. & Lane, M. D. Commitment of C3H10T1/2 pluripotent stem cells to the adipocyte lineage. *Proc Natl Acad Sci U S A* **101**, 9607-9611, doi:10.1073/pnas.0403100101 (2004).

252   Hesse, E. *et al.* Zfp521 controls bone mass by HDAC3-dependent attenuation of Runx2 activity. *J Cell Biol* **191**, 1271-1283, doi:10.1083/jcb.201009107 (2010).